Progress in Retinal and Eye Research 57 (2017) 134–185

Contents lists available at ScienceDirect

Progress in Retinal and Eye Research

journal homepage: www.elsevier.com/locate/prer

Pharmacokinetic aspects of retinal drug delivery

Eva M. del Amo [b, 1], Anna-Kaisa Rimpelä [a, 1], Emma Heikkinen [b, 1], Otto K. Kari [a, 1], Eva Ramsay [b, 1], Tatu Lajunen [a, 1], Mechthild Schmitt [a, 1], Laura Pelkonen [b, 1], Madhushree Bhattacharya [a, 1], Dominique Richardson [a, 1], Astrid Subrizi [b, 1], Tiina Turunen [a, 1], Mika Reinisalo [b, 1], Jaakko Itkonen [a, 1], Elisa Toropainen [b, 1], Marco Casteleijn [a, 1], Heidi Kidron [a, 1], Maxim Antopolsky [a, 1], Kati-Sisko Vellonen [b, 1], Marika Ruponen [b, 1], Arto Urtti [a, b, *]

[a] Centre for Drug Research, Division of Pharmaceutical Biosciences, University of Helsinki, Helsinki, Finland
[b] School of Pharmacy, University of Eastern Finland, Kuopio, Finland

ARTICLE INFO

Article history:
Received 23 August 2016
Received in revised form
25 November 2016
Accepted 1 December 2016
Available online 24 December 2016

Keywords:
Retina
Vitreous
Choroid
Topical
Intravitreal
Sub-conjunctival
Suprachoroidal
Clearance
Distribution
Pharmacokinetic modeling
Transport

ABSTRACT

Drug delivery to the posterior eye segment is an important challenge in ophthalmology, because many diseases affect the retina and choroid leading to impaired vision or blindness. Currently, intravitreal injections are the method of choice to administer drugs to the retina, but this approach is applicable only in selected cases (e.g. anti-VEGF antibodies and soluble receptors). There are two basic approaches that can be adopted to improve retinal drug delivery: prolonged and/or retina targeted delivery of intravitreal drugs and use of other routes of drug administration, such as periocular, suprachoroidal, sub-retinal, systemic, or topical. Properties of the administration route, drug and delivery system determine the efficacy and safety of these approaches. Pharmacokinetic and pharmacodynamic factors determine the required dosing rates and doses that are needed for drug action. In addition, tolerability factors limit the use of many materials in ocular drug delivery. This review article provides a critical discussion of retinal drug delivery, particularly from the pharmacokinetic point of view. This article does not include an extensive review of drug delivery technologies, because they have already been reviewed several times recently. Instead, we aim to provide a systematic and quantitative view on the pharmacokinetic factors in drug delivery to the posterior eye segment. This review is based on the literature and unpublished data from the authors' laboratory.

Contents

* Corresponding author. Centre for Drug Research, Division of Pharmaceutical Biosciences, University of Helsinki, Viikinkaari 5 E, P.O. Box 56, 00790, Helsinki, Finland.
E-mail addresses: arto.urtti@helsinki.fi, arto.urtti@uef.fi (A. Urtti).

[1] Percentage of work contributed by each author in the production of the manuscript is as follows: Eva M. del Amo - 10%; Anna-Kaisa Rimpela - 10%; Emma Heikkinen - 5%; Otto k. Kari - 5%; Eva Ramsay - 4%; Tatu Lajunen - 4%; Mechthild Schmitt - 4%; Laura Pelkonen - 4%; Madhushree Bhattacharya - 4%; Dominique Richardson - 4%; Astrid Subrizi - 4%; Tina Turunen - 4%; Mika Reinisalo - 3%; Jaakko Itkonen - 3%; Elisa Toropainen - 3%; Marco Casteleijn - 2% Heidi Kidron - 2%; Maxim Antopolsky - 2%; Kati-Sisko Vellonen - 3%; Marika Ruponen - 5%.

http://dx.doi.org/10.1016/j.preteyeres.2016.12.001

1. Introduction

Drug delivery and pharmacokinetics play important roles in current retinal therapeutics and the development of new medications. Retinal diseases lead to visual impairment and in many cases blindness. The number of patients suffering from retinal disease is increasing due to the aging population; it has been predicted that the number of patients suffering from age-related macular degeneration (AMD) will reach 288 million in 2040 (Wong et al., 2014). Large patient populations with glaucoma and diabetic retinal

complications also increase in prevalence due to the aging population. In addition, there are numerous inherited rare retinal degenerations that lead to blindness at a young age.

As the mechanisms of retinal diseases are investigated and revealed, new potential drug targets will emerge. The delivery of drugs to retinal targets is challenging and various routes of drug administration have been investigated (Fig. 1). Unfortunately, most of them result in sub-therapeutic drug levels in the retina. Intravitreal injection is currently the method of choice in retinal drug delivery (Fig. 1). Intravitreal injections are used widely in the clinics, especially in the delivery of anti-VEGF proteins (bevacizumab, ranibizumab, aflibercept) to patients suffering from the wet form of AMD. These injections should be given every month or two months, but in practice the compliance is poor and the injections are given at longer intervals (Cohen et al., 2013; Holz et al., 2015). This decreases the efficacy of the AMD treatments and there is a need for longer acting intravitreal injections. It is important to note that monthly and bimonthly injection intervals are feasible in the case of anti-VEGF proteins, because these antibodies and soluble receptors have long intravitreal half-lives (about one week), they are highly potent compounds that show effects even at very low concentrations, and they are tolerated at relatively high doses. In fact, the vitreal drug concentrations show about 100-fold changes during the AMD treatment. Small molecules have much shorter half-lives (usually less than 10 h) than protein drugs in the vitreous (Maurice and Mishima, 1984). Therefore, their dosing intervals are too short to be clinically acceptable in chronic multiple dose treatment. Also, many protein drugs (e.g. growth factors) have much more narrow therapeutic indices than anti-VEGF antibodies and would require frequent intravitreal dosing. For these reasons, controlled release delivery systems are being investigated for intravitreal drug delivery to the retina (see Fig. 1).

Retinal drug delivery could also be accomplished using other methods, such as systemic, topical, periocular (sub-conjunctival, sub-Tenon's, posterior juxtascleral, peribulbar and retrobulbar injections), sub-retinal and suprachoroidal drug administration (Fig. 1), but these approaches may not result in adequate drug concentrations in the retina with currently available technologies. These routes of drug delivery may become clinically feasible if new improved drug delivery systems are developed.

This review aims to present systematic, critical and quantitative treatise of the *pharmacokinetic factors* in retinal drug delivery of small molecular weight drugs, biologics and controlled drug delivery systems. The delivery technologies and general ocular

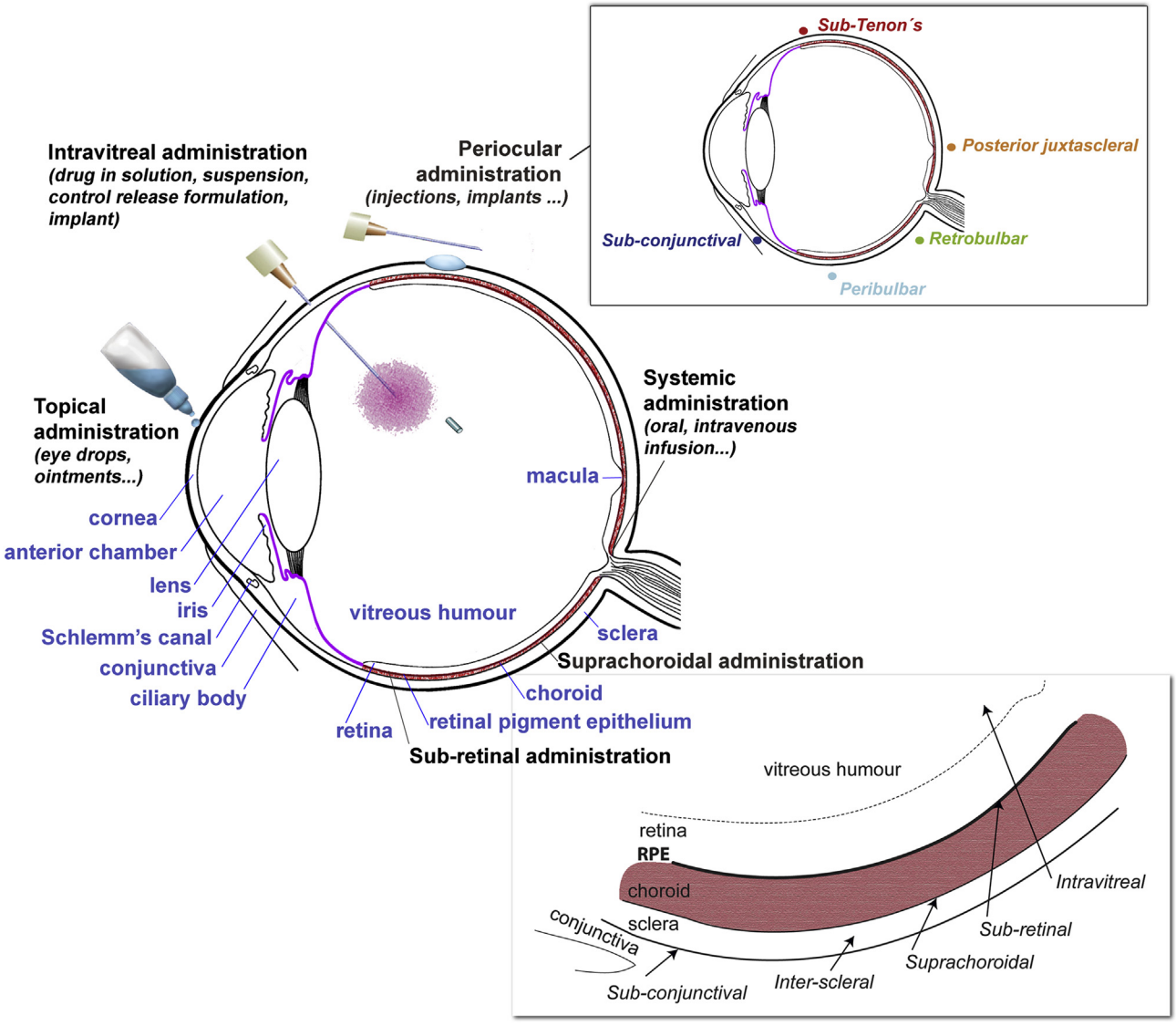

Fig. 1. Routes of drug administration for retinal drug delivery, adapted from del Amo (2015).

pharmacology are not discussed in detail, because there are recent reviews that present these aspects in detail (Hamdi et al., 2015; Herrero-Vanrell et al., 2014; Novack and Robin, 2016; Yasin et al., 2014).

2. Blood-ocular barriers

After intravitreal administration the drugs distribute in the vitreous, and to the surrounding ocular tissues. Drug elimination from the vitreous cavity takes place via blood-ocular barriers and aqueous humor outflow to the systemic blood circulation. In the case of systemic, suprachoroidal and periocular drug administration, the drug must cross the blood-ocular barrier before it can reach the targets in the retina. Therefore, blood-ocular barriers play an important role in defining drug permeation into the eye and from the eye to the blood circulation.

The blood-ocular barriers consist of the anterior blood-aqueous barrier (BAB) and posterior blood-retinal barrier (BRB) (Fig. 2) (Raviola, 1977). The posterior iris, inner non-pigmented ciliary epithelia and the tight endothelia around the iris and ciliary muscle capillaries form the BAB. The BRB consists of the endothelia of the retinal capillaries (inner BRB) and retinal pigment epithelium (RPE) (outer BRB). Unfortunately, the permeability values for the vascular components of the BAB are difficult to determine. Permeability of the retinal pigment epithelium is easier to determine experimentally and, therefore, its role in the blood-ocular barrier is easier to quantitate. Qualitative data have been generated in experiments using fluorescent tracers of various sizes. In other tight epithelial membranes (intestine, conjunctiva, cornea), the diameters of paracellular holes have been determined to be in the range of 1–3 nm (Hämäläinen et al., 1997; Linnankoski et al., 2010). We can assume that the proteins of tight junctions will form a similar barrier in the blood-ocular barriers. The experiments with fluorescent and radiolabeled tracers support this notion. Note that the cited size values of the tracers were obtained from the original articles and they may differ from the values in some other sources.

2.1. Inner blood retinal barrier: retinal capillaries

Tracer experiments have revealed that the retinal capillary walls in various species (rat, monkey, pig) prevent permeation of i.v. carbon nanoparticles (20 nm in diameter), ^{125}I-albumin (7.2 nm), horseradish peroxidase (4 nm), and microperoxidase (2 nm) (Ashton and Cunha-Vaz, 1965; Smith and Rudt, 1975; Törnquist et al., 1990), but small molecules (molecular weights a few hundred Daltons) (e.g. mannitol, glycerol, fluorescein) were shown to be permeable (Cunha-Vaz and Maurice, 1969, 1967; Tachikawa et al., 2010; Thornit et al., 2010). These compounds are clearly smaller than the size of typical paracellular spaces in the membranes with tight junctions (about 2 nm) (Hämäläinen et al., 1997). In addition, some compounds, like fluorescein, may permeate transcellularly by passive diffusion and active transport (Cunha-Vaz and Maurice, 1969, 1967). The reported *in vivo* permeability values reflect the permeation in the entire BRB, not only the retinal capillaries, and so it is difficult to quantitate the permeability in the retinal capillaries. Some investigators have reported permeabilities in cellular models, but the relevance of these capillary cell models is not certain, as the reported values are much higher than one would expect for the membranes with tight junctions, i.e. in the range of 10^{-4} cm/s (Haselton et al., 1998, 1996). Based on the existing data, we can conclude that the retinal capillaries form a barrier that prevents permeation of molecules with a diameter of 2 nm and higher, while small molecules are able to permeate across the inner BRB to some extent.

2.2. Outer blood retinal barrier: retinal pigment epithelium

The retinal pigment epithelium is a tight cellular monolayer that is located between the photoreceptors and choroid (Fig. 2). It has important functions in the homeostasis of the neural retina and as the outer part of the BRB. The roles of Bruch's membrane and choroidal tissue as barriers to small molecules and neutral macromolecules (up to 500 kDa) are negligible in comparison with the RPE (Pitkänen et al., 2005). The transepithelial resistance of the RPE is typically in the range of 0.10–0.15 kOhm cm^2 (Kimura et al., 1996; Pitkänen et al., 2005; Tsuboi and Pederson, 1986). Smith and Rudt (1975) showed that microperoxidase (size 2 nm) does not permeate through the RPE *in vivo* in monkeys.

Permeability of the RPE has been investigated in more detail using Ussing chambers and *ex vivo* bovine RPE-choroid specimens (Pitkänen et al., 2005). Permeation of small molecules was dependent on their lipophilicity; the permeability of small hydrophilic compounds (e.g. nadolol) was in the range of 2×10^{-6} cm/s, while lipophilic drugs (e.g. betaxolol) permeated much faster (16×10^{-6} cm/s). The paracellular permeability of hydrophilic solutes decreased with increasing molecular size, clearly highlighting the size dependent molecular exclusion by the RPE (Table 1).

It is important to note that the inward permeability of FITC-dextran 77,000 was only 0.027×10^{-6} cm/s; about 36 and 618

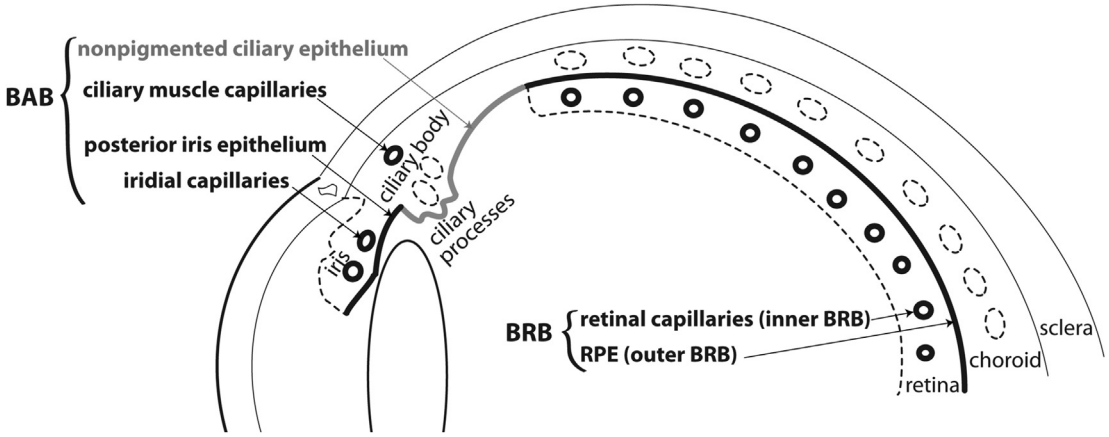

Fig. 2. Blood-ocular barriers. The thicker lines indicate tight endothelium/epithelium while the dashed ones indicate leaky endothelium/epithelium.

Table 1
Permeability of hydrophilic and lipophilic solutes in the *ex vivo* bovine RPE-choroid membranes (Pitkänen et al., 2005).

Compound	Lipophilic/hydrophilic	Molecular weight (Da)	Molecular diameter (nm)	Permeability (10^{-6} cm/s)
Betaxolol	Lipophilic ($LogD_{7.4}$) = 1.59	307	0.9	10.3 ± 4.48 (outward) 16.7 ± 3.65 (inward)
Carboxyfluorescein	Hydrophilic	376	1.0	2.33 ± 1.06 (outward) 0.96 ± 0.38 (inward)
FITC dextran	Hydrophilic	4400	2.6	0.24 ± 0.16 (inward)
FITC dextran	Hydrophilic	21,200	6.4	0.13 ± 0.18 (inward)
FITC dextran	Hydrophilic	38,200	9.0	0.046 ± 0.029 (inward)
FITC dextran	Hydrophilic	77,000	12.8	0.027 ± 0.032 (inward)

times less than the permeability of carboxyfluorescein and betaxolol respectively. This demonstrates the steep relationship between the RPE permeability and molecular size. For comparison, the choroidal tissue permeability is 1–2 orders of magnitude higher, ranging from 100 × 10^{-6} cm/s (^{51}Cr-EDTA) to 0.3 × 10^{-6} cm/s (albumin) (Törnquist et al., 1990). The permeability of the fenestrated choroidal blood vessel walls is high, allowing rapid entry of drugs to the extravascular choroid from the blood circulation (Bill et al., 1980). After intravitreal administration the drug is cleared rapidly to the blood circulation in the choroid after RPE passage. The choroidal vessels have openings of 60–80 nm allowing permeation of large molecules (e.g. albumin) (Bill et al., 1980).

Clear outward directionality of carboxyfluorescein and fluorescein permeation in the RPE indicates active transport (Tsuboi and Pederson, 1986), but in later studies the directionality of carboxyfluorescein permeation was not as obvious (Kimura et al., 1996; Pitkänen et al., 2005, Table 1). Cunha-Vaz and Maurice (1967) showed active transport of fluorescein *in vivo*, but the roles of different tissues (RPE, retinal capillaries) in these findings are not clear.

2.3. Blood-aqueous barrier

The blood-aqueous barrier consists of endothelial (iris and ciliary muscle vasculature) and epithelial barriers (posterior iris epithelium and non-pigmented epithelium) (Fig. 2). It has been shown that i.v. microperoxidase (2 nm), horseradish peroxidase (4 nm) and carbon particles (20 nm) did not escape from the iris vessels in rat, cat, rabbit and monkey healthy eyes (Ashton and Cunha-Vaz, 1965; Bill, 1975; Raviola, 1974; Smith and Rudt, 1975; Vegge, 1971). Butler et al. (1988) and Shakib and Cunha-Vaz (1966) claimed species differences in the iris vessel permeability, but the conclusions were contradictory (see also Ashton and Cunha-Vaz, 1965; Cole, 1974). Also, in ciliary muscle vessels, horseradish peroxidase does not escape from the blood circulation to the extravascular space (Raviola, 1977). However, the vessels of ciliary processes are leaky in rabbits and monkeys allowing permeation of proteins (myoglobin 4 nm; albumin 7 nm; gammaglobulin 11 nm) across their walls (Bill, 1968; Bill et al., 1980; Smith and Rudt, 1975).

The epithelial components of BAB also have tight intercellular junctions (Fig. 2). The iris posterior epithelium does not allow permeation of horseradish peroxidase (4 nm) (Raviola, 1977; Tonjum and Pedersen, 1977). Likewise, the non-pigmented epithelium of monkey did not allow permeation of microperoxidase or horseradish peroxidase (Raviola, 1974; Smith and Rudt, 1975).

It is difficult to assess the permeability of the BAB and BRB separately because an intravitreal drug is usually eliminated through the BAB and BRB simultaneously (Fig. 2). Likewise, an intravenously administered drug distributes to the eye through the BAB and BRB (Fig. 2), therefore, it is difficult to assess the contribution of each route separately. Some insight might be obtained from intracameral elimination data. Intracameral drugs are eliminated from the eye mainly via aqueous humor outflow and the veins of the iris and ciliary body (Urtti, 2006). Aqueous humor outflow is relatively constant and therefore the contribution of the iris and ciliary body veins can easily be calculated when the intracameral total clearance has been determined. Clearance via the blood flow is essentially zero for large molecules (like inulin) and approximately 10–20 μl/min for small lipophilic compounds (Urtti, 2006; Urtti et al., 1990). This means that the BAB, like the BRB, is a tight barrier for proteins and other macromolecules (2 nm and larger), but allows permeation of small molecules. The total blood flow in the iris and ciliary body of rabbit is about 144 μl/min (del Amo and Urtti, 2015; Nilsson and Alm, 2012). This indicates that the small molecules have extraction ratios of approximately 0.07–0.14 in the rabbit iris and ciliary body.

2.4. Active transport in blood-ocular barrier

The physical structure of the blood-ocular barrier defines the level of passive drug permeation in the barrier. Obviously, the permeability also depends on the chemical drug properties as discussed above, however active transporters may affect permeation of drugs that are substrates of transporter proteins. Transporters have been reviewed thoroughly (Hosoya et al., 2011; Mannermaa et al., 2006) and, therefore, we do not review this aspect here in detail. It is important to note, however, that transporter proteins have not been systematically quantitated in the eye at the protein level. The expression levels of transporters vary between cell types (different *in vitro* models) and also contradictory results have been published (e.g. P-gp expression in the ARPE19 cell line) (for more information, see section 9.3). Little is known about the localization of the transporter proteins (apical or basolateral surface).

Physicochemical molecular descriptors (H-bonding and $LogD_{7.4}$) show good correlation with intravitreal half-life and clearance of small molecular drugs without outliers (del Amo et al., 2015; Kidron et al., 2012). This indicates that the active transport is not an important factor in intravitreal clearance among those compounds in the data sets (del Amo et al., 2015; Kidron et al., 2012). On the other hand, *in vivo* fluorophotometry estimates of blood-ocular barrier permeability suggest an important role of active transport. The inward permeability of fluorescein is 10^{-7} - 10^{-6} cm/s, while outward permeability is about 10^{-5} cm/s in monkeys and humans (Blair and Rusin, 1986; Cunha-Vaz and Maurice, 1967; Oguro et al., 1985) indicating directionality and active transport in the blood-ocular barrier. Other examples, investigated in rats, include pravastatin that was eliminated from the vitreous via active transport (OATP1A4 and OAT3) after intravitreal injection (Fujii et al., 2015), propranolol that was transported via influx transporters across BRB, and inhibitors (pyrilamine, TEA, verapamil) that reduced the retinal uptake of propranolol in the *in vivo* study (Kubo et al., 2013). Active influx and efflux transport phenomena are complex and

sometimes it is difficult to make firm conclusions when multiple processes are active simultaneously. For example, SLC and ABC transporters share many common substrates and, therefore, functional consequences of the interactions are unclear (Chapy et al., 2016).

Overall, the pharmacological significance of active transport in the posterior eye segment is still unclear. More information about the expression and localization of the transporters in the blood-ocular barrier components is needed. Furthermore, it is important to note that the importance of transporter activity is relative and dependent on the rate of passive drug diffusion (Sugano et al., 2010). For example, if the passive diffusion is much faster than the maximal active transport (V_{max}), it is obvious that the transporters do not have a significant role. Extensive passive diffusion tends to decrease the relative impact of active transport. Unlike passive diffusion, active transport is saturable and its relative efficacy and importance are pronounced at low drug concentrations, but decreased at high drug concentrations. Drug concentrations at the blood-ocular barriers after intravitreal administration are clearly higher than after systemic or topical drug delivery.

2.5. Summary on barriers

Blood-ocular barriers do not allow permeation of proteins and other large molecules, but they do allow permeation of small molecules. For this reason, the intravitreal clearance of small molecules is much faster than the clearance of biologics and it is also easier to deliver small drugs inwards into the eye. This aspect will be discussed more quantitatively in the following chapters. It is important to note that the role of barriers depends on the permeating species (small molecule, biological, drug delivery system).

3. Intravitreal drug administration

There are numerous acquired and inherited posterior segment diseases with existing and emerging drug targets. Some recent reviews discuss the various drug targets in the retina and chroroid (Campochiaro, 2015; Doonan et al., 2012; Grassmann et al., 2015; Guadagni et al., 2015). Some of these targets are located in the ganglion cells, photoreceptors, retinal pigment epithelial cells, and chroroidal endothelial cells.

3.1. Drug distribution and interactions with the vitreous

After intravitreal injection, drugs distribute within the vitreal cavity and they enter the extracellular and intracellular drug targets in the posterior eye segment (Fig. 1). The vitreous acts as a barrier in drug delivery, but its role is strongly dependent on the drug molecules and formulations: the barrier function ranges from insignificant to important.

3.1.1. Vitreous humor

The vitreous humor consists of hyaluronan, an anionic hydrophilic polymer with a high molecular weight (MW 2–4 million Da), and collagen fibres that provide strength and resistance to tractional forces. Hyaluronan attracts counterions and water, but yet it bears an overall net negative charge (Le Goff and Bishop, 2008). Hyaluronan also provides swelling pressure that pushes apart the fibrillar proteins. However, hyaluronan is not uniformly distributed within the vitreous; the highest concentrations are in the posterior vitreous cortex and the central vitreous is more liquid than the cortical vitreous (Le Goff and Bishop, 2008) (Fig. 3). The kinematic viscosity of the vitreous humor has been determined to be 300–2000 cSt (Yang et al., 2014) and hydraulic resistivity is $1.725 \times 10^{13}\ M^{-2}$ (Missel, 2012). It should be noted that, as a person ages, the rheological properties of the vitreous change and tend towards a more liquid form (Laude et al., 2010). Rabbit vitreous is often considered to be more viscous than the vitreous in humans, but this issue is not clear in the scientific literature. It is important to note that, like in humans, the vitreous viscosity decreases with age in rabbits (Los, 2008; Munger et al., 1989). It is known that the hyaluronic acid concentration in rabbit and human vitreous are 20–40 and 100–400 μg/ml, respectively (Balazs, 1983; Boruchoff and Woodin, 1956). Collagen concentrations in rabbit and human do not show clear differences either. Proper rheological determinations are needed to show the real vitreous viscosity parameters in the rabbit, man and other species.

Compared to the plasma, the average protein concentration in the healthy human vitreous is low. The vitreous contains both structural proteins (collagen II, IX and V/XI, fibrillin and cartilage oligomeric matrix protein) (Bishop, 1996; Nguyen and Fife, 1986) and non-structural proteins (albumin, immunoglobulin, complement proteins, globulins, transferrin) (Chen and Chen, 1981; Laicine and Haddad, 1994; Ulrich et al., 2008). In vitreoretinal disease, protein concentrations may rise; it was reported in a recent study that the vitreous protein concentration in a normal vitreous was 4.7 ± 1.2 mg/ml, while in proliferative diabetic retinopathy it was 5.1 ± 1.8 mg/ml (Loukovaara et al., 2015). From a pharmacokinetic viewpoint this increase is insignificant.

The human vitreous has been analysed using proteomic methods, such as 2D-PAGE, ESI-MS, MALDI-MS and LC-MS/MS. These studies have compared the healthy and diseased eye (proliferative diabetic retinopathy, proliferative vitreo-retinopathy, diabetic retinopathy, diabetic macular oedema) (Gao et al., 2008; Kim et al., 2007; Koyama et al., 2003; Nakanishi et al., 2002; Ouchi et al., 2005; Robinson et al., 2006; Shitama et al., 2008; Wang et al., 2012). The protein classes in the healthy eye include proteases, protease inhibitors, complement and coagulation cascade hormones, growth factors, cytokines, receptors, apoptosis regulation, and proteins related to signalling activity and visual perception (Murthy et al., 2014). Like other biological fluids, human vitreous samples also showed heterogeneity between individual test samples (Aretz et al., 2013). In the diseased eye (proliferative diabetic retinopathy) some unique proteins (enolase, catalase) were identified (Lee et al., 2004; Yamane, 2003). This suggest that these proteins are specifically expressed in the diseased eye.

3.1.2. Diffusion in the vitreous

Diffusion of molecules and nanoparticles has been measured in the vitreous using particle tracking methods and confocal microscopy. The mesh size in the bovine vitreous was estimated to be in the range of 500 nm (Peeters et al., 2005; Xu et al., 2013) and even in a non-liquefied state the vitreous is not a tight barrier for diffusion (Turunen, 2016). In comparison with the mesh size in the tight epithelia and endothelia (about 2 nm), the vitreous is quite open allowing relatively unrestricted molecular mobility. The vitreal hindrance of diffusion can be estimated by comparing diffusion in the vitreous to diffusion in water. Upon liquefaction, the viscosity of the vitreous is approaching that of water in some regions, but detailed rheological data about these changes is still missing. Despite this, we can assume that the diffusion coefficient in water is the maximal diffusivity that could be achieved upon complete liquefaction. Xu et al. (2013) measured diffusivity of fluorescently labelled nanoparticles in the bovine vitreous and compared the diffusion coefficient values to the diffusivity in water (calculated using Stokes-Einstein equation). The conclusion was that the diffusion coefficient of neutral PEG-coated polystyrene nanoparticles (up to the size of about 0.5 μm) is only about two times smaller than in water, whereas the diffusivity of anionic nanoparticles showed similar changes (about two times higher

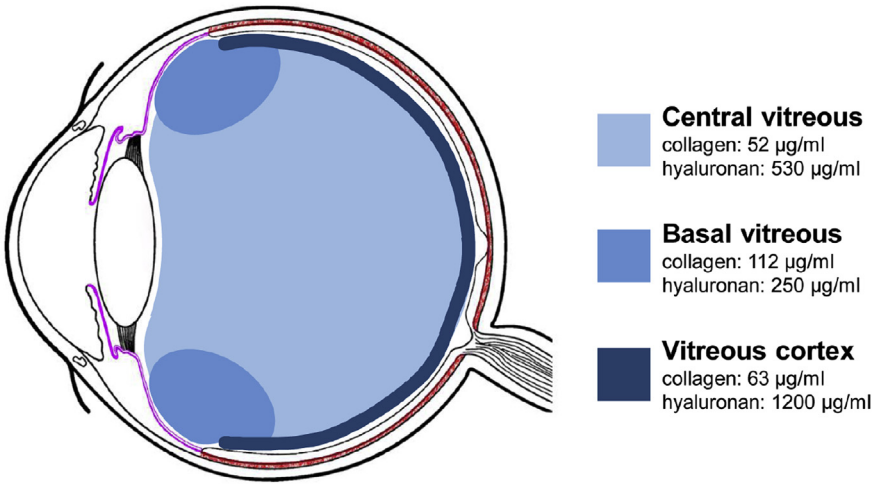

Fig. 3. Zones of hyaluronic acid concentrations in the vitreous (Bos et al., 2001).

than in water) when the particle size was 200 nm or less (Xu et al., 2013). As the diffusion hindrance factor of the vitreous humor is very small even for nanoparticles, it is obvious that the diffusion of anionic and neutral molecules is not restricted in the vitreous. For example, biologics are typically less than 10 nm in diameter (bevacizumab 6.5 nm; ranibizumab 4.1 nm) (Li et al., 2011), which is very small compared to the mesh size in the bovine vitreous (≈500 nm). Thus, their movement is not restricted in the vitreous. Peeters et al. (2005) also showed that the diffusivity of FITC-dextrans is not significantly restricted in the vitreous humor. Furthermore, it is unlikely that the vitreal liquefaction in elderly patients would have any significant effects when the mesh size, even before liquefaction, does not restrict diffusion.

In Fig. 4 we have collated diffusion coefficients from the literature (Xu et al., 2013) and from unpublished experiments with similar method (Turunen, 2016) (see Figure legend). The experimental diffusion coefficients in the vitreous were compared to the calculated diffusion coefficients in water (Stokes-Einstein equation). Moreover, diffusion coefficients of small MW compounds (Gisladottir et al., 2009; Tojo et al., 1999) and macromolecules (Dias and Mitra, 2000) were included. Their radii were obtained from the literature (Ambati et al., 2000; Prausnitz and Noonan, 1998; Shatz et al., 2016). Overall, the vitreous humor is a relatively loose structure both in the normal and liquefied state (after hyaluronidase treatment): the diffusivities were not significantly different from water. Even though the vitreous has hardly any effect on the diffusion of molecules or anionic nanoparticles, it may significantly hinder the diffusion of particles with a size range above 500 nm (Xu et al., 2013, Fig. 4). Importantly, the diffusion of positively charged nanoparticles and polymers is dramatically restricted in the vitreous (reduction of diffusion coefficient by factor of 10^3), both in the liquefied and normal state (Fig. 4). This is understandable as the vitreous is a negatively charged polymer network capable of interacting with the cationic particles based on electrostatics. Unfortunately, the impact of cationic charge density of hydrophobic regions on the mobility of macromolecules or particles in the vitreous is unclear. Surprisingly, the available data of experimental diffusion in vitreous of the small molecule ganciclovir (Tojo et al., 1999) and dexamethasone (Gisladottir et al., 2009) and the bigger molecule FITC-dextran 4 kDa (Dias and Mitra, 2000) seemed to be higher than their theoretical diffusivity in water (for more detailed information see Supplementary Table 1). Overall, the conclusions about the vitreal barrier are quite obvious: 1) for dissolved molecules and small nanoparticles, the vitreous does not represent a significant restriction to drug diffusion as compared to water; 2) increased particle size decreases the mobility in the vitreous; 3) liquefaction causes a modest increase in particle diffusion in the vitreous; 4) multiple cationic charges in the particles cause major restriction to particle movement in the vitreous.

Microspheres, suspension particles, and implants are much bigger than nanoparticles and they do not diffuse through the vitreous. PLGA microparticles are not expected to move in the vitreous as they have the tendency to aggregate after injection (Barcia et al., 2009; Giordano et al., 1995; Herrero-Vanrell et al., 2014; Herrero-Vanrell and Refojo, 2001). Microsphere movement may change in some cases, for example in aphakic eyes and after liquefaction of the vitreous. The influence of the lens on the movement of microspheres has been described in rabbits (Algvere and Bill, 1979). Intravitreously injected non-degradable plastic microparticles (7–10 µm size) were retained in the vitreous cavity in phakic eyes, while some particles moved to the anterior chamber in aphakic eyes (Algvere and Bill, 1979). Intracameral injections of non-degradable polystyrene microbeads (about 10 µm) to rats have been used in purpose to elevate the intraocular pressure in animal experiments (Smedowski et al., 2014). However, the impact of particle size and surface characteristics on pharmaceutical particles on the outflow facility is not known.

3.1.3. Convection in the vitreous

In addition to diffusion, also convection may play a role in intravitreal drug distribution. The velocity of convective fluid flow from the ciliary body across the retina has been estimated to be about 2×10^5 cm/min in rabbit eyes (Araie and Maurice, 1991). Velocity of posterior fluid movement is negligible compared to the aqueous humor flow to the anterior chamber. Distribution contours in the rabbit eyes after intravitreal injection of FITC-dextran (66 kDa) indicated that convective flow towards the retina had only a minor contribution in its ocular distribution (Araie and Maurice, 1991). Later Missel (2012) investigated the role of convective flow in the intravitreal molecular distribution using finite element modeling. Based on current experimental evidence the convective flow towards retina is not a major contributing factor in the distribution of dissolved intravitreal drugs. The role of convective flow in the distribution of drug formulations has not been investigated.

3.1.4. Drug interactions with the vitreous

Compared to human plasma the number of proteins in the

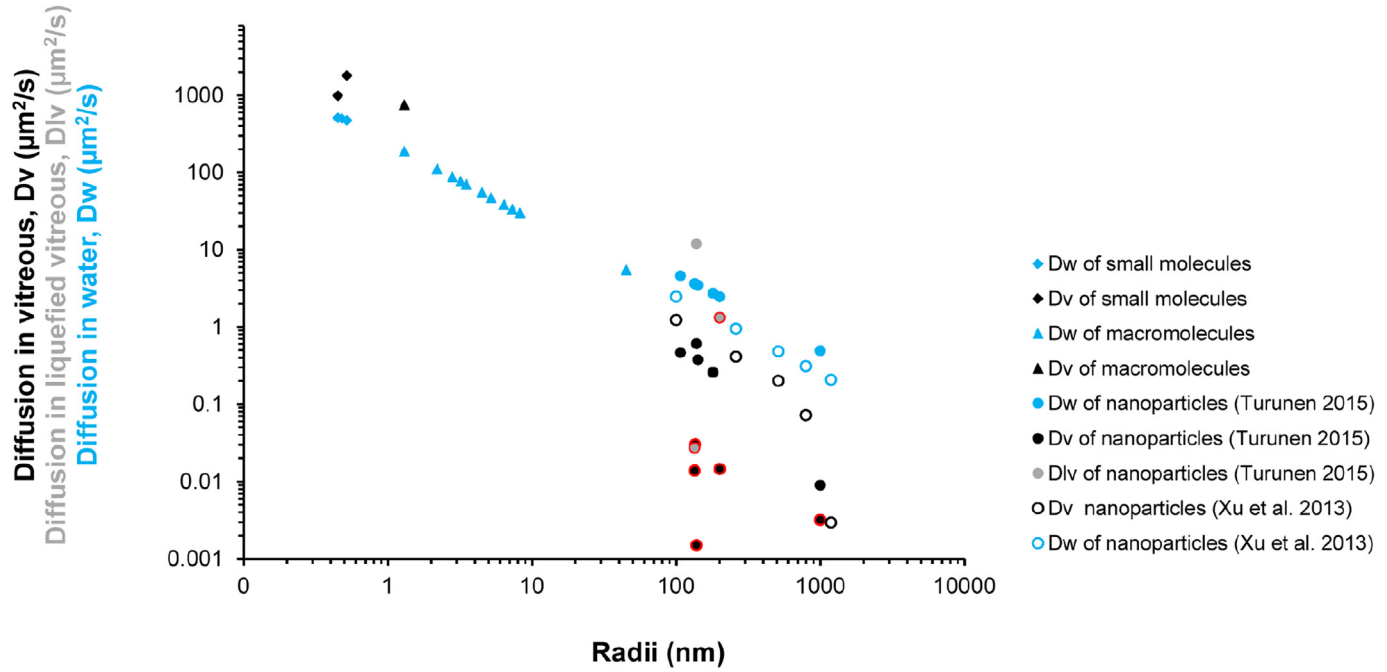

Fig. 4. Diffusion coefficients of molecules and particles in the vitreous. The nanoparticle data have been extracted from Xu et al. (2013) and Turunen (2016). Xu et al. (2013) used polystyrene and PLGA nanoparticles, whereas Turunen (2016) carried out the experiments using liposomes. In both studies diffusion coefficients were determined using particle tracking with confocal microscope in intact posterior segment of the bovine and porcine eye, respectively. Liquefaction of the vitreous was done using hyaluronidase treatment (Turunen, 2016). The red symbols correspond to cationic nanoparticles. For small compounds and macromolecules, the diffusion coefficients in water were calculated using the radii obtained from literature for fluorescein, dexamethasone, ganciclovir, hyaluronic acid 500 kDa, pegaptanib, aflibercept, bevacizumab, albumin, ranibizumab, FITC-dextran 150 kDa, FITC-dextran 80 kDa, FITC-dextran 40 kDa, FITC-dextran 20 kDa, FITC-dextran 10 kDa and FITC-dextran 4 kDa. The experimental diffusion coefficient in rabbit vitreous was obtained for dexamethasone and FITC-dextran 4 kDa (Dias and Mitra, 2000; Tojo et al., 1999) and in porcine vitreous for ganciclovir (Gisladottir et al., 2009).

human vitreous is smaller (about 1300 compared to 3000 in plasma) and the protein concentration is less (<5 mg/ml, typically 0.5–1.5 mg/ml) than in the plasma (60–80 mg/ml) (Angi et al., 2012). Only sparse data is available about the protein binding of drugs in the vitreous, even though this factor might affect the pharmacokinetics of small molecule drugs in the eye. Even though the protein levels in vitreous are less than in the plasma, yet protein binding is possible. Protein binding and other binding events in the vitreous are expected to slow down drug elimination from the vitreous, because the proteins have much slower elimination from the vitreous than the small molecules (this may be analogous situation with the effect of plasma protein binding on renal clearance of drugs). Two reports have studied protein binding of antibiotics (fosfomycin, levofloxacin, vancomycin) in the human vitreous. The binding was negligible unbound fraction being 90–99% (Petternel et al., 2004; Schauersberger and Jager, 2002). The data about this issue is so sparse that the outcome of that study should not be generalized.

Protein stability involves physical phenomena and conformation changes that are not relevant for small molecules (Manning et al., 2010). Intravitreal injection is challenging because the protein drug should remain stable during manufacturing, sterilization, shelf-life and *in vivo* within the vitreous. In the case of controlled release formulations, the protein drug must remain stable within the formulation at vitreous temperature for weeks, even months. After its release from the delivery system, the protein drug will be exposed to the vitreous components without stabilizing excipients, leaving the protein subject to possible destabilization. Aggregation and conformational changes may decrease the efficacy of the protein drug and may also have immunological consequences. Patel et al. (2015) investigated the stability of two antibodies and one antibody fragment in three porcine vitreous models. It seems that the pH rise was the major factor that lead to the protein aggregation. Aggregation was avoided in a semi-dynamic model where pH drift has been addressed. Proteins are also susceptible to proteolytic enzymes. The levels of proteolytic enzymes (e.g. serine proteases) are elevated in the aging human vitreous (Vaughan-Thomas et al., 2000), but it is not yet clear if this has impact on protein drugs.

3.1.5. Distribution to the surrounding ocular tissues

Intravitreal drugs distribute to the surrounding tissues depending on their membrane permeability and binding affinity to lipids, proteins, melanin and other cell components. Particularly, drug binding to melanin may increase drug concentration in the cells substantially (Potts, 1964). The cellular drug delivery issues are discussed more in chapter 9.

The volume of distribution is a pharmacokinetic parameter that describes the extent of drug distribution and binding after its administration. After intravitreal injection, the eye behaves like an isolated tissue, because the blood circulation acts like a sink where the drug is diluted so much that the drug concentrations in the plasma do not have influence on ocular drug concentration profiles. Therefore, a separate volume of distribution can be determined for the eye. Del Amo et al. (2015) collected all available intravitreal injection data from rabbit and human experiments and determined the intravitreal volumes of drug distribution. Interestingly, the intravitreal volumes of drug distribution were nearly constant (80% in the range 1.2–2.2 ml in the rabbits) and the volumes were not dependent on drug properties (e.g. molecular weight and lipophilicity) (see Section 3.2.3). The volume of drug distribution in rabbit eyes is close to the anatomical volume of the vitreous humor, indicating that the surrounding tissues (retina, lens, ciliary body, iris) have only a minor impact on the volume of distribution. This is due to two factors: 1) the anatomical size of the surrounding tissues

is much less than the volume of the vitreous humor. The equation for volume distribution is as follows: $V_{ss} = V_v + K_{p1} V_1 + K_{p2} V_2 \ldots$, where V_v is the volume of vitreous, K_{p1}, K_{p2} and so on are the partition coefficients between the tissue and vitreous, and V_1, V_2 etc. describe the anatomical volumes of the surrounding tissues. In the eye $V_v \gg V_1, V_2 \ldots$; 2) Most surrounding tissues (except the lens) are not only drug distribution sites, but they also act as routes for drug elimination towards the systemic blood circulation. Therefore, back diffusion from these sites to the vitreous is limited and it does not affect volume of distribution significantly.

3.2. Drug elimination from the vitreous

In principle, drug elimination from the vitreous could take place via biotransformation or physical elimination to the blood circulation. Mostly, drugs are eliminated using the second mechanism and from the blood circulation, are then eliminated from the body by metabolic clearance (mostly in the liver) and renal excretion to the urine.

3.2.1. Metabolic drug elimination

Drug metabolism in the vitreous has not been explored in a systematic manner. There is, however, some evidence for the presence of minor amounts of metabolic enzymes in the vitreous humor. For example, esterase and peptidase activity exists in the vitreous humor (Dias et al., 2002). This has been used in the case of ester pro-drugs of acyclovir and ganciclovir (Duvvuri et al., 2004), even though the esterase activity in many other ocular tissues (e.g. iris, ciliary body) and plasma is much higher (Järvinen et al., 1995). Dipeptide prodrugs of ganciclovir are also converted to the parent compound in the vitreous humor (Majumdar et al., 2006). However, there are no reports showing the presence of any phase I or phase II metabolic enzymes in the vitreous humor. This may explain the low importance of metabolic drug clearance in the vitreous.

There are other enzymes in the vitreous that are relevant for the action of some drug delivery systems: matrix metalloproteinases (MMP's), Trypsin −1 and Trypsin-2 are present in the vitreous humor and are capable of digesting collagen II (van Deemter et al., 2013). Alcohol dehydrogenase and various other enzymes are involved in the production of hyaluronic acid and lipid metabolism in the vitreous (Berman, 1991). In the ageing human vitreous the levels of certain matrix metalloproteinases (MMP's), cysteine proteases and serine proteases were found to be elevated (Vaughan-Thomas et al., 2000).

3.2.2. Drug elimination through blood-ocular barriers

After intravitreal injection, drugs are eliminated from the eye either via the anterior route or posterior route (Fig. 5) (Maurice and Mishima, 1984). The anterior route is available for all drugs and it is based on drug diffusion through the vitreous humor towards the posterior chamber where it enters the aqueous humor. Thereafter, the drug will be subject to elimination in the outflow of aqueous humor (arrow 1 in Fig. 5). The posterior route is available only for the compounds that are capable of crossing the endothelia and epithelia of blood-ocular barriers (see section 2). These barriers are selective, allowing passage of small molecules, while restricting the permeation of large molecules (appr. 2 nm and bigger). Posterior routes involve drug elimination through the blood-aqueous barrier (vascular endothelia and epithelia in the ciliary body and iris) (arrows 2 and 3 in Fig. 5B), and blood-retinal barrier (retinal capillaries and retinal pigment epithelium) (arrow 4 in Fig. 5B). Therefore, small molecules with lipophilic properties are cleared from the vitreous faster than large molecules. The half-lives of small molecules are typically in the range of 1–10 h, while the half-lives of proteins and other large molecules are several days (del Amo et al., 2015; Kidron et al., 2012; Maurice and Mishima, 1984).

Recently thorough analysis of the drug elimination from the vitreous in rabbits and humans were carried out (del Amo et al., 2015; del Amo and Urtti, 2015). The published intravitreal injection data were subjected to curve fitting analyses to determine the clearance and volume of distribution. Herein, three new compounds were added to the previous data set of 52 intravitreal drugs in rabbit eye (del Amo et al., 2015): melphalan (MW = 305.2 Da, $V_{ss,ivt}$ = 1.62 ml, CL_{ivt} = 1.033 ml/h, $t_{1/2,\ ivt}$ = 1.1 h); daptomycin (MW = 1620.67 Da, $V_{ss,\ ivt}$ = 1.47 ml, CL_{ivt} = 0.041 ml/h, $t_{1/2,\ ivt}$ = 24.6 h) and ziv-aflibercept (MW = 97,000 Da, $V_{ss,ivt}$ = 4.04 ml, CL_{ivt} = 0.028 ml/h, $t_{1/2,ivt}$ = 100 h) (pharmacokinetic data was extracted from Buitrago et al. (2016), Ozcimen et al. (2015) and Park et al. (2015) respectively). The results are shown in Fig. 6 (more detailed data are found in the Supplementary Material Table 2). It is

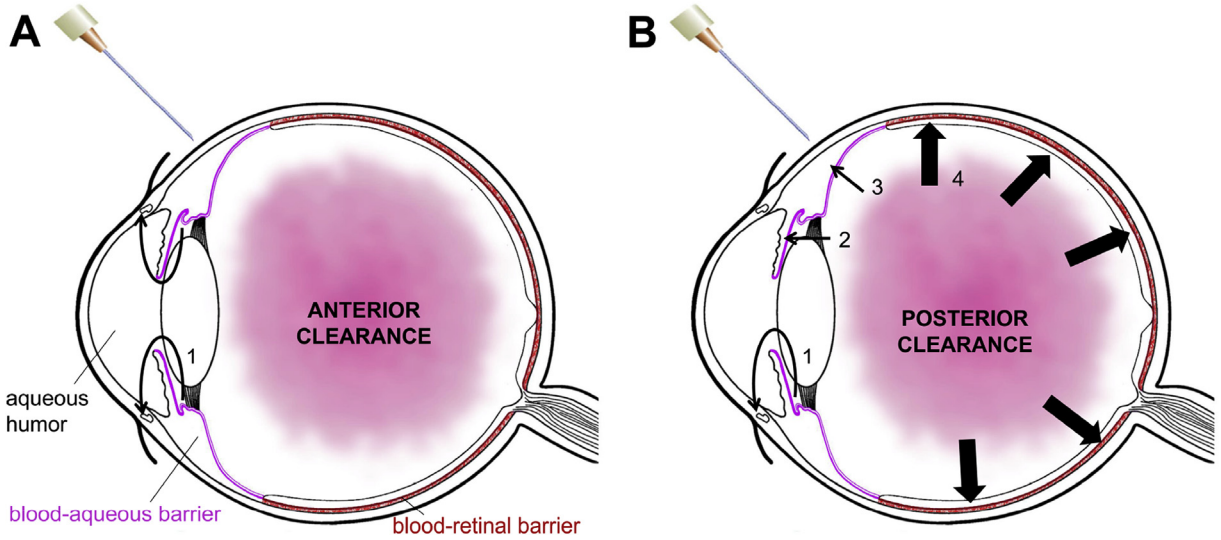

Fig. 5. Elimination routes of drugs from the vitreal cavity. Anterior clearance route means diffusion in the vitreous to the posterior chamber and, thereafter, flow in the aqueous humor via outflow channels in the trabecular meshwork (A), while posterior clearance takes place when the drug is eliminated through blood-retinal and blood-aqueous barriers (B).

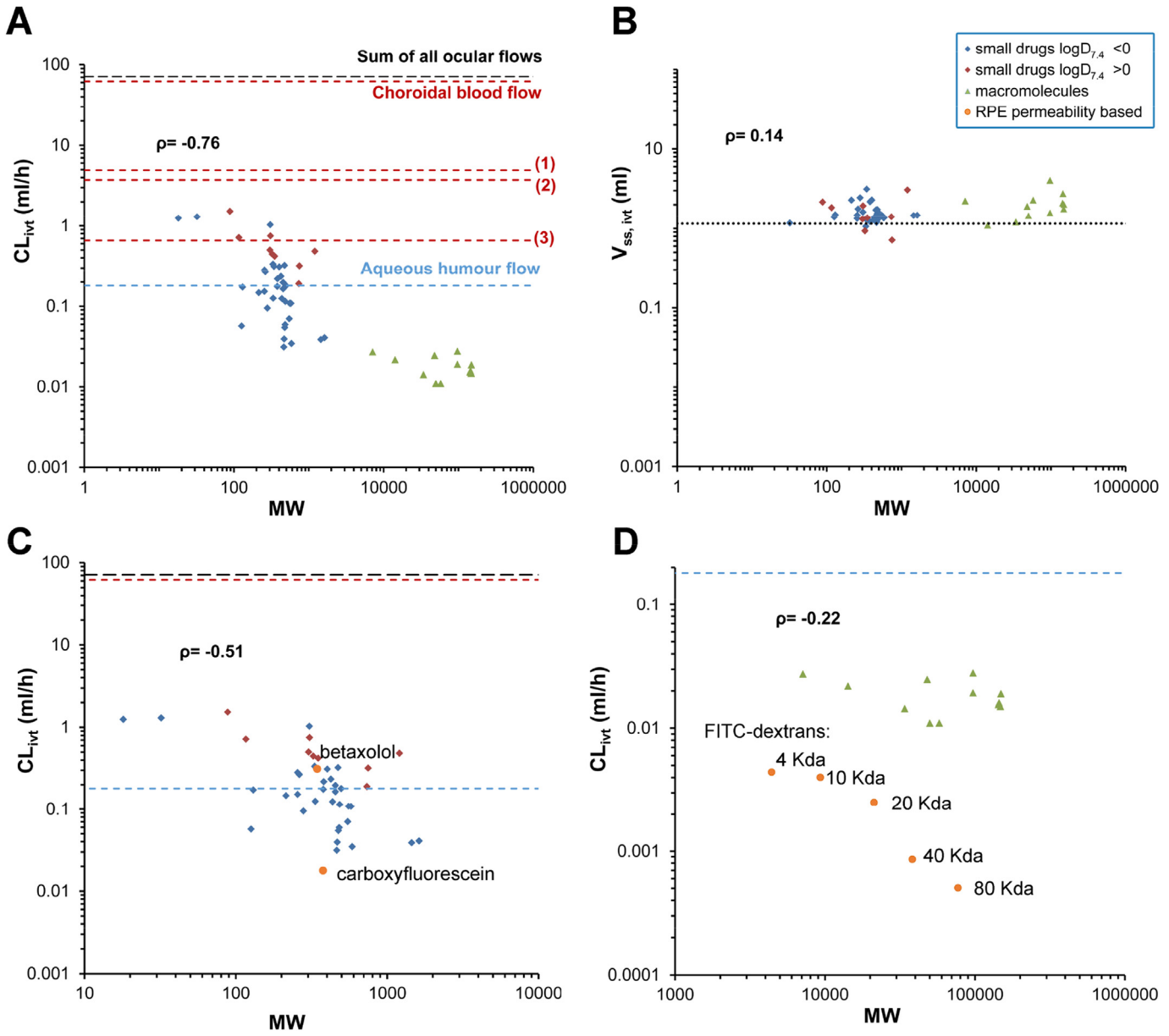

Fig. 6. Pharmacokinetics of intravitreal drugs in the rabbit eyes. The data presents all published literature till 2016 that fulfilled the quality criteria (del Amo et al., 2015) with a final set of 55 compounds. A) Clearance from the vitreous for small lipophilic ($LogD_{7.4} > 0$) (red symbols), small hydrophilic ($LogD_{7.4} < 0$) (blue symbols), and macromolecules (green symbols). For the full data, see Supplementary Material Table 2 and del Amo et al. (2015). Flow rates in the choroid and aqueous humor are presented for comparison. Also, ciliary body (1), iridial (2) and retinal (3) blood flows are presented. B) Volume of distribution of drugs in the rabbit vitreous. Symbols are the same as in 6A. The dotted line is average anatomical volume of the rabbit vitreous. C) RPE contribution to the vitreal clearance was calculated for betaxolol and carboxyfluorescein (orange symbols) based in their permeability in the RPE (Pitkänen et al., 2005) and surface area of the rabbit RPE. The RPE mediated clearance is in the same range with the expected total *in vivo* clearance from the vitreous indicating a major role of the RPE in the elimination of these compounds. D) RPE contribution to the vitreal clearance was calculated in the same way for FITC-dextrans (orange symbols). The RPE mediated protein clearance is much smaller than the expected total *in vivo* clearance from the vitreous (green symbols). This indicates that the RPE is a major barrier for macromolecule elimination from the vitreous, and only 3–20% of the injected dose is eliminated through the RPE.

obvious that the clearance values of large molecules are clearly smaller than the clearance of small molecules or the rate of aqueous humor outflow (Fig. 6A).

For small molecular weight compounds, the clearance values are higher than for proteins and the clearance values of small molecules show about 50-fold range (Fig. 6A). The highest clearance values are much higher than the aqueous humor outflow, while the smallest values are far below the rate of aqueous humor turnover (Fig. 6A). This indicates that the compounds with high clearance values are eliminated through blood-ocular barriers and the permeability in these barriers is the most important determinant of the clearance. Clearance values of small molecules were correlated with molecular descriptors using the quantitative structure property relationship (QSPR) approach. The model demonstrated that intravitreal clearance (CL_{ivt}) can be predicted with a simple equation based on hydrogen bonding (HD) and $LogD_{7.4}$ values: $\text{Log } CL_{ivt} = -0.25269 - 0.53747\ (\text{Log HD}) + 0.05189\ (\text{Log } D_{7.4})$ (del Amo et al., 2015). These molecular descriptors ($LogD_{7.4}$, HD) are relevant for permeability in the lipid membranes, such as blood-ocular barriers, supporting the notion that the clearance depends on the membrane permeability. Small molecular diffusion is expected to be nearly constant in the vitreous, but the clearance values show

large differences. Therefore, diffusion in the vitreous humor is not an important parameter for the clearance of small molecular drugs. Rather, the permeability in the blood-ocular barriers is the rate-limiting step.

3.2.3. Elimination via anterior route

For anterior elimination, the drug must diffuse in the vitreous and gain access to the aqueous humor in the posterior chamber. Accordingly, the differences in the diffusivity of biologicals in the vitreous determine the anterior clearance that is relatively constant (maximally about 3-fold range over MW range of 7100–177,000 Da) (Fig. 6A, green triangles). This is in line with the relatively unrestricted diffusion in the vitreous and modest differences that are expected from Stokes-Einstein equation for molecular diffusion. Niwa et al. (2015) studied the elimination and efficacy of the anti-VEGF proteins ranibizumab and aflibercept in normal and vitrectomized monkey eyes. The area under the concentration–time curve (AUC) values of intravitreal ranibizumab and aflibercept changed slightly after vitrectomy: ranibizumab (normal: 171,000 ± 65,200 day x ng/ml, vitrectomized: 154,000 ± 42,400 day x ng/ml) and aflibercept (normal; 174,000 ± 35,200 day x ng/ml, vitrectomized 124,000 ± 64,300 day x ng/ml). These results are in line with the modest effects of vitreal liquefaction on the diffusivity (Fig. 4) and narrow (3-fold) range of clearance values for anteriorly eliminated biologics (Fig. 6A). Recently, it was shown that intravitreal clearance of antibodies correlates well with the hydrodynamic molecular radii (Shatz et al., 2016). This was explained based on the relationship between the diffusion coefficient in the vitreous and hydrodynamic radii of the compounds. These conclusions also indicate that investigations on the macromolecule diffusion in the vitreous may be useful in predicting the clearance of large molecules from the vitreous. It seems that the vitreous has an impact on protein drug elimination, but the range of clearance values is narrow.

Intravitreal clearance should be equal with the rate of aqueous humor outflow if the vitreous and aqueous humors act as a single mixed tank, but they do not. The iris, ciliary body, lens and vitreous humor are limiting the access of the drug to the aqueous humor (Fig. 5). It is unlikely that the drugs would diffuse through these tissues, but they do diffuse through the vitreous humor to the aqueous humor. Interestingly, the clearance values of macromolecules are about 5–50 times higher than the expected clearance through the RPE (calculated as permeability x surface area ; based on RPE permeability values of FITC dextrans with similar MW range than the macromolecules) (Fig. 6D; del Amo and Urtti, 2015; Pitkänen et al., 2005). This indicates that the posterior elimination of proteins via BRB is negligible and they are eliminated via the anterior pathway (Fig. 5A). Some investigations have claimed that proteins, like bevacizumab, permeate through the BRB and are eliminated mostly via this route to the blood circulation (Gal-Or et al., 2016; Stewart, 2014). These claims are not on solid ground quantitatively, because bevacizumab permeation to retinal layers and the choroid has been shown only qualitatively with immunohistochemistry (Heiduschka et al., 2007). Bevacizumab entrance to the blood stream has been quantitated, but this drug also enters the blood stream via the anterior route, and this does not prove posterior clearance either. A study by Nomoto et al. (2009) has also been used as an argument for posterior elimination of bevacizumab, but this study is an outlier; three other rabbit and human studies indicate an anterior elimination (Bakri et al., 2007; Krohne et al., 2008; Meyer et al., 2011) (for detailed data analyses, see del Amo and Urtti (2015)). The anterior route of elimination has been observed for ranibizumab in human eyes (Krohne et al., 2012) and for ^{125}I-albumin and fluoresceinated-dextran (MW of 66 kDa) in rabbit eyes (Araie and Maurice, 1991; Johnson and Maurice, 1984; Maurice, 1976, 1959; Maurice and Mishima, 1984).

Pharmacological activity of anti-VEGF proteins (ranibizumab, bevacizumab, aflibercept) leads to reduced choroidal vessel leakiness and oedema. This does not mean that these proteins would permeate to a great extent through blood retina barrier. Firstly, the exact sites of action for VEGF binding activity of the drugs are not known. They may bind VEGF in the retina leading to sequestration of VEGF and reduced VEGF-receptor occupancy. Secondly, these compounds are active at low concentrations so that only a small fraction of the dose is needed for pharmacological activity in the choroidal vessels. Thirdly, blood retina barrier may be compromised in the disease and facilitating drug access to the choroid. This is discussed in more detail in the chapter 10.1.

3.2.4. Roles of blood-ocular barrier components in vitreal drug elimination

The flux of a drug across a biomembrane (J; μg/h) is defined by the equation J = C x CL = C x P x S, where C is the concentration gradient (e.g. vitreous vs. blood) (μg/ml), CL is the drug clearance from the donor compartment through the membrane (ml/h), P is the drug permeability in the membrane (cm/h) and S is the surface area of the membrane (cm^2). Importantly, the permeability depends on the partition coefficient of the drug between the vitreous and the blood-ocular barrier membrane, membrane thickness and the diffusion coefficient of the drug in the membrane. Therefore, the drugs with high partitioning and permeation in the blood-ocular barriers will have high intravitreal clearance. Using individual clearances for different parts of blood ocular barrier, it should be possible to dissect the roles of each barrier, but unfortunately the experimental data and methods do not provide adequate support for this approach.

In the blood-retinal barrier, the RPE is a major barrier and its role can be dissected because RPE permeability can be studied reliably *ex vivo* (Pitkänen et al., 2005). Based on the equation above, the clearance values of small molecules through the RPE are estimated to be 0.02–0.36 ml/h depending on the RPE permeability of the compounds ($S = 5.2\ cm^2$; $P = 1–19 \times 10^{-6}$ cm/s) (Mannermaa et al., 2010; Pitkänen et al., 2005). Blood circulation in the choroid is high (62 ml/h in rabbits, 96 ml/h in pigs), the blood vessels have high surface area (400–600 mm^2 in rabbits) (Bill et al., 1980), and leaky structure with openings of 70–80 nm. The openings are much bigger than the size of drug molecules, and choroidal tissue is an order of magnitude leakier than the RPE (Törnquist et al., 1990). Therefore, the choroid acts as a sink that efficiently removes drugs to the blood circulation. Drug concentrations in the extravascular choroidal tissue are expected to equilibrate rapidly with the plasma. Two conclusions can be obtained from the RPE mediated clearances (0.02–0.36 ml/h): 1) The process is membrane controlled, because the clearance values are low compared to the blood flow in the choroid (62 ml/min); 2) Comparison of total clearance values from the vitreous and the RPE mediated clearance values (Fig. 6A) indicates that the RPE permeation constitutes a major fraction of the vitreal clearance for the high clearance compounds (Fig. 6C), but the RPE is insignificant player in the vitreal clearance of macromolecules (Fig. 6D).

Permeability of retinal capillaries is difficult to measure and there are no reliable estimates. It is obvious from the anatomy that the surface area of the capillaries (20–25 mm^2) (Maurice and Street, 1957) is much smaller than that of the RPE (520 mm^2) in rabbits (Reichenbach et al., 1994) and also in humans. Retinal capillary endothelia have tight junctions, and therefore it is likely that the contribution of retinal capillaries to the vitreal drug clearance is much smaller than that of the RPE.

In the blood-aqueous barrier, the surface area of the non-pigmented ciliary epithelium in human eye is relatively large

(845 mm^2) (Weiss, 1897). The quantitative contributions of ciliary and retinal elimination in overall posterior route clearance are not known, but based on the large surface area of the non-pigmented epithelium (in the same range with human RPE, 1204 ± 184 mm^2) (Panda-Jonas et al., 1994), modest blood flow of ciliary body (4.91 ml/h in rabbit, 5.34 ml/h in monkey) and iris (3.72 ml/h in rabbit, 1.02 ml/h in monkey) (Alm and Bill, 1973; Nilsson and Alm, 2012) and large surface area of leaky blood vessels in the ciliary processes (670 mm^2 in rabbits) (Bill et al., 1980), this route may play a significant role in the vitreal drug clearance. However, more research is needed to quantitate the contribution of blood-aqueous barrier in vitreal drug clearance.

Leakiness of the blood-ocular barriers may be altered in the pathological conditions. This aspect depends on the disease state and drug properties. Often times the disease effects are considered to be prominent by definition. However, based on our literature analyses of the real pharmacokinetic data indicate that these effects are surprisingly small (for more information, see chapter 10.1.). There are two aspects to be considered herein. Firstly, in the case of highly permeable drugs, the clearance is already quite high and membrane leakiness may increase the clearance only modestly. Secondly, clearance of large molecules (like anti-VEGF compounds) takes place predominantly via anterior route (Fig. 6D). Therefore, even 10-fold increase in the RPE permeability is expected to increase protein clearance only modestly (about 1.5 fold; calculation based on the clearance data in del Amo and Urtti (2015)). Excellent correlation and only 40% difference was seen between the intravitreal clearance values of healthy rabbits and human patients (del Amo and Urtti, 2015). This difference can be explained based on the eye size.

3.2.5. Other mechanisms

Target mediated elimination kinetics imply that the drug binds to its extracellular target at such an extent that it has influence on the overall drug clearance. This has been shown with some proteins in the systemic circulation, including bevacizumab (Panoilia et al., 2015) and aflibercept (Stewart, 2012). For example, Stewart, (2012) points out that free aflibercept in the circulation has a half-life of 1–3 days, but the half-life is extended to 18 days when the drug is bound to its VEGF-target. Thus, binding to VEGF plays a role in aflibercept clearance also noted by Dixon et al. (2009). Because molecular weight affects drug clearance from the vitreous (Fig. 6A), it is possible that VEGF binding could reduce the clearance of aflibercept if a large fraction of the dose would be VEGF bound, but this has not been proven yet. Currently, there is no evidence for target-mediated elimination from the vitreous.

The neonatal Fc receptor (FcRn) protects immunoglobulin G (IgG) from catabolism, controls its transport between cell layers and extends its serum half-life by preventing lysosomal degradation. The Fc portion of IgG binds with high affinity to FcRn at an acidic pH (<6.5) but not at a physiological pH (7.4). In systemic pharmacokinetics FcRn is involved in recycling of monoclonal antibodies so that the half-life of the drug is prolonged in the systemic circulation. In principle, this kind of recycling might contribute to intraocular pharmacokinetics as FcRn is expressed in the blood-ocular barrier of several species (rat, mouse, pig, human) (Kim et al., 2009a; Powner et al., 2014; van Bilsen et al., 2011). Kim et al. (2009a) showed that FcRn is expressed in the blood-ocular barrier and that it plays a role in the elimination of intravitreally administered IgGs across the BRB. A recent study on porcine eyes suggests that the FcRn recycling function in the RPE could play a role in the pharmacokinetics of the posterior eye segment by maintaining the bevacizumab concentration in the retina (Dithmer et al., 2016). Also, Deissler et al. (2016) showed that there is an active FcRn mediated transcytosis of bevacizumab in the retinal endothelial cells. Even though it seems that FcRn is present and active, it does not seem to have a true quantitative pharmacokinetic impact in the vitreous like it has in plasma (Gadkar et al., 2015). Moreover, for aflibercept FcRn related mechanisms of transport have been shown (Kuo and Aveson, 2011; Zehetner et al., 2015), but their impact on intravitreal pharmacokinetics has not been proven.

3.3. Drug delivery to the retinal layers from the vitreous

The retina is a crucial tissue as it contains the light sensing cells and supporting cells that are needed for the vision. The light information is transferred from the retina to the brain via the optic nerve. The cellular structure of the retina is complex and drug distribution and delivery in the retina is not well understood (Fig. 7). The roles of the retinal pigment epithelium and retinal endothelia as barriers to drug delivery have been discussed earlier in this review. The inner limiting membrane, outer limiting membrane and Müller cells represent additional barriers for drug delivery from the vitreous to the retina.

3.3.1. The inner limiting membrane (ILM)

The inner limiting membrane (ILM) is located at the vitreal border of the retina, between the end feet of retinal Müller cells and the vitreous. The ILM also acts as the basement membrane for Müller cells. The main components of the ILM are collagen and glycosaminoglycans and it is a mechanical and electrostatic barrier with a net negative charge. The pore size of human ILM is suggested to be approximately 10 nm (Jackson et al., 2003).

It is clear that the hydrophilic ILM structure based on glycosaminoglycans and collagen cannot block the diffusion of small molecules (Jackson et al., 2003). The small molecular drugs diffuse relatively freely in the vitreous and enter the extracellular space in the retina easily. The RPE and retinal endothelia constitute barriers, especially for the hydrophilic compounds. Intracellular delivery of small molecules into the retinal cell types depends on the usual factors (passive diffusion and active transport). Unfortunately, there are only sparse data about the expression of membrane transporters in different cell types in the retina.

In the case of biologics, the ILM does not seem to limit retinal drug delivery when the molecular weights of the compounds are below 100 kDa (Jackson et al., 2003). These investigators determined the maximum molecular sizes that freely penetrate to the retina in pig, cattle, and rabbit to be 60 ± 11.5, 78.5 ± 20.5 and 86 ± 30 kDa, respectively. Other studies also indicate that there is a molecular size cut-off, but many biologics have relatively unrestricted access to the retina from the vitreous. For example, tissue plasminogen activator (70 kDa) and rhodamine labelled dextran (20 kDa) permeated from the vitreous into the sub-retinal space (Kamei et al., 1999). Likewise, heat shock protein (70 kDa) and tenecteplase (70 kDa) penetrated to various layers of the retina in rats and pigs (Yu et al., 2001). These conclusions are supported by the findings of Pitkänen et al. (2004), who used *ex vivo* bovine eyes in their studies. In these experiments, access of fluorescently labelled materials to the RPE was determined with flow cytometry in the presence and absence of the neural retina. The data indicated that the ILM posed an insignificant barrier for the diffusion of FITC-dextrans of 20 kDa and 500 kDa. However, the neural retina almost completely blocked the permeation of highly cationic poly-L-lysine (20 kDa) to the RPE, suggesting the important role of an electrostatic barrier. There are still important open questions related to the retinal penetration of biologicals: 1) What is the real actual cut-off size in terms of molecular radius? FITC-dextran is a polydisperse material, and therefore, it is difficult to make firm conclusions about the size cut-off; 2) Poly-L-lysine has a high cationic charge density, but what is the effect of cationic charges at a smaller charge

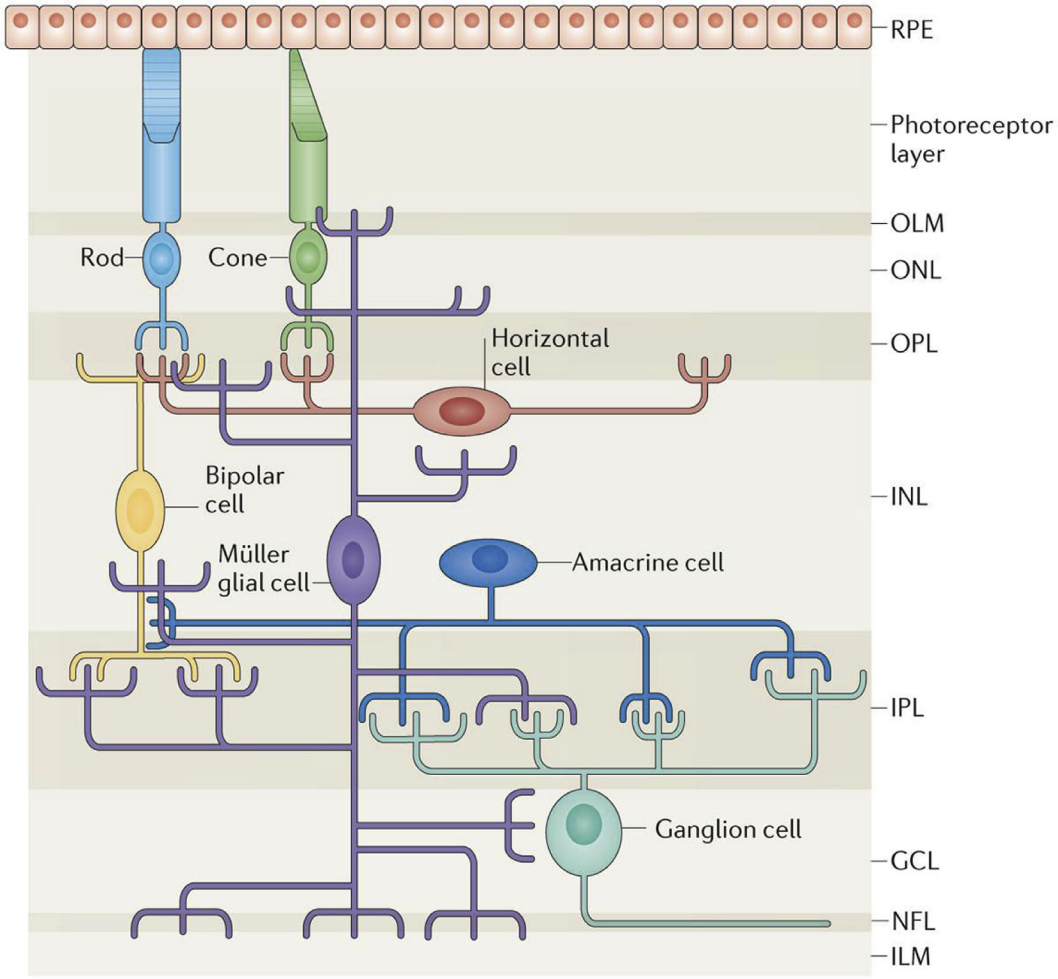

Fig. 7. Retinal layers: the outer limiting barrier (OLM), the outer nuclear layer (ONL), outer plexiform layer (OPL), the inner nuclear layer (INL), inner plexiform Layer (IPL), the ganglion cell Layer (GCL), nerve fibre layer (NFL) and the inner limiting membrane (ILM). Among them the layers that may restrict movement of some molecules and particles are the inner limiting membrane (ILM), Müller glial cells, outer limiting barrier (OLM), besides the already discussed RPE and the endothelial walls of the retinal capillaries between the retinal tissue and blood circulation (not shown in the figure). Figure is from Goldman (2014); with permission from Nature Publishing Company.

density? 3) The published data is mostly based on the images and histology. Integrity of the tissue becomes an issue. Moreover, these data are qualitative, not quantitative. What is the quantitative impact of different retinal layers on the distribution of biologicals?

Quantitation and more accurate cell specific data on the retinal delivery are needed, because many drugs have intracellular targets and they must be delivered to the target cells in the retina. The cellular delivery aspect is more critical for the drugs, especially biologicals that have intracellular target sites. The ILM and Müller cell barriers could be significant for nanocarriers (liposomes, nanoparticles) that are typically larger than the ILM pore size and many studies suggest that the ILM limits the access of nanoparticles to the retina (Gan et al., 2013; Kim et al., 2009b; Koo et al., 2012; Merodio et al., 2002). However, confocal images of Bourges et al. (2003) showed some permeation of poly(lactide) nanoparticles (sizes 140 and 300 nm) to the retina. The authors discussed that the permeation may have been facilitated by ILM rupture, inflammation or microglial cell activation.

Currently used anti-VEGF drugs (ranibizumab, bevacizumab, aflibercept, pegaptanib) have extracellular targets, i.e. they bind extracellular VEGF. Furthermore, it is not clear how deep these drugs must permeate to the retinal tissue in order to be active. It is also possible that they sequester VEGF from a distance. Based on the ILM pore size these drugs should be able to permeate to the retinal layers, but it is unlikely that they would permeate through the RPE. Julien et al. (2014) showed that ranibizumab penetrated to the monkey retina via inter-cellular clefts, whereas aflibercept was distributed to the neuronal and RPE cells. Heiduschka et al. (2007) showed that bevacizumab crossed the retina despite a transitory accumulation in ILM. A possible involvement of retinal glial cell activation in the permeation is speculated. However, these drugs are primarily eliminated from the eye via the anterior route (see section 3.2.3).

There are also variations in the condition of inner limiting membrane. Thickness of the inner limiting membrane varies being thicker at the macular region than elsewhere (Heegaard, 1997; Heegaard et al., 1986). Furthermore, its thickness is increased in diabetics (To et al., 2013). The impact of the regional and disease related changes on drug permeation have not been investigated. Peeling of the inner limiting membrane might increase material permeation from the vitreous to the retina, but there are no published experiments to prove this issue.

3.3.2. *Müller cells*

Müller cells are major glial cells in the retina and they contribute to the normal retinal structure and homeostasis. These cells span all

the retinal layers from the vitreal border to the distal end of the outer nuclear layer (Fig. 7). They also contribute to the formation of ILM and outer limiting membrane (OLM). Importantly, like the RPE cells, the Müller cells are phagocytosing cells and represent part of the defence mechanism of the eye.

The active receptor mediated endocytosis processes of Müller cells may play an important role in the retinal pharmacokinetics of nanoparticles. Dalkara et al. (2009) studied the retinal distribution of fluorescently labelled AAV-viruses of different serotypes after intravitreal injection in rats. They showed that only serotypes having binding sites on ILM and/or Müller cell end feet had access to retinal layers. Also, studies with hyaluronan- and albumin coated nanoparticles suggest that active uptake by Müller cells would provide particles a pathway through the retina (H. Kim et al., 2009b; Koo et al., 2012). Similarly Kim et al. (2015) postulated that retinal delivery of albumin nanoparticles with neurotrophic brimonidine may be mediated via TGF beta receptor mediated uptake into the Müller cells and retinal ganglion cells. The data is based on qualitative assays and no truly quantitative data exists in the literature.

3.3.3. Outer limiting membrane (OLM)

Outer limiting membrane (OLM) is formed by adherent and tight junctions between the apical processes of Müller cells and inner segments of the photoreceptor cells. The work by Omri et al. (2010) suggests that tight junctions may exist in OLM and it should be considered as part of a retinal barrier that can be disrupted in pathological conditions. The pore radius of OLM has been estimated to be 3.0–3.6 nm in rabbit retina. This means that, for example, albumin and gamma-globulin are too large to diffuse through an intact OLM (Bunt-Milam et al., 1985). FITC-dextrans were injected in sub-retinal space of rabbits and their diffusion to the vitreous was followed by fluorophotometry (Marmor et al., 1985). Carboxyfluorescein and FITC-dextran 10-S diffused quickly into the vitreous and disappeared in 8 and 30 h, respectively. However, diffusion of FITC-dextran 70-S and 150-S (both larger than albumin) was slow, and about 80% of the 150-S was still in the sub-retinal space after 3 days (Marmor et al., 1985). Table 2 shows information about the permeation of various macromolecules across the OLM in the rabbits suggesting that the molecular weight cut-off is about the size of an albumin molecule (Bunt-Milam et al., 1985).

However, the size limit and barrier role of OLM is not quite clear. There are other reports that do not support the barrier role of OLM. Several studies are showing permeation of macromolecules and even nanoparticles from the vitreous through OLM (Bourges et al., 2003; Julien et al., 2014) suggesting that it is much leakier structure than suggested by Bunt-Milam et al. (1985).

3.3.4. Summary

Several barriers in the neural retina may affect permeation of large molecules and particles to the retina. The roles of these barriers have not been quantitated and their roles are still not fully clear. These barriers are difficult to study in quantitative ways, because they cannot be isolated and placed to diffusion chambers and the permeants cannot be quantitated in the intact neural retinal layers.

3.4. Intravitreal drug delivery systems

3.4.1. Macroscopic drug delivery systems

Currently, intravitreal drug delivery is carried out using injections (solutions, suspensions) and implants (del Amo and Urtti, 2008). There are some controlled release intravitreal drug delivery systems in clinical use, for example non-degradable (polyvinyl/silicone laminate, Retisert) and degradable (polylactic acid - glycolic acid matrix; Ozurdex) implants. They provide long dosing intervals of 6 months for dexamethasone (Ozurdex) and 3 years for fluocinolone acetonide (Retisert, Iluvien). Intravitreal drug delivery systems are widely studied, because there is a need to prolong the dosing intervals in retinal drug treatment using implants, refillable injection ports and gels. There are several excellent reviews about these technologies for interested readers (Hamdi et al., 2015; Herrero-Vanrell et al., 2014; Yasin et al., 2014). Pharmacokinetics of the injected solutions was discussed earlier in this review (section 3.2). In the case of implants, the relevant kinetic issues are discussed in section 3.5 (i.e. design of the required release rate, biodegradation and sink condition aspects).

3.4.2. Particulate drug delivery systems

Particulate systems, such as microspheres and nanoparticles, have been used for intravitreal drug delivery, because they can be injected with a small needle. The particles have more complex intravitreal kinetics than the implants making their design more difficult. In contrast to the implants, the particles may move in the vitreous cavity. Therefore, particles may be useful for drug targeting in the posterior eye segment, but on the other hand, particle movement may be unpredictable and lead to toxicity. Particle movement depends on the material, and in some cases particles may be immobile in the vitreous.

Diffusion in the vitreous is a key parameter that affects the particle distribution in the vitreal cavity. As shown earlier, polystyrene and PLGA nanoparticles with negative or neutral charge and a size below 500 nm diffuse in the bovine vitreous with little hindrance (Xu et al., 2013), and the enzymatic cleavage of hyaluronic acid slightly changes their diffusivity in porcine vitreous (Turunen, 2016) (Fig. 4). Cationic liposomes (116–139 nm) showed about 10^3 times slower diffusion in the porcine vitreous than anionic liposomes (138–170 nm), and their diffusion is only slightly affected by the liquefaction of the vitreous (Fig. 4) (Turunen, 2016). Microspheres and suspension particles are not capable of diffusing through the normal vitreous and, therefore, liquefaction should make a major difference. The changes in the aging vitreous and its heterogeneous nature (Fig. 3) may change microparticle and suspension distribution potentially leading to interspecies differences and inter-subject variability (Awwad et al., 2015; Laude et al., 2010). Quantitative experimental data is, however, needed to prove this commonly presented clinical viewpoint.

Macromolecules are primarily eliminated from the vitreous via aqueous humor outflow, because they have insignificant permeation across blood-ocular barriers that limit the permeation to the entities smaller than 2–4 nm (section 2). Therefore, it is expected that the anterior, rather than the posterior route, would be relevant in the elimination of nanoparticles (typically 50–500 nm) and microparticles (typical diameter in the range of 1–50 μm) from the vitreous. However, biodegradable polymers may be degraded to soluble polymer fragments (e.g. polylactide-*co*-glycolide polymers) that may be eliminated also across the blood-ocular barriers. As illustrated in Fig. 8, particle diffusion, material degradation, and diffusion of degradation products are significant factors in the elimination process. In addition, there are some active cellular

Table 2
Permeation of various molecules across the outer limiting membrane in the rabbit retina (Bunt-Milam et al., 1985).

Compound	Source	Molecular weight (Da)	Traverses OLM
Myoglobin	Horse muscle	18,000	Yes
Peroxidase	Horseradish	44,000	Yes
Albumin	Bovine serum	67,000	No
Gamma globulin	Rabbit serum	160,000	No

mechanisms that may play a role in particle elimination from the vitreous (Fig. 8). The mechanisms are not well understood, because no mechanistic and quantitative studies have been done to explore the routes of particle elimination. Most published studies are qualitative, but a quantitative understanding of the elimination pathways would be important for the development of particulate drug delivery systems.

Many nanoparticle and microparticle formulations have been investigated as intravitreal injectables. Nanoparticles have been shown to retain in the vitreous or retina for days or weeks (Gan et al., 2013; Koo et al., 2012; Merodio et al., 2002), whereas the retention times of microspheres (e.g. PLGA, porous silicon) are 1–6 months depending on the formulation (Giordano et al., 1995; Moritera et al., 1991; Nieto et al., 2015; Shelke et al., 2011). For example, bovine serum albumin based nanoparticles with ganciclovir (size: 290–303 nm; zeta-potential −27.8 to −25.1 mV) retained in the rat retina for two weeks (Merodio et al., 2002). Gan et al. (2013) showed that 75% hyaluronan modified core-shell lipononanoparticles (size: 420 nm; zeta-potential −25 mV) were present in the posterior eye segment of rats seven days post-injection. Long retention of polylactide microparticles (mean size 7.6 μm) was shown in the study Shelke et al. (2011): after three months 17% of injected particles were still found in the vitreous of rabbits. The longer retention times of microspheres can be explained in various ways: 1) Diffusion in the vitreous could be the explanation, since microspheres have much lower mobility in the vitreous than nanoparticles (Fig. 4). Therefore, nanoparticles would reach the aqueous humor more rapidly and become eliminated via the anterior route; 2) Drug release kinetics may explain the results, because nanoparticles have higher surface area per weight unit. They have also a shorter diffusion pathlength for contents release and the carrier material is more available for hydrolytic and enzymatic degradation processes; 3) Nanoparticle studies have been done in rats (Gan et al., 2013; Koo et al., 2012; Merodio et al., 2002), whereas microspheres have been tested in rabbits (Moritera et al., 1991; Nieto et al., 2015; Shelke et al., 2011). Because diffusion time increases as a function of the distance squared (l^2), shorter distance from injection site in the rat might lead to faster elimination than in the rabbits; 4) Cellular uptake of the nanoparticles is more effective than the cellular removal of microspheres (Fig. 8). There are indeed several reasons that might explain the experimental results. Certainly, it is possible to tune the particle processes in the vitreous with particle design (Fig. 8).

Microspheres retain longer in the vitreous than nanoparticles, but the overall picture of particle behaviour in the vitreal cavity is still far from complete. Only one study has attempted to analyse retention of both drug and particle material. Shelke et al. (2011) analysed the retention of particle mass and remaining drug (TG-0054) in the vitreous of New Zealand White albino rabbits. Biodegradable poly(L-lactide) microparticles (mean diameter 7.6 μm) were used. In this case, the drug elimination was slightly faster (17% remaining at 3 months) than the elimination of the particles (27% remaining at 3 months). In many cases, the analyses are based only on drug concentrations, but drug release can be much faster than particle elimination from the vitreous, thereby leading to erroneous conclusions. Many studies are based on visual fundus examination and observation of the particles (Giordano et al., 1995; Moritera et al., 1991; Nieto et al., 2015) or histological analyses (Gan et al., 2013; Koo et al., 2012; Merodio et al., 2002) without true quantitation of intact particles or degradation products.

The vitreal elimination processes compete with each other (Fig. 8). Particle degradation in the vitreous is not dependent on particle diffusion, and thus degradation could be the major elimination mechanism of biomaterial if the degradation takes place more rapidly than the physical elimination of the particles. Biodegradation can take place via chemical hydrolysis in the bulk polymer (PLGA) or at its surface (polyesteramides; Andrés-Guerrero et al., 2015). Enzymatic degradation of the delivery system might be subject to inter-subject and inter-species variations of enzyme expression (section 3.2). As discussed later, the rate of degradation and the size of the resulting fragments have impact on the polymer borne material that is present in the vitreous during the treatment (see section 3.5.).

Without biodegradation the material elimination is expected to take place mostly via the anterior route. In this case, the choice of animal species and vitreous viscosity can play a role. It has been observed that the particles may enter the anterior chamber in the monkey eyes after intravitreal injection, but not in the rabbit eyes (Daugherty, conference presentation, Controlled Release Society

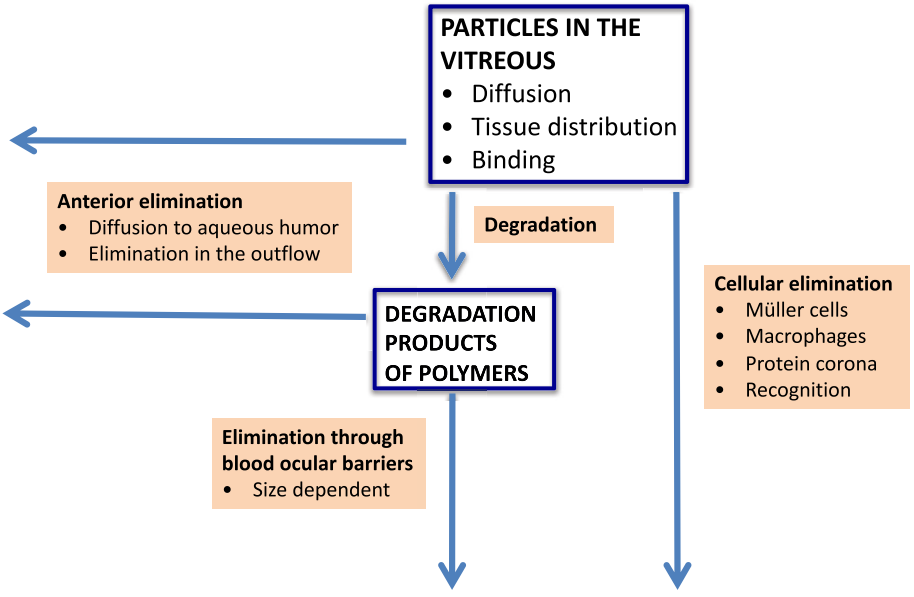

Fig. 8. Possible routes of elimination of particulate drug delivery systems from the vitreous.

Annual Meeting, 2015). A less viscous vitreous may allow particle movement to the anterior chamber in primates, but in rabbits this movement may be restricted by the more viscous vitreous humor, but there may be other explanations (e.g. different obstruction by the lens and iris). Theoretically, obstruction of the outflow channels is a potential risk related to particle entrance to the anterior chamber. The critical size and surface characteristics that cause outflow blockade are not completely known, but intracameral injection of polystyrene particles with diameter of 6–10 μm has been used to block outflow and generate animal models for elevated intraocular pressure (Smedowski et al., 2014), but it is not known whether smaller particles may cause obstruction during long-term exposure.

Lymphatic drainage is another putative route for particle elimination from the anterior chamber. De Kozak et al. (2004) injected tamoxifen intravitreally as free drug in solution and in polyethylene glycol coated polymeric nanoparticles of about 100 nm in diameter to the rats with experimental autoimmune uveoretinitis. Drug loaded nanoparticles inhibited ocular inflammation more efficiently than the free tamoxifen and some nanoparticles were detected in macrophages in the cervical lymph nodes, but not in the inguinal lymph nodes. Yücel et al. (2009) showed recently that nanoparticles (carboxylate modified FluoSpheres, 20 nm) are localized after intracameral injection to the lymphatic vessel like structures in the ciliary body in sheep. Lymphatic uveoscleral clearance from the aqueous humor was also shown with radiolabeled albumin that was localized to the lymph nodes (Yücel et al., 2009). However, the concentration of radioactivity in the lymph nodes (per gram) was one order of magnitude smaller than in plasma, suggesting that even though such a clearance mechanism exists, its role is much smaller than the clearance via trabecular meshwork that leads to systemic circulation. There also seems to be species differences, since lymphatic clearance was not seen in cats. Overall, the nanoparticles and macromolecules are cleared from the vitreous and aqueous humor using several mechanisms, but current evidence supports the major role of aqueous humor outflow mediated elimination.

Cellular elimination is the main route of nanoparticle elimination from plasma (Gregoriadis and Ryman, 1972; Poste et al., 1982). Phagocytosing macrophages of mononuclear phagocyte system remove the particles effectively in the liver and spleen after their recognition. Cellular recognition is enhanced by binding of opsonin proteins (e.g. antibodies, complement components) on the particle surface in plasma (Owens and Peppas, 2006). This defence mechanism has been partly overcome with coated particles that have reduced protein adherence and slowed removal from the blood circulation (Illum and Davis, 1984; Owens and Peppas, 2006; Vonarbourg et al., 2006). In the eye, the phagocytosing defence cells include Müller cells, astrocytes, and RPE cells. Obviously, the cellular elimination may be activated in inflamed eye with macrophages (Zeng et al., 2008). These cells phagocytose particles (even micron size scale) and the Müller cells have similar functionality. Particle recognition and immunological aspects play a role, but these factors are discussed in section 10 of this review. Quantitatively, it is not clear how large fraction of the injected particles can be ingested by the cells and subsequently degraded. Overall, quantitation of the particle elimination processes is needed, but this is methodologically challenging.

3.5. PK and PK/PD models for intravitreal drugs

3.5.1. Models for drugs

Pharmacokinetic (PK) and pharmacodynamic (PD) models are useful scientific tools in drug development. The models integrate the PK and PK/PD processes in mathematical models that are necessary in 1) the determination of kinetic parameters; 2) sorting out the influence of patient related factors in drug kinetics and responses; 3) preclinical to clinical translation in drug discovery and development; 4) drug delivery system development; 5) design of dosing regimens and route of drug administration. Pharmacokinetic models can be divided into top-down and bottom-up models. Top-down models are used with the existing *in vivo* data to solve kinetic parameters. Bottom-up models are based on *in silico* and *in vitro* data that are used as components in integrating models. In general pharmacology, the use of PK/PD models is increasing, because they may speed up drug discovery and development. In addition, reliable PK/PD models may reduce, replace and refine animal experiments. Furthermore, the FDA encourages the pharmaceutical industry to use pharmacokinetic modeling in the documentation of new drug applications. In ophthalmology, PK/PD modeling has similar advantages as it has in general pharmacology. In the following paragraphs we present an update and viewpoints concerning ocular PK/PD modeling of intravitreal drugs.

The top-down approach has been used to solve intravitreal ocular PK parameters, such as clearance, volume of distribution and half-life (for complete analyses of the rabbit data in the literature, see supplementary materials of del Amo et al. (2015) and Supplementary Table 2). During the analysis of the intravitreal PK data, several problems were noticed in the design of the published studies. For that reason, 58% of the studies could not be included in the estimation of clearance and volume of distribution values. Typical problems were related to the sampling times, such as missing initial, intermediate or terminal phase samples, too short duration of the study or too sparse sampling (del Amo and Urtti, 2015). These problems undermine the reliability of the PK parameter estimates. Intravitreal drug studies involve invasive sampling procedures and typically the animals are killed at each time point. Therefore, it is important to design the studies so that maximal information can be gained with minimal number of laboratory animals. Pharmacokinetic parameters are important because they can be used to simulate different situations, such as dosing scenarios, thereby being information rich and generalizable. Therefore, proper design of intravitreal PK studies is important for progress in the field (for more advice, see del Amo and Urtti (2015)).

Despite some progress in non-invasive sampling (microdialysis of drugs from the vitreous) and analysis (e.g. magnetic resonance imaging, *in vivo* fluorophotometry) intravitreal pharmacokinetic studies are still invasive. Microdialysis can be used only for a relatively short time (a few hours) and the non-invasive analytical methods are not applicable for most drugs (see section 10). On the other hand, the pharmacodynamic responses can be determined non-invasively using optical coherence tomography, electroretinogram or fluorescence angiography. Furthermore, these methods are also feasible in clinical studies. Thus, pharmacodynamics (PD) data is easier to obtain than the pharmacokinetics (PK) data.

Population PK/PD analyses are widely used in systemic pharmacology, but still only a few examples are found in the ocular literature. Yet, population PK/PD would be a suitable approach for ocular studies, because this method is capable of maximally utilizing data from sparse samples from large number of patients. Audren et al. (2004) carried out population PK/PD modeling of intravitreal triamcinolone acetonide for diabetic macular oedema. PK and PD data was obtained from phase II studies. Central macular thickness was used as the drug response PD parameter that was measured by optical coherence tomography (OCT). This study did not include analyses of intraocular concentrations of triamcinolone. Instead, a previous human study of intravitreal triamcinolone acetonide was used. Central macular thickness changes with time were described with an indirect PD model and triamcinolone inhibited the increase of thickness in a concentration-dependent

manner according to an empiric sigmoidal model (Hill's equation). The authors were able to simultaneously model all data with nonlinear mixed-effect modeling and extract the typical parameters and interindividual and residual variability. This approach allowed them to estimate the duration of activity, maximal drug response, and phases of drug response in the patients.

Other population PK/PD analyses include the VEGF-A suppression effect in the aqueous humor after intravitreal ranibizumab administration. In this case, ranibizumab concentrations were analysed and the VEGF-A levels were used as the indicator for drug response. This analysis helped to estimate the dosing interval of ranibizumab (Saunders et al., 2015). A PK/PD model of another antibody, lambalizumab against complement factor D, was developed based on cynomolgus monkey data (Le et al., 2015). This model helped to evaluate target-mediated drug disposition, target turnover, drug distribution across ocular tissues and systemic circulation.

Interestingly, Hutton-Smith et al. (2016) developed a mechanistic hybrid model for ranibizumab that includes several aspects of PK/PD including pharmacokinetics (based on clinical data of Saunders et al. (2015)), *in vivo* drug and VEGF dissociation constants and duration of VEGF suppression. This model uses partly top-down data (from Saunders et al. (2015)) and partly bottom-up parameters. This kind of model is useful in the design of dosing regimens or drug release. Importantly, modeling revealed that the effective affinity of ranibizumab to VEGF *in vivo* was different from the *in vitro* affinity.

The current trend is to build bottom-up models that include anatomical and physiological factors, pharmacokinetic parameters, and take into account physico-chemical features of drugs. Such models are called physiologically based pharmacokinetic models (PBPK) that can be extended to pharmacodynamics (PBPKPD). PBPK models require knowledge of the physiological processes and rich prior data that is used in the model parameterisation. A typical approach in PBPK modeling is to use *in silico* and *in vitro* data for model building. Then, the model performance is tested in *in vivo* animal experiments. PBPK models can be conveniently scaled up to humans, because the physiological processes are the same, but the sizes and rates are different. This approach has not been used for intravitreal drug administration even though it could provide certain advantages. Firstly, PBPK models are useful in inter-species scaling. Secondly, the disease state effects on PK can be taken into account in these models. Thirdly, growing *in silico* and *in vitro* data can be incorporated to the models to improve their predictability continuously. Fourthly, QSPR models and other generalized approaches can be used to define parameters in PBPK models. This will provide breadth to the applicability domain of the models, particularly helping the use of the models to predict ocular PK of new compounds.

Finite element modeling is a modeling type that is related to the PBPK. This is also a bottom-up approach where a 3D 'virtual eye' is built using CAD systems and then drug movement in different tissues can be defined accurately, because the eye is composed of thousands of voxels (elements of volume) (Missel, 2012; Missel et al., 2010). Since so many voxels are included in the model, the concentration gradients can be simulated within the small ocular tissues. Finite element modeling allows simulation of accurate injection sites within the vitreous. The drawback of this modeling type is that it requires plenty of computing power. It also includes plenty of details and therefore its reliability depends on the availability of the supporting data. For some issues the data is available, for example diffusion in the vitreous, but in some cases the data is lacking (e.g. permeation across the non-pigmented epithelium). Elegant finite element models have been built for rabbit, monkey and human eyes (Missel, 2012; Missel et al., 2010), but the performance of these models in broad sense is uncertain, since no wide comparisons to the experimental data has been performed.

In summary, intravitreal PK/PD modeling has progressed well due to technical advances in the modeling tools (Missel, 2012) and integrating approaches to predict compound clearance from the vitreous (del Amo et al., 2015). The challenge is to integrate the broader chemoinformatic aspects to the PBPK modeling. Other major aspects include integration of drug responses and disease progression (Hutton-Smith et al., 2016), and the retinal tissue, for example inner and outer limiting membranes, to the models.

3.5.2. PK modeling in controlled release system design

Controlled drug release is an important goal in intravitreal drug delivery, because long dosing intervals are desirable to reduce the burden of injections to the patients and health care (del Amo and Urtti, 2008). Drug release rate from the delivery system (J_{ivt}) and clearance (CL_{ivt}) of free drug determine the steady-state concentration in the vitreous:

$$C_{ss} = J_{ivt}/CL_{ivt}$$

Clearance can be determined *in vivo* after intravitreal injection or it can be predicted for small molecules using the QSPR model (see section 3.2.) (del Amo et al., 2015), where the required parameters HD and $LogD_{7.4}$ can be calculated *in silico* when the chemical structure is known. Del Amo et al. (2015) demonstrated recently how clearance values could be used to determine the required release rate to achieve certain target concentration in the vitreous. We assumed that the injected doses are 0.1, 1, 10, 100, 1000 and 10,000 μg. Note that the highest dose of 10 mg would mean that the drug constitutes about 10% of the total weight of the injection (maximal volume of 100 μl). First order drug release rate constants for the drug delivery systems were varied and drug concentrations in the vitreous just before the next dose (i.e. 3 months after previous injection) was simulated as a function of the release rate constant and initial drug dose in the device (Fig. 9). Three example drug profiles are shown: tobramycin (CL_{ivt} 0.04 ml/h, $V_{ss,ivt}$ 1.22 ml), fluconazole (CL_{ivt} 0.753 ml/h, $V_{ss,ivt}$ 1.93 ml) and bevacizumab (CL_{ivt} 0.019 ml/h, $V_{ss,ivt}$ 2.02 ml). It is obvious from these graphs that high clearance drug (fluconazole) requires high drug doses (1–10 mg) in the device and a slow release rate constant to maintain the concentration above 1 μg/ml. In the case of tobramycin much higher concentrations can be reached and many dose and rate constant combinations yield concentrations above 1 μg/ml. For example, drug loading of 10 μg is adequate at many rate constants. The influence of clearance is even clearer in the case of bevacizumab that shows about 40 fold higher concentrations in the vitreous than fluconazole. Formulation of drugs to small devices is challenging and a low required dose is an advantage. In the case of high clearance compounds, a long duration of action may be achieved only with potent compounds that are active at very low drug concentrations, whereas requirements are more relaxed in the case of low clearance compounds. Note that in these simulations we assume that the delivery system remains in the vitreous (e.g. implant). Pharmacokinetic simulations can be exploited in the design of drug delivery systems for intravitreal administration. Knowing or predicting the clearance it is possible to simulate the release rate and drug loading in the delivery system that are required to achieve certain drug concentration profiles.

3.5.3. Degradation rate of polymers

Drug delivery systems can be non-degradable (e.g. Iluvien) or degradable (e.g. Ozurdex). In the latter case, the polymer is degrading to smaller fragments that dissolve within the vitreous and are eliminated from the eye. Unfortunately, there are no reports

that inform us about the *in vivo* degradation rate of the polymers. This is due to the analytical challenges, since the methods in polymer degradation studies (e.g. size exclusion chromatography, free flow fractionation) are not sensitive enough to analyse the concentrations of polymer fragments *in vivo*. There are some reports that are based on visual inspection or imaging of delivery system retention in the vitreous or analysis of the remaining mass (de Almeida et al., 2015), but these data do not provide an exact view on the polymer degradation or dissolution in the vitreous. The investigated materials include poly(lactide –co-glycolides (de Almeida et al., 2015; Jansen et al., 2011), poly(orthoesters) (Einmahl et al., 2003, 2000), poly(trimethylene carbonate) (Jansen et al., 2011), polyesteramides (Andrés-Guerrero et al., 2015), and poly-e-caprolactone (Silva-Cunha et al., 2009). In some cases, the polymer degradation is much slower than drug release, resulting in retention of an empty 'ghost' device in the eye after drug release (Andrés-Guerrero et al., 2015; de Almeida et al., 2015; Jansen et al., 2011).

Tolerability of the material in the eye is one of the major hurdles in the development of drug delivery systems. The degradation products from the delivery system impose a potential risk of toxicity. Toxicity is dependent on the intrinsic toxicity of the compound and exposure to the material (i.e. concentration and duration). Degradation of the drug delivery system can take place by different mechanisms, for example chemical hydrolysis to smaller fragments or erosion that leads to polymer dissolution without changes in the molecular weight (Kohn et al., 2004). Herein degradation refers to all mechanisms that lead to the elimination of a polymer or its fragments from the eye.

It is known that molecular size has an impact on the clearance from the vitreous (Fig. 6A) and thus it is expected that the degradation rate of the polymer should have an influence on the rate of material elimination and concentration of the polymer fragments in the vitreous. We simulated the impact of these processes using hypothetical rates for polymer degradation and molecular weight dependent rates of vitreal clearance. Two models were constructed with STELLA software (ISEE Systems 10.0). The models are not based on a specific polymer carrier, but instead they illustrate the inter-dependencies of the processes (dissolution, hydrolysis and clearance). In the first model, a polymer carrier needs to be dissolved before undergoing hydrolysis and elimination (Fig. 10). In the second model, dissolution and hydrolysis take place simultaneously within the polymeric device (Fig. 11).

In both models the polymer carrier dose was set as 5 mg. The dissolution rate was defined as P x K x $(C_s - C)/C_s$, where P = intact polymer remaining (mg), K = dissolution rate constant (1/h), C_s = polymer solubility (high value of 1000 mg/ml was used; i.e. we simulate a process that is not solubility limited) and $C_{vitreous}$ = free polymer concentration in the vitreous (mg/ml). In the simulations both dissolution and hydrolysis rates were varied to investigate different scenarios. The range of dissolution rates was 0–0.07 h^{-1} (i.e. polymer dissolution in 2, 20 or 200 days). Hydrolysis rates in the simulations were 0–7 h^{-1} (hydrolysis times: no hydrolysis, 30 min, 5 h, 2 days, 20 days). In the models we took into account the route of elimination of the degraded fragments, either through the anterior route or both the anterior and posterior route. Anterior clearance for polymeric species (0.01–0.04 ml/h) was estimated based on the known values for the vitreal clearance of hydrophilic compounds with different molecular weights (vancomycin 0.04 ml/h; proteins 0.01–0.03 ml/h) (del Amo et al., 2015). The values representing both anterior and posterior clearance were 0.01, 0.04, 0.055 ml/h (value of netilmicin) and 0.501 ml/h (value of hesperetin) (del Amo et al., 2015). The volume of distribution for all degradation products was set to 1.18 ml.

Fig. 12 shows that the polymer exposure in the vitreous depends

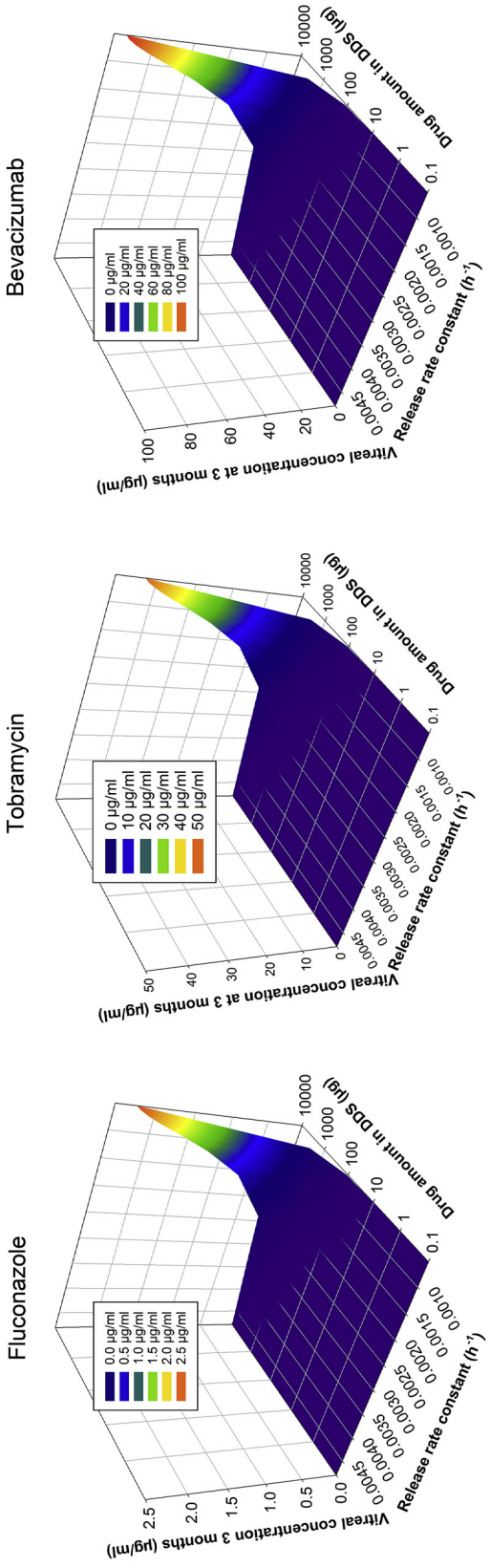

Fig. 9. Simulated drug concentrations in the vitreous after injection of controlled release system that releases drug during 3 months (unpublished simulations). The colour range shows the different drug concentrations in rabbit vitreous (µg/ml) at 3 months. The simulations were done using the clearance values for fluconazole (0.75 ml/h), tobramycin (0.04 ml/h) and bevacizumab (0.019 ml/h). Effects of the first order release rate (h^{-1}) and initial drug load on the drug concentration in the vitreous are illustrated.

on the polymer dissolution rate and hydrolysis rate, in the first scenario (Fig. 10). Obviously, slow dissolution leads to prolonged exposure at smaller concentrations than fast dissolution. Compared to the case without polymer hydrolysis (blue lines) the hydrolysis of polymer decreases the levels of polymer borne species in the vitreous significantly (10–100 fold), especially when the posterior clearance is present. This is understandable because the clearance of smaller fragments is faster than the clearance of intact polymer or larger fragments. The impact of the hydrolysis rate is pronounced at the highest rate of dissolution, because in that case the hydrolysis becomes the rate-controlling factor in elimination. Rapid hydrolysis to small fragments is expected to facilitate removal of materials from the vitreous. Exposure to the polymer fragments is at the lowest levels when polymer dissolution is slow (20 or 200 d), but the dissolved polymer is hydrolysed fast (5 h or 2 d).

The simulation results from the second scenario are shown in Fig. 13. In this case, dissolution and hydrolysis take place at the same time (Fig. 11). Again, fast hydrolysis causes accelerated material elimination from the vitreous. In this case, faster hydrolysis leads also to a higher peak concentration of degradation products independently from the polymer dissolution rate. Without hydrolysis the elimination of the polymer takes longer, but the peak concentration is lower than for polymer carriers that undergo hydrolysis. From toxicity point of view, a fast hydrolysis is beneficial regarding the total exposure. Intravitreal AUC is dramatically decreased with fast hydrolysis of the polymer to small fragments with increased clearance (Fig. 13).

The kinetic simulation models for polymer degradation could be used in the design of drug delivery systems. Firstly, *in vitro* estimates for polymer dissolution and hydrolysis rates in the vitreal conditions are needed. Thereafter, total concentration profiles of polymer and degradation products can be simulated. This concentration range can be compared to the *in vitro* cellular toxicity data, particularly the concentration ranges for toxic responses. This gives early prediction for the risk of toxicity in the eye and may help in the design of the polymers and material quantities to be used in the eye. Secondly, drug release and polymer degradation needs to

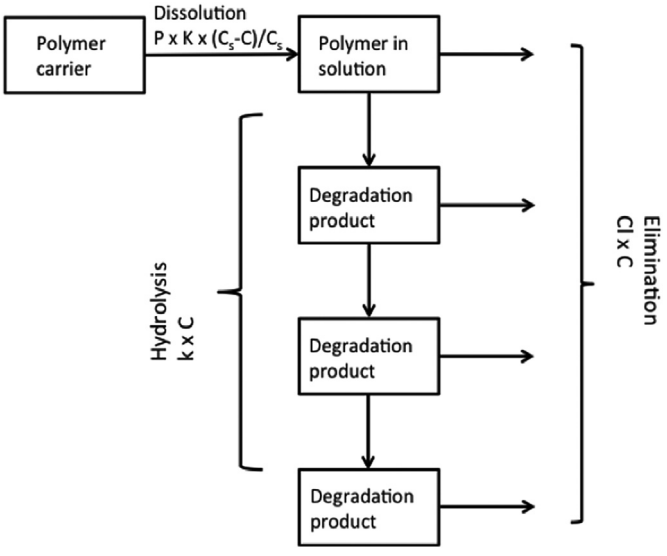

Fig. 10. Scheme for polymer biodegradation simulation #1. It is assumed that the intact polymer is dissolved and thereafter degraded in the vitreous. Different rates of dissolution and hydrolytic degradation were simulated. Polymer solubility is not limiting the dissolution in the model. In the simulations, the clearances of each three degradation products are dependent on the molecular size of the degradation products.

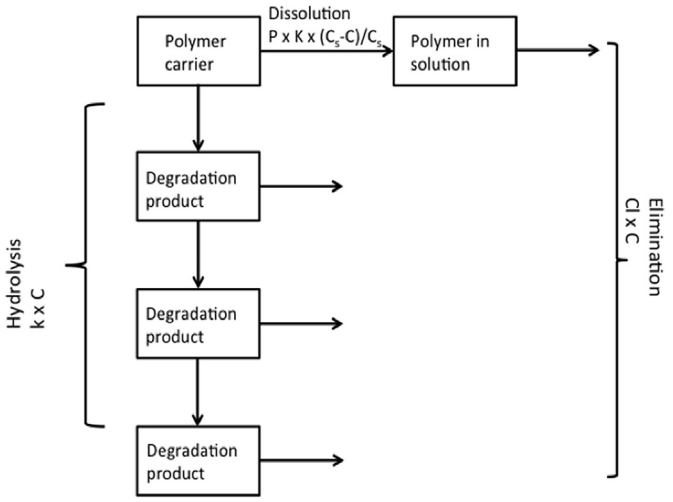

Fig. 11. Scheme for polymer biodegradation simulation # 2. It is assumed that the intact polymer is dissolved and eliminated as such. In addition, the polymer is degraded in the delivery system to smaller fragments that are released from the device and eliminated from the vitreous. Different rates of dissolution and hydrolytic degradation were simulated. Polymer solubility is not limiting the dissolution in the model. In the simulations, the clearances of each three degradation products are dependent on the molecular size of the degradation products.

be synchronized. Often a drug is released from the device much faster than the polymer degradation. In chronic drug treatment, this leads to the situation when a new drug dose is injected before the previous polymeric implant has degraded. Simulations are useful in estimating the disappearance of the 'ghost' devices from the eye and exposure to the free polymer and fragments.

3.5.4. Relationship between drug solubility and release rate

Normally drug release from the formulations is tested in sink conditions. This means that solubility in the dissolution medium should not limit drug release from the delivery system. Typically, this is arranged so that the dissolved drug concentration in the medium is less than 10% of drug solubility. Sink conditions prevail in some cases *in vivo*, but not always. For example, drug release from the transdermal patches is much lower on the skin as compared to the release rate in sink conditions (Sutinen et al., 2000). This is due to the low permeability of the skin causing drug accumulation on the skin surface and loss of the drug concentration gradient between the patch and skin subsequently leading to decreased rate of drug release. This could happen in the vitreous, if the drug clearance is not fast enough to maintain the free drug concentration in the vitreous below the limit (<10% of drug solubility or drug concentration in the device). If these conditions are not met, the concentration of free drug in the vitreous increases and leads to a decreased rate of drug release from the device. Then, drug release gradually shifts from device-controlled situation to solubility-limited release. In the case of poorly water-soluble corticosteroids, low solubility has been used to achieve prolonged drug action. Due to the low solubility of triamcinolone acetonide, it dissolves slowly during several weeks after the intravitreal injection of suspension.

Drug release testing should preferably be carried out using a system that mimics the release conditions in the vitreous (including vitreal enzymes, pH, viscosity, clearance). Recently, a release methodology with anterior clearance component was introduced for intravitreal drug release studies (Awwad et al., 2015). Optimal release system should mimic the intravitreal clearance conditions (CL = P x S; where P = membrane permeability;

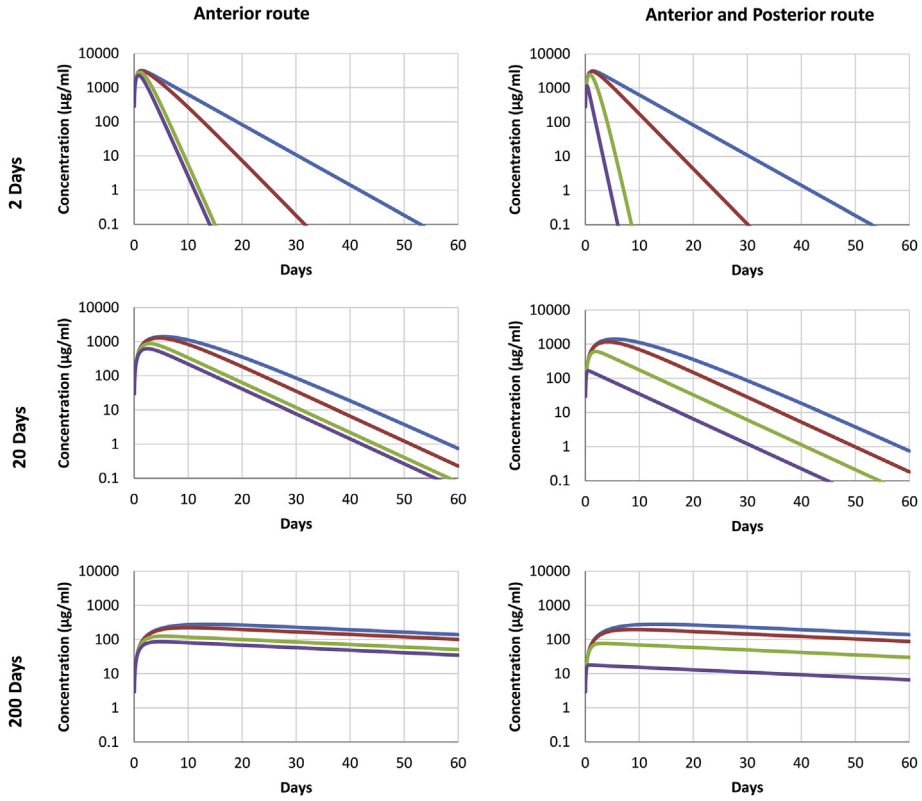

Fig. 12. Simulations of free concentrations of polymer borne species in the vitreous over time after intravitreal injections (unpublished simulations). The initial polymer content in the biodegradable device was 5 mg. Three durations of polymer dissolution (2, 20 and 200 days) were simulated. The times of polymer hydrolysis (i.e. 5 half-lives) were 20 d (red lines), 2 d (green lines), and 5 h (purple lines). Blue line shows the simulation without hydrolysis. The simulations were done using the model from Fig. 10. The clearance values of the degradation products were 0.01, 0.02, 0.03 and 0.04 ml/h for anterior elimination and 0.01, 0.04, 0.055 and 0.501 ml/h for anterior and posterior elimination.

S = surface area), but these conditions are not necessarily sink conditions. Simulations can also be used to extrapolate from *in vitro* testing to *in vivo* conditions. We carried out simulations on the effects of drug solubility and *in vitro* release rate (sink conditions) on the expected steady-state concentration of released drug in the rabbit vitreous. In the simulations we assume that the zero-order release rate *in vivo* decreases proportionally if the concentration of released drug increases in the vitreous (*in vivo* release rate = *in vitro* release rate×(drug solubility − drug concentration in the vitreous)/drug solubility). Two clearance values were used in the simulations: 0.03 ml/h (low clearance) and 1 ml/h (high clearance).

The simulations demonstrate that sink conditions prevail in the vitreous at all release rates (up to 5 µg/h) only when the drug solubilities are at least 0.1 mg/ml or 1 mg/ml at clearance levels of 1 ml/h and 0.03 ml/h, respectively (Fig. 14). At lower solubility values the expected rates of drug release *in vivo* are much less than *in vitro* at sink conditions (Fig. 14). It is evident that the clearance values are affecting the conditions for drug release. At higher clearance levels sink conditions are easier to maintain than at lower values of clearance (Fig. 14A and B).

It is important to develop predictive *in vitro* release methods and simulation tools to provide relevant and predictive data before *in vivo* testing. Important considerations in the method development include: 1) *In vitro* clearance should mimic *in vivo* drug clearance so that the concentration gradient between the device and free drug is relevant; 2) Dissolution medium should mimic the vitreous in terms of pH, enzymatic activity and viscosity. The relevance of the enzymes depends on the susceptibility of the delivery system to the enzymes. The role of viscosity is not known, but in principle higher viscosity could lead to a thicker hydrodynamic diffusion layer that may reduce the release rate, especially in the case of lipophilic and large molecules. Obviously, the sink conditions are lost easier when the drug has low solubility and/or low intravitreal clearance.

4. Systemic drug delivery to the retina

Systemic drug administration as tablets is the most common way of drug delivery in the clinical practice, but not so common in ophthalmology. Drugs that do not absorb adequately to the blood circulation from the intestine are given as parenteral s.c., i.m. and i.v. injections. In ophthalmic treatment the systemic route has been used to deliver antibiotics to treat endophthalmitis, carbonic anhydrase inhibitors to treat elevated intraocular pressure, and methotrexate and parenteral antibodies to treat uveitis (Bartlett and Cullen, 1989; Schwartz and Budenz, 2004; Yanoff and Duker, 2014). Systemic drugs that are intended for other indications may also enter the eye, and in this case, they may cause adverse effects (Blomquist and Palmer, 2011; Miguel et al., 2014; Potts, 1974). For example, chloroquine, sildenafil, chlorpromazine, alendronate and tamoxifen may cause retinal side effects. Understanding drug distribution across blood-ocular barriers from systemic circulation to the eye is a key factor in effective ocular treatment with systemic medications, and on the other hand, it determines the ocular exposure to the systemic drugs.

4.1. Drug distribution from blood circulation to the retina

Properties of blood-ocular barriers have been described in detail

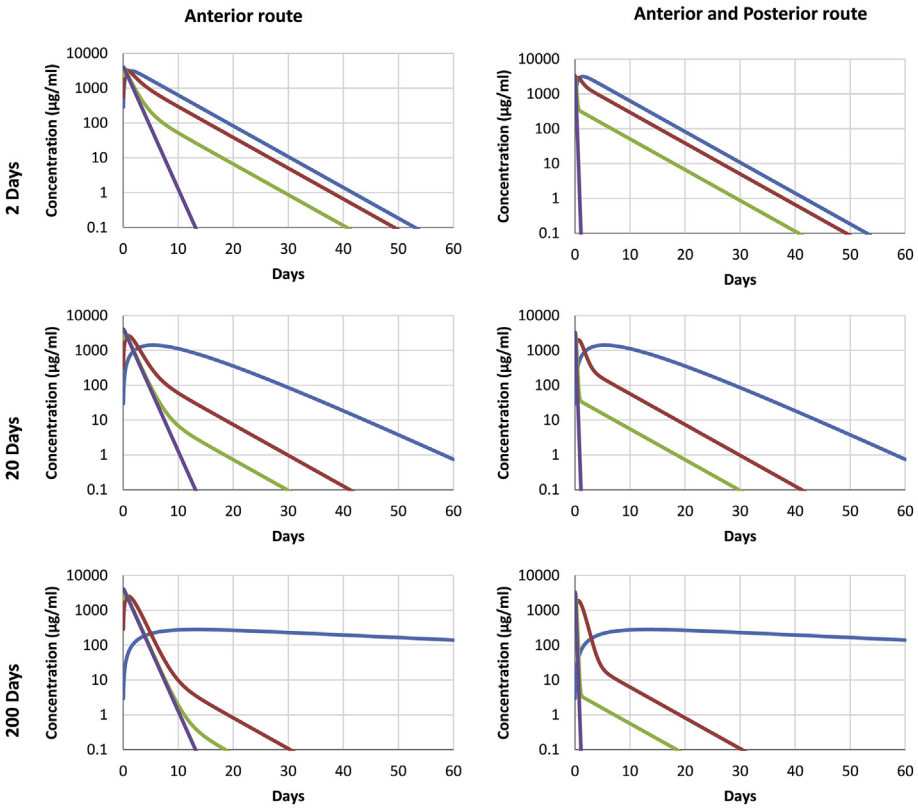

Fig. 13. Simulations of free concentrations of polymer borne species in the vitreous over time after intravitreal injections (unpublished simulations). The initial polymer content in the biodegradable device was 5 mg. Three durations of polymer dissolution (2, 20 and 200 days) were simulated. The polymer hydrolysis times (5 half-lives) were 2 d (red lines), 5 h (green lines), and 30 min (purple lines). Blue line shows the simulation without hydrolysis. The simulations were done using the model from Fig. 11. The clearance values of the degradation products were 0.01, 0.02, 0.03 and 0.04 ml/h for anterior elimination and 0.01, 0.04, 0.055 and 0.501 ml/h for anterior and posterior elimination.

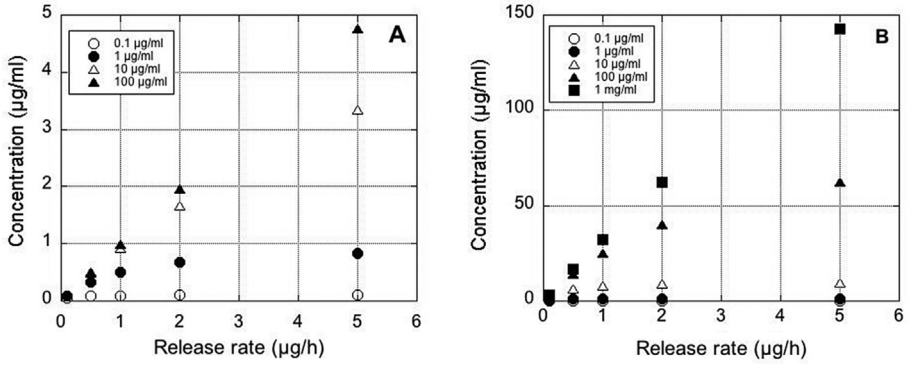

Fig. 14. Simulated steady state concentrations in the vitreous humor for compounds having different vitreous solubilities (0.1, 1.0, 10, 100, and 1000 µg/ml), release rates in the sink conditions (0.1, 0.5, 1, 2 and 5 µg/h) and vitreal clearances (A: 1 ml/h; B: 0.03 ml/h).

in section 2. These barriers regulate drug transfer between the blood circulation and the eye in both directions. Ocular distribution of systemic drugs has been studied in rabbits (for references, see Vellonen et al. (2016)). The studies that report drug concentrations both in plasma and in vitreous humor are particularly useful for understanding the drug distribution from plasma to the posterior eye segment.

Drug distribution from rabbit plasma to the vitreous was recently analysed in a systematic manner (Vellonen et al., 2016). A simulation model was built to describe pharmacokinetics in the systemic circulation and drug distribution to the vitreous (Fig. 15). The model was based on two key factors: 1) Free drug concentration in plasma ($C_u = f_u C$, where f_u is the free fraction of the drug in plasma); 2) Distribution clearance between plasma and vitreous was assumed to be the same as drug clearance from the vitreous. Previously, clearance from the vitreous was modeled using the QSPR approach (del Amo et al., 2015). This model provides clearance estimates computationally from the chemical structure. The predicted clearance values were used as estimates of the distribution clearance of drugs in the ocular drug distribution model (Fig. 15) (Vellonen et al., 2016). The assumption of similar clearance across blood-ocular barriers in both directions is valid if there is no active transport that would lead to significant directionality in the barrier.

Drug concentrations in the rabbit vitreous were simulated and the vitreal drug exposure obtained (area under the drug concentration vs. time curve in the vitreous; AUC) correlated well with the real experimental values (Fig. 16). Among ten drugs the deviation was less than 2.0-fold in 80% of cases and the maximal deviation from the experimental values was 3.8 fold in rabbit eyes (Fig. 16). The AUC values in plasma and the vitreous were spanning over three orders of magnitude, but the model provided an accurate match with the real data. It seems that the computational estimates of ocular distribution clearance values are useful in this context. The clearance values are conveniently calculated for small molecules based on the chemical structure (del Amo et al., 2015). This approach is not applicable to protein drugs, and the QSPR model was originally built using small molecules with low or medium lipophilicity ($LogD_{7.4}$ range from −10.59 to 2.19). Therefore, its reliability for more lipophilic compounds is uncertain. Plasma protein binding and distribution clearance were needed for the prediction; lipophilicity or protein binding alone lead to poor predictions of ocular drug distribution from plasma (Vellonen et al., 2016).

In the case of passive diffusion, the distribution clearance does not depend on the direction of drug transfer, but transporter-mediated permeation could lead to preferred direction of drug transport in the blood-ocular barrier (either inwards or outwards). CL_{ivt} was predicted with two physicochemical factors, $LogD_{7.4}$ and hydrogen bonding capacity (HD), without outliers suggesting that the transporters do not have a major influence on drug clearance from the vitreous (del Amo et al., 2015). In accordance with this, no substantial deviations are seen in the plasma-to-vitreous simulations (Fig. 16). However, many compounds in the data set are substrates of transporters and in some cases transporter effects may be present. For example, ciprofloxacin, fleroxacin, and ofloxacin are transporter substrates. This is in line with the simulated AUC values that are greater than the experimental values (Fig. 16). Mercaptopurine also shows higher simulated AUC values than experimental values in the vitreous, and this could be due to the actions of influx transporter OAT3 (ocular side) and efflux transporter MRP4 (blood side) (Hosoya et al., 2011; Tagami et al., 2009). Thus, it seems that the transporter activity may modulate the ocular distribution of systemic drugs.

Protein binding in plasma was taken into account in the model assuming that the protein bound drug does not permeate across the blood-ocular barrier. This is reasonable assumption in the light of the properties of the blood-ocular barrier (section 2). This rationale is also supported by the data from post-mortem human plasma and vitreous (Holmgren et al., 2004). In that study, a correlation between the degree of protein binding of the drugs and vitreous/femoral blood concentration ratio was found. The model of Vellonen et al. (2016) does not take into account the protein binding or other binding events in the vitreous, because no quantitative data exists about these factors. It is known that the protein quantity in the vitreous is less than in plasma (section 3). It is likely that the protein binding in the vitreous is less important than it is in plasma, since model predictions were successful even without the vitreal binding factor. Certainly, the model can be improved if the vitreal protein binding data will become available.

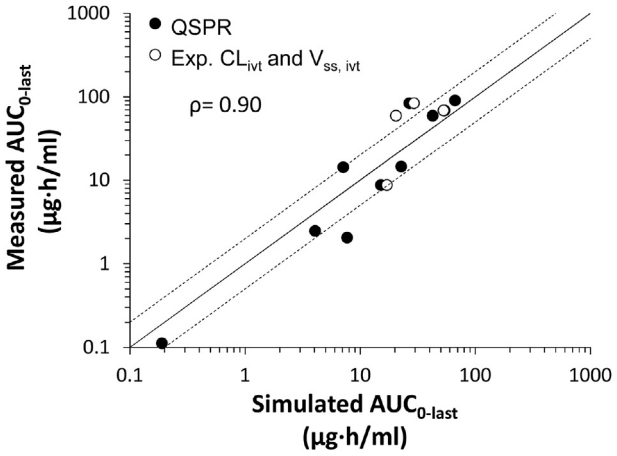

Fig. 16. Correlation of measured and simulated AUC_{0-last} in rabbit vitreous after intravenous administration. Drug distribution clearance between systemic circulation and the eye (CL_{ivt}) was defined computationally (QSPR; solid circles) and $V_{ss,ivt}$ of 1.48 mL was used. Also, experimental values of CL_{ivt} and $V_{ss,ivt}$ (Exp.; open circles) were used for comparison. Solid line represents the slope of 1 and dotted lines are 2-fold deviation from 1:1 relationship. Reprinted (adapted) with permission from Vellonen et al. (2016), Copyright (2016) American Chemical Society.

Overall, small molecular drugs do permeate across blood-ocular barriers to the eye and it is in principle possible to treat the retina with systemic drugs. However, systemic aldose reductase inhibitors failed in the clinical studies due to their minimal efficacy in the treatment of diabetic retinopathy (Ramana, 2011). Sometimes systemic toxicity may become limiting factor for systemic drugs. It is also known that systemic use of carbonic anhydrase inhibitors (like acetazolamide) is associated with serious adverse effects (such as tiredness, anorexia and dysesthesia in the fingers and around the mouth) (Inoue, 2014).

Drug distribution from plasma to the eye is also often seen in preclinical animal studies when a drug is dosed only to one eye and the other eye serves as a control. Systemic drug absorption is rapid and nearly complete after topical eye drop instillation and subconjunctival injections (Amrite et al., 2008; Lee and Robinson, 2004; Urtti and Salminen, 1993). In rabbit experiments, the dose is usually the same as in humans, but the systemic drug clearance

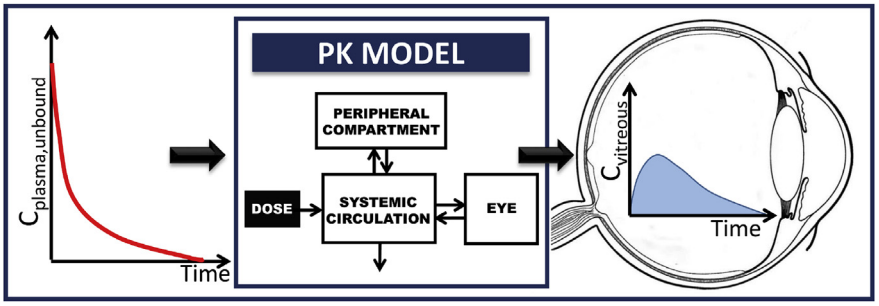

Fig. 15. Drug distribution from plasma to vitreous humor. A simulation model was used to predict vitreal drug concentrations that result from known drug concentration profiles in plasma. The model was based on free drug concentration in plasma and computational distribution clearance between systemic circulation and the eye (del Amo et al., 2015). Reprinted (adapted) with permission from Vellonen et al. (2016), Copyright (2016) American Chemical Society.

and volume of distribution are much smaller. This will lead to overestimation of systemic drug distribution to the contralateral eye. After chronic dosing of timolol (six days, twice daily) drug levels in the contralateral eye in the rabbits (four hours after the last dose) reached high levels in vascularized ocular tissues (10–60% of the values in the treated eye), but low levels (2% of the concentration in the treated eye) in the avascular cornea (Salminen and Urtti, 1984).

4.2. Retinal targeting from the blood stream

Distribution of free drug from the blood stream to the vitreous is driven by the concentration gradient and ability to cross the blood-ocular barriers (i.e. distribution clearance) (Vellonen et al., 2016). Free drug may accumulate more than expected to the retina and choroid if the drug is binding to cellular components (especially melanin) or it is a substrate for a significant active transport process (for more, see section 9.3.). Another option is formulating the drug into a targeting system.

Targeted drug delivery from systemic circulation to the tumours, central nervous system and other tissues is widely studied topic in pharmaceutical literature. Targeted drug delivery from systemic blood circulation to the tissues is often accomplished using nanoparticles and liposomes (Goyal et al., 2014), antibody-drug and polymer-drug conjugates (Sassoon and Blanc, 2013), and small molecular prodrugs (Huttunen and Rautio, 2011). Active drug targeting relies on homing compounds that have a high affinity to the target cells or tissues (Steichen et al., 2013), while passive targeting is based on accumulation of the nanoparticles or polymers to the tumour tissue due to its leaky vasculature and inefficient lymphatic removal from the tumours (i.e. enhanced permeation and retention (EPR) effect (Maeda, 2001)). Carrier mediated drug delivery may have safety related advantages, because the encapsulated drug does not cause side effects (e.g. liposomal encapsulation of doxorubicin protects from the cardiac toxicity of the drug). Similar principles should also be applicable for retinal drug targeting (Liu et al., 1989). It should be noted, however, that intravenously administered nanoparticles are mostly distributed from blood circulation to the cells of the reticuloendothelial system of the liver and spleen (Lehtinen et al., 2012b).

Targeted retinal drug delivery from the systemic circulation has been investigated in preclinical animal models, but not in humans. Most studies are qualitative investigations where microscopy, immunohistochemistry, and fluorescein angiography have been used as end-points. Investigated materials include gold nanoparticles (J. H. Kim et al., 2009), liposomes with conjugated targeting antibodies (Zhu et al., 2002), liposomes with conjugated peptides (Salehi-Had et al., 2011), PLGA nanoparticles with targeting moieties (Singh et al., 2009), antibody-drug conjugate (Kamizuru et al., 2001), and externally triggered liposomes (Gross et al., 2013). Unfortunately, no general conclusions can be drawn from these studies regarding the impact of particle or conjugate size, charge, or affinity of targeting ligand to the retinal targets. Some results show effective drug targeting to the retina. For example, liposomal delivery systems (mean size 45 nm; zeta potential + 35 mV) with targeting to choroidal neovascularization lead to transgene expression in the choroidal vessels (Salehi-Had et al., 2011) and anti-angiogenic efficacy of paclitaxel (Gross et al., 2013). Also, systemically given antibody conjugates of mitomycin C were shown to reduce choroidal neovascularization (Kamizuru et al., 2001). Likewise, targeted PLGA nanoparticles (size 270–430 nm; decorated with RGD peptide and transferrin) alleviated choroidal neovascularization in rats (Singh et al., 2009). Liposomes with transferrin were shown to transfect the RPE and ciliary body after systemic delivery in mice and monkeys (Zhang et al., 2003; Zhu et al., 2002). Despite many positive results (Zhang et al., 2003; Zhu et al., 2002) no follow up or confirming studies have been performed. Therefore, it is difficult to assess the true potential of this approach at this point. The results suggest that poly(lactide-*co*-glycolide) nanoparticles (270–420 nm in diameter; negatively charged) are targeting to the neovessels (Singh et al., 2009). This was explained by the increased leakiness of the blood-retinal barrier, but this could also reflect changes in the endothelial cells (over-expression of target receptors, changes in the endocytic capacity). Small liposomes (85 nm) were needed to reach the RPE cells in healthy eyes, which is in line with the limits set by the choroidal vessel pores (Zhang et al., 2003; Zhu et al., 2002). Quantitative information about the retinal bioavailability or mechanistic data about targeting at different layers in the retina still does not exist.

Targeted drug delivery requires homing of the delivery system to the desired tissue. On top of that, the drug should be released from the carrier, but this is often a difficult task and only rarely drug release is at the cellular level quantitated (Soininen et al., 2016). Drug release can be triggered using endogenous (e.g. reduced pH in the cellular endosomes) or exogenous factors (e.g. light) (Lajunen et al., 2016a). The eye is particularly well suited for exogenous triggering of drug release, because it is transparent and ophthalmologists routinely investigate the retina with an ophthalmoscope and use lasers for diagnostics and treatment. Early works of Khoobehi et al. (1988) demonstrated that it is possible to induce contents release from i.v. liposomes in the posterior eye segment with microwaves. Furthermore, the light activated systems are interesting in ophthalmology, because the light can be accurately projected to the site of interest with excellent spatial resolution. It is important to 'sensitize' the delivery system to the light signal so that effective release can be achieved using safe levels of light intensity. Light triggering agents can be divided to metallic nanoparticles, light induced chromophores, degradable lipids, photopolymerizable liposomes, and indocyanine green (Lajunen et al., 2016b). All these agents are capable of inducing light triggered release from the liposomes or other particles, but many systems are based on toxic compounds that cannot be used in clinical drug delivery. Gold nanoparticles absorb light and release the absorbed energy as heat to the lipid bilayer that becomes permeabilised, inducing the contents release from the liposomes (Paasonen et al., 2010, 2007). The appropriate wavelength depends on the size and shape of the gold nanoparticles. Visible and near-infrared light can induce relatively large gold particles (diameters 20–50 nm) thereby making formulation of small liposomes smaller than the pore size of choriocapillaries (70–80 nm) impossible. Recently, we reported the use of indocyanine green (ICG) as a light induction agent in liposomes with similar actions as gold nanoparticles (Lajunen et al., 2016a). As a clinically used imaging agent ICG should be safe. In addition, it can be formulated to small liposomes for effective induction of drug release with near-infrared light (Lajunen et al., 2016b). The idea of light triggered release in retinal drug targeting is an interesting possibility, but the retinal safety of the light (wavelength, intensity, pulse duration) must be ascertained before these systems can be used in the clinics. Light activation has already been used in the clinics in the case of Verteporfin, a photodynamic therapy treatment of age-related macular degeneration (Lai et al., 2015).

Some background facts support the rarely studied approach of targeted retinal drug delivery. Firstly, choroidal blood flow relative to the tissue size is extremely high and the choriocapillaries are leaky, having pores of 70–80 nm, thereby allowing extravasation of polymers or nanoparticles. Secondly, the target cells (e.g. RPE and neural retina cells) are in close proximity of the extravascular choroid. Thirdly, RPE is active in internalization of materials

allowing targeting to these cells. Fourthly, the posterior eye segment is easy to reach with various methods of external release triggering signals (e.g. light, ultrasound, magnetic fields). Huge activity has been undertaken to target drugs to tumours, whereas retinal drug targeting has been only rarely investigated. There may be possibilities for breakthroughs in this field, since many relevant nanotechnologies have been developed in other fields of drug delivery.

5. Periocular drug administration

Periocular administration means drug injection to a region surrounding the eye, for example sub-conjunctival, sub-Tenon's, peribulbar, retrobulbar or posterior juxtascleral injections (see upper insert in Fig. 1). These injections differ on the location/direction of the injection in the proximity of the sclera. The scleral thickness diminishes near the equator region (from 0.53 ± 0.14 mm into 0.39 ± 0.17 mm) (Olsen et al., 1998) potentially leading to increased drug penetration (e.g. posterior juxtascleral injection). On the other hand, sub-conjunctival injections have been used for a long time in the clinics to deliver drugs to the anterior part of the eye. In this chapter, sub-conjunctival injection will be discussed. Higher concentrations in the anterior chamber tissues are reached with such injections as compared to the topical eye drop administration and this mode of delivery has been investigated as an option for posterior segment drug delivery.

Sub-conjunctival injections result in drug distribution to the anterior chamber at higher levels than after topical instillation of eye drops. The drug bioavailability to the aqueous humor is about 10% after sub-conjunctival injection, because the corneal barrier is circumvented and the retention at the injection site is longer than after eye drop administration. Systemic absorption from the sub-conjunctival space is often rapid and it limits the bioavailability (Maurice and Mishima, 1984).

Drug delivery from the sub-conjunctival space to the retina is more challenging than the delivery to the anterior chamber. Sub-conjunctival administration has been investigated as an alternative to intravitreal injections for retinal drug delivery (for ref. see, Ranta and Urtti (2006)). The overall conclusion is that the retinal bioavailability is in the range of 0.1% after sub-conjunctival injections (Kim et al., 2004). This is better than after topical administration (Weijtens et al., 1999), but less than the retinal bioavailability after intravitreal injections. Sub-conjunctival injection volumes can be high (even 0.5 ml) which makes loading of an adequate drug dose easier.

Retinal bioavailability after sub-conjunctival injections is low, because there are several barriers between the injection site and retina (Maurice and Mishima, 1984, Fig. 17). The sub-conjunctival drug delivery to the retina has been simulated, to explore the roles of various barriers in defining the low retinal bioavailability (Ranta et al., 2010). The simulation model was based on experimental results: 1) drug elimination rates *in vivo* from the sub-conjunctival depot; 2) scleral permeability in Ussing chambers; 3) known diffusion coefficients in similar tissues to the extravascular choroid; 4) *in vivo* elimination rate from the choroid; 5) drug permeability in the *ex vivo* RPE; 6) *in vivo* clearance from the vitreal compartment. The simulation model integrates these factors in the rabbit eye for three model drugs; a small lipophilic compound, a small hydrophilic drug and a macromolecule. All aforementioned pieces of data were not available for any single compound, but the values for the compound classes were distinct from each other. Thus, simulations were carried out as 'typical profiles' for each class.

As shown in the schematic model structure (Fig. 17) the barriers can be divided to two groups: 1) flow barriers (elimination to blood flow and lymphatic flow from the sub-conjunctival space and choroid); 2) penetration barriers (sclera, extravascular choroid, RPE). After sub-conjunctival injection about 80–95% of the small molecular drug absorbs rapidly to the systemic circulation, and only a minority permeates across the sclera, but the systemic absorption of proteins (e.g. Gd-albumin) can be even 70 times slower than the absorption of small drugs (Amrite et al., 2008; Kim et al., 2008; Ranta et al., 2010). In sclera, the permeability of small molecules is relatively constant and independent on lipophilicity, whereas the macromolecules permeate about ten times slower than the small molecules (Olsen et al., 1995; Prausnitz and Noonan, 1998). In the extravascular choroid diffusivity is relatively fast and the distance is short; therefore, the drugs reach the choroidal vessels rapidly, and depending on drug properties they do reach to the systemic circulation (Ranta et al., 2010). Blood flow in the choroid is extremely high for such a small tissue (62 ml/h in rabbit) (Nilsson and Alm, 2012) and the leakiness of the vessels leads to rapid transfer to the blood stream, especially in the case of small molecules (Bill, 1968; Bill et al., 1980; Törnquist, 1979). Recent experimental study shows that the choroidal blood flow decreases the retinal bioavailability of periocularly administered triamcinolone acetonide (Li et al., 2016). In the RPE, the permeability of small lipophilic compounds is about 8 and 500 times faster than the permeability of small hydrophilic and large molecules, respectively (Mannermaa et al., 2010; Pitkänen et al., 2005). Overall, there is a clear trend: the small molecules, especially lipophilic ones, permeate faster than macromolecules through the penetration barriers (Pitkänen et al., 2005; Prausnitz and Noonan, 1998), but they are eliminated faster to the blood stream than the macromolecules. Apparently, the flow factors have a bigger impact and eventually the small molecular weight does not facilitate retinal bioavailability, but rather decreases drug distribution to the vitreal cavity (Ranta et al., 2010).

In addition to the blood flow, lymphatic flow also plays a role in drug clearance from the sub-conjunctival and choroidal spaces (Kim et al., 2004; Robinson et al., 2006). The role of lymphatic flow may be particularly important in clearing the particles and macromolecules from the interstitial fluid and shuttling them to the lymphatic nodes (Muthuchamy and Zawieja, 2008). The role and existence of lymphatic vessels in the inner eye is still somewhat controversial (Schroedl et al., 2014), but the presence of lymphatics in the conjunctiva is well established. A rich network of lymphatic vessels is found in the conjunctiva, representing approximately 50% of its surface area (Guo et al., 2012). Activity of the lymphatic system in removing the sub-conjunctival compounds has also been demonstrated (Kim et al., 2004), but the role of this system in the removal of nanoparticles has not been studied.

Because drugs in solution are rapidly eliminated from the injection site, the duration of action of the sub-conjunctival injections is short, unless slow drug dissolution or release is involved. Thus, it is necessary to prolong drug retention and release in the sub-conjunctival space before this approach can be used in chronic multiple dosing drug treatment. It is not feasible in clinics to have frequent sub-conjunctival injections. Several technologies have been developed to prolong and improve retinal drug delivery from the sub-conjunctival injections, but we are not reviewing the sub-conjunctival delivery systems here, because they are well covered in the literature (Imai et al., 2015; Kim et al., 2007, 2014; Kompella et al., 2003; Misra et al., 2009; Sabzevari et al., 2013). Instead, we have simulated pharmacokinetics of sub-conjunctival depots to estimate required drug doses and release rates for retinal drug action. The simulations were carried out using the previous model (Ranta et al., 2010). A first order release rate from the drug delivery device was added as input, with a dose range of 0.1 μg–10 mg.

Fig. 18 illustrates the impact of release rate constant on the

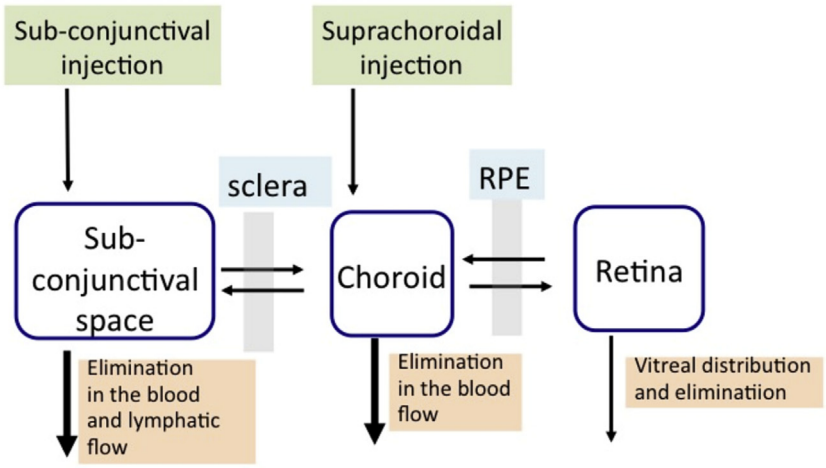

Fig. 17. Schematic presentation of the kinetic phases of sub-conjunctival and suprachoroidal injections for retinal drug delivery.

simulated vitreal drug concentrations after sub-conjunctival administration. Equal dose (1 mg) results in clearly higher concentrations of macromolecule than in the case of small hydrophilic and lipophilic compounds. Lipophilicity has relatively small influence, because the increased lipophilicity improves the permeation across the RPE, whereas it increases also drug loss from the sub-conjunctival and choroidal space to the blood stream. For macromolecule prolonged action of 2–4 months can be obtained if the limit of drug activity is about 1–10 ng/ml, but for small molecules the limit for target site concentration is around 0.01–1 ng/ml. Sub-conjunctival drug dose can be increased at least by one order of magnitude. At the dose of 10 mg the simulations suggest that the required concentrations would be in the range of 10^{-10}–10^{-8} M; meaning that this approach is suitable only for very potent compounds. This is due to the low retinal bioavailability (0.1%) after sub-conjunctival drug delivery. In the case of choroid, the bioavailability is much better (5–20%) (Ranta et al., 2010). For choroidal targets concentrations of 10^{-8}–10^{-6} M may be reached over prolonged periods. Sub-conjunctival injection is given on one side of the eye and drug bioavailability to the other side of the eyeball is lower than the values above. For example, in the case of topical application of controlled release devices the drug concentrations in the superior and inferior halves of the eyeball differ substantially (even 60 fold) (Urtti et al., 1988).

The loss of drug to the systemic circulation from the injection site is rapid, especially for small lipophilic molecules (elimination half-life from injection site is about 5 min) and hydrophilic small molecules (half-life ≈ 25 min) (Amrite et al., 2008; Kim et al., 2008). It is possible to prolong the retention and release times in the sub-conjunctival space with formulations, such as particles and implants (for ref. see Kim et al. (2014)) In principle, polymeric conjugates should also result in increased retention, since it is known that large molecules (e.g. albumin) retain much longer in the sub-conjunctival injection site (elimination half-life ≈ 6 h). Controlled release is a feasible strategy to prolong the concentration profiles, but it does not change the bioavailability in the ocular tissues. The relative rates of transfer towards the inner eye and systemic circulation are expected to remain the same (Fig. 17; Ranta et al., 2010).

Increased retinal bioavailability after sub-conjunctival injection is achieved only if the drug transfer to the eye is increased relative to the rate of systemic drug loss (Fig. 17). Permeability of the sclera is the key point in this case. Permeability of macromolecules (FITC dextrans up to the size of 6.5 nm) in the sclera is relatively high (10^{-6}–10^{-5} cm/s) both in rabbits and humans (Ambati et al., 2000; Olsen et al., 1995). Thus, it is also likely that synthetic polymers permeate well in the sclera. Nanoparticles have been used to enhance drug delivery from posterior periocular space to the retina and choroid (Amrite et al., 2008). Small bodipy labelled carboxylated polystyrene nanoparticles (20 nm) permeated across the sclera slowly (less than 0.5% in 24 h), whereas 200 nm particles did not permeate across the sclera. On the other hand, the 20 nm nanoparticles were eliminated rapidly (half-life 5.5 h) to the systemic circulation, but 200 nm nanoparticles retained at the injection site for months. Thus, periocular small nanoparticles are not feasible for retinal drug delivery due to the particle loss to the systemic and lymphatic flow (Amrite et al., 2008). There are, however, problems associated with this approach. If the particles enter choroid from one side it is not clear whether they can distribute in the choroid and reach the diseased areas on the other side of the eye. Furthermore, if the target site is located in the neural retina, the particles should permeate across the RPE that is about 100 times tighter barrier than sclera to macromolecules (Pitkänen et al., 2005). Indeed, polystyrene nanoparticles (20 nm) were not able to permeate at all across sclera-choroid-RPE specimens (Amrite et al., 2008). At cellular level the particles might get internalized to the choroidal endothelial cells and the RPE cells with endocytic processes, but the spatial distribution within the tissues may be limited.

Sub-conjunctival injection is less invasive than intravitreal injection, avoiding the risks of endophthalmitis and cataract, but currently retinal bioavailability is still too low (about 0.1%) and it is more suitable for anterior segment drug delivery (bioavailability about 10%). In this case, the most evident advantage of drug delivery systems is the prolonged action and controlled release at the injection or implantation site. The potential in drug targeting and enhanced bioavailability to the retina is still poorly defined. The potency of the drug needs to be considered: for retinal treatment the drug should be active at nM levels. Then, dosing of 10 mg subconjunctuvally might lead to adequate drug response.

6. Suprachoroidal drug delivery

Suprachoroidal drug delivery is a relatively new mode of drug administration that was introduced recently (Einmahl et al., 2002), but it is not yet used clinically. The drug dose is injected to the

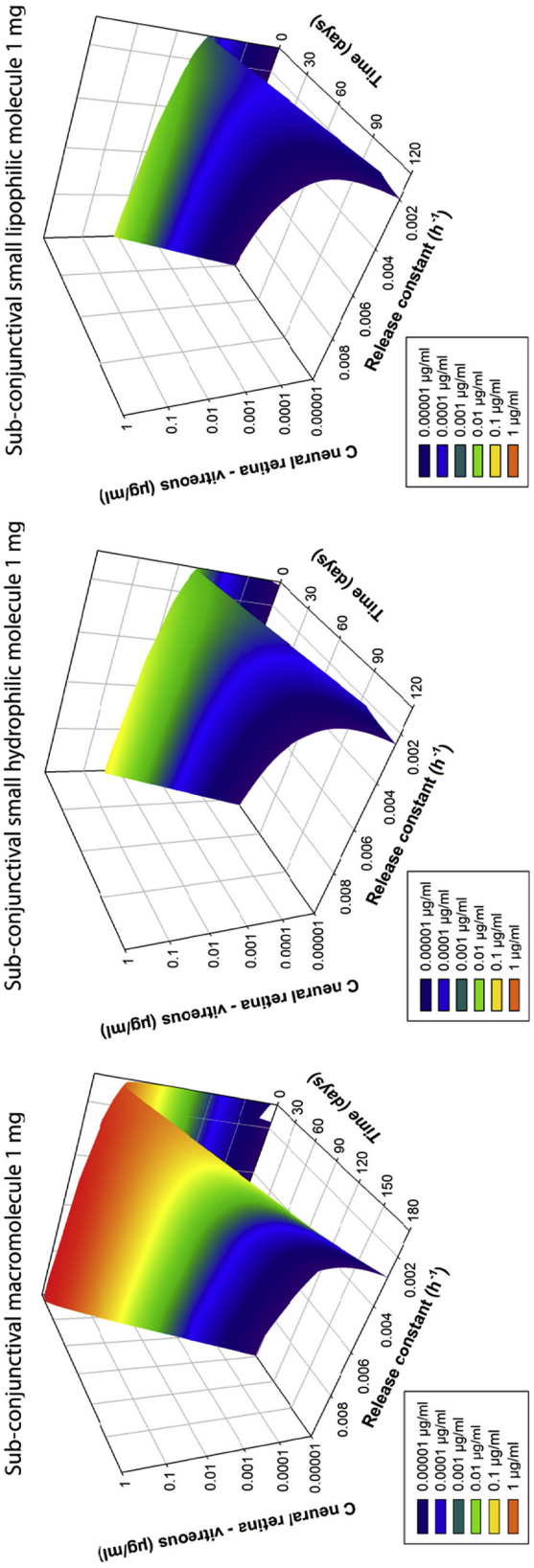

Fig. 18. Simulations on sub-conjunctival delivery with controlled release systems (unpublished simulations). The simulated drug concentrations in the neural retina-vitreous compartment are represented by the colour range.

suprachoroidal space, just beneath the inner surface of sclera. The injection volume is small, about 50 µl and typically these injections are given with microneedles (Olsen et al., 2011; Patel et al., 2012, 2011), but also cannulation is possible (Olsen et al., 2006). After the injection, the fluid distributes around in the suprachoroidal space that is limited anteriorly by the scleral spur and posteriorly by the optic nerve. The spreading is probably due to the pressure that the injection exerts on the small suprachoroidal space (Patel et al., 2011). With suprachoroidal injection it is possible to a reach wider area around the eyeball than in the case of sub-conjunctival injection. However, the spreading is not complete and it seems that the ciliary arteries of the choroid limit the spreading (Chiang et al., 2016). The suprachoroidal route avoids direct entry into the inner eye and decreases the risks for endophthalmitis, retinal detachment, and cataract formation. Compared to the sub-conjunctival delivery the injection site is closer to the retina and choroid and higher bioavailability is expected. Pharmacokinetics of suprachoroidal drugs in solution has been studied in animal models. For example, suprachoroidal bevacizumab reached mainly the choroid, RPE and photoreceptor outer segments, whereas intravitreal drug distributed more to the inner retina (Olsen et al., 2011). Suprachoroidal microneedle injections were also used recently in humans (Morales-Canton et al., 2013). Suprachoroidal drug delivery has been recently reviewed in more detail (Rai et al., 2015).

Bioavailability of suprachoroidal drug to the retina and vitreal cavity depends on the rate of drug elimination to the choriocapillaries and permeability of the drug across the RPE (Fig. 17). The drug must pass through the RPE to reach the neural retina, but a major part of the drug dose will be lost to the choroidal blood flow (Ranta et al., 2010). Clearance to the blood flow is significant based on the high blood flow in the choroid (62 ml/h in rabbit, 43 ml/h in man) and leakiness of these vessels (70–80 nm holes) (del Amo and Urtti, 2015). *In vivo* studies demonstrated that the choroidal compounds disappeared to the blood circulation rapidly in minutes or hours (Abarca et al., 2013; Bill, 1968; Bill et al., 1980; Kim et al., 2014; Törnquist, 1979). Delivery to the vitreous, sclera and retina increased by an order of magnitude in non-perfused eyes, further demonstrating the importance of blood flow as mechanism of drug loss (Abarca et al., 2013). Obviously, choroidal bioavailability at least at the injection site is 100%, but the retinal bioavailability depends on the competing processes of the RPE permeation and choroidal drugs loss. Based on the kinetic model of Ranta et al. (2010) the retinal bioavailability can be estimated to be in the range of 0.2–4%.

Even though retinal bioavailability of suprachoroidally injected drug in solution would be adequate, the duration of drug action is too short after injection of the drug solution. Half-lives of compounds in the suprachoroidal space vary between 1.2 and 7.9 h for sodium fluorescein, dextrans and bevacizumab (Patel et al., 2012). This means that the solution-based injections should be given frequently and this is not acceptable in the clinical practice. Prolongation of action is necessary to make suprachoroidal drug administration attractive in a clinical setting. Controlled drug release formulations have been tested for suprachoroidal administration. Compared to the solution, non-biodegradable fluorescent polystyrene particles (20 nm-10 µm in size) stayed in the suprachoroidal space much longer (at least 1–2 months) (Patel et al., 2012). Clinically, non-degradable particles are not feasible for suprachoroidal administration, because they would accumulate to the tissue and their rescue from the tissue is difficult. The study of Patel et al. (2012) demonstrated that the polystyrene particles are not effectively cleared from the suprachoroidal space and prolonged drug release would be a possible approach for biodegradable formulations. Triamcinolone acetonide suspension has been given as suprachoroidal injection and the drug produced high concentrations in the retina and vitreous (Chen et al., 2015). In this

case, triamcinolone acetonide was continuously delivered to the retina over a prolonged time and this treatment was found effective in the porcine model of posterior uveitis (Gilger et al., 2013).

We used the model from Ranta et al. (2010) to evaluate the relationships between dose, drug release rate and expected drug concentrations in the neural retina-vitreous compartment (Fig. 17). We simulated the pharmacokinetics after suprachoroidal injections of 10 μl. Drug bioavailability to the vitreal compartment was simulated for a small lipophilic drug, a small hydrophilic drug and a macromolecule. Compared to the sub-conjunctival injection the bioavailability increased 6–23 fold: 1.5%, 0.19% and 4.2%, for lipophilic, hydrophilic and macromolecule compound, respectively. These findings suggest that lipophilic drugs and biomacromolecules benefit more than small hydrophilic drugs from the suprachoroidal route when the scleral barrier is avoided. The simulated concentrations in the retina/vitreous for the small molecules and macromolecule are shown in Fig. 19. The simulated dose was 1 mg. We can conclude that a long duration of action (2–4 months) can be reached for macromolecules that require at least concentration of 0.01–0.1 μg/ml for activity. For small molecules, it is difficult to obtain long duration: only the slow release (0.001 h^{-1}) and potent drug (active at 1 ng/ml) are expected to yield long duration of drug action (2–4 months). If we assume that the molecular weights are 500 and 50,000 for small drugs and macromolecule, respectively, the potency limits for the macromolecules would be 10^{-8}-10^{-7} M and 10^{-9} M for small molecules at the dose of 1 mg. In the case of choroidal targets the situation is easier, because the bioavailability is practically 100%. However, the rapid choroidal clearance decreases these concentrations. We can estimate that the potency limit for long action in the choroidal extracellular targets is in the range of 2 x 10^{-7} - 10^{-6} nM.

Retinal and choroidal bioavailability of drugs after suprachoroidal injection is higher than the bioavailability after transcleral drug delivery. The overall conclusion is that suprachoroidal drug administration shows approximately one order of magnitude higher retinal and choroidal bioavailability than sub-conjunctival drug delivery. Suprachoroidal drug delivery is suitable for potent drugs that are active at low concentrations, especially in the case of retinal targets. Prolonged retention of the formulation and controlled release over months is preferable. Otherwise, this mode of administration is not clinically attractive. Other pending issues are reproducibility of injections to the small tissue and the requirement for biodegradable formulations, because the delivery system cannot be rescued from this tissue in the case of problems.

7. Sub-retinal drug delivery

Sub-retinal injections are used in some specialized experimental purposes when delivery of therapeutics is aimed to reach the RPE or photoreceptors. The injection is applied between the RPE and neural retina. This leads to formation of a bleb that disappears later when the aqueous solution is resorbed to the body. This is technically demanding delivery method that is used only in quite specialized clinical applications and in early phase ocular pharmacological experiments with mice and rats.

Sub-retinal injection of tissue plasminogen factor is used to assist the removal of sub-retinal haemorrhage (Sandhu et al., 2010). Sub-retinal implant (i.e. artificial retina) product has been recently accepted for clinical use (Stingl et al., 2015), but this is not drug containing system. Furthermore, stem cell derived retinal cells and viral vectors for gene therapy have been applied sub-retinally. Namely, some adeno associated virus 2 based systems are in clinical trials with promising results in the treatment of retinal degenerations (Bainbridge et al., 2015; Maguire et al., 2008; Weleber et al., 2016). However, it is important to note that these are special

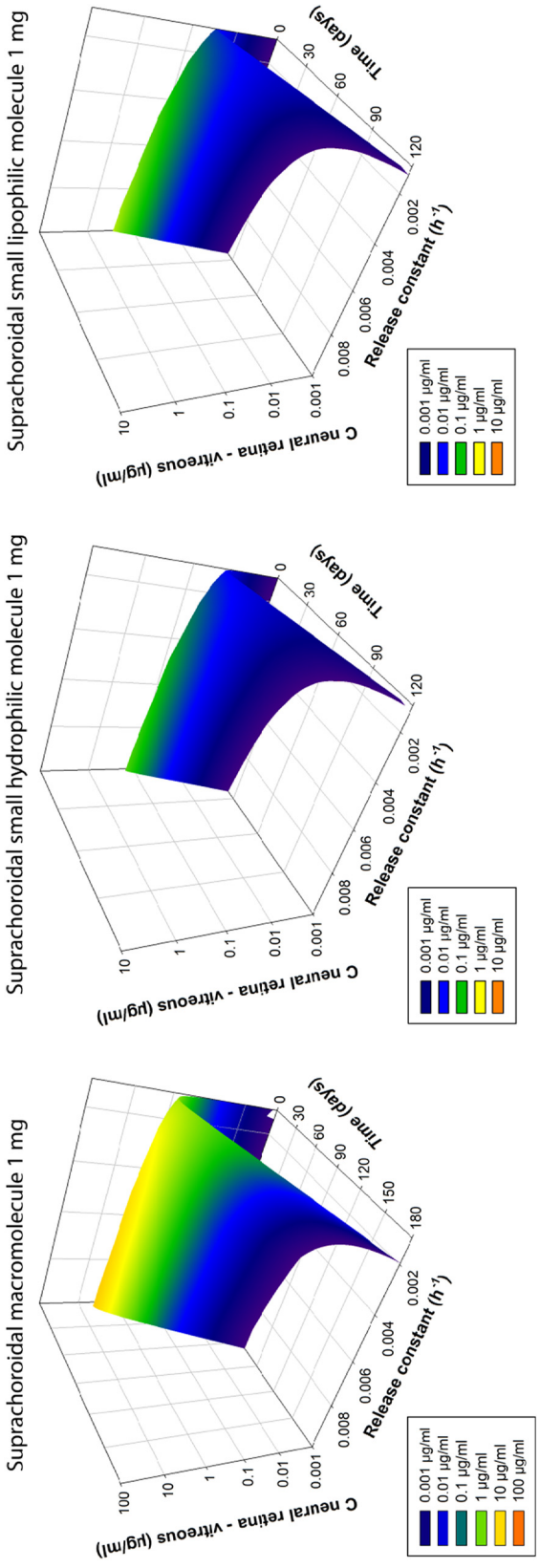

Fig. 19. Simulated time courses of drug concentrations in the neural retina-vitreous compartment after suprachoroidal drug delivery at dose of 1 mg in formulations with different rates of drug release (unpublished simulations). The simulated concentrations are represented by the colour range.

applications. In chronic treatments sub-retinal injections should have long duration of action (preferably years per injection).

8. Topical drug delivery

8.1. Drug absorption, distribution and efficacy

Topical ocular drug delivery with eye drops is commonly used in the treatment of anterior segment disorders, such as elevated intraocular pressure, infections and inflammations. The eye drops are instilled daily or several times per day to deliver small molecular weight drugs to the anterior segment tissues. Most clinical drugs have adequate corneal permeability for transcorneal drug absorption into the anterior chamber. Ocular bioavailability, determined from aqueous humor, is typically in the range of 1–4%, but much less for small hydrophilic drugs and practically zero for proteins (Maurice and Mishima, 1984; Urtti et al., 1990). Low bioavailability is due to the rapid drainage of eye drops from the ocular surface and systemic absorption through conjunctiva (Maurice and Mishima, 1984; Urtti et al., 1985). From aqueous humor the drugs distribute easily to the iris, ciliary body and lens, and they are eliminated via aqueous humor outflow and venous blood flow of the anterior uvea (Maurice and Mishima, 1984; Urtti, 2006). Corneal permeation of the drug depends on its lipophilicity (Huang and Schoenwald, 1983; Kidron et al., 2010), and results in typical drug distribution pattern with concentrations in the tissues following the order lacrimal fluid $\gg$ cornea $>$ aqueous humor $\approx$ iris $\approx$ ciliary body $>$ anterior sclera $>$ lens $\gg$ retina $\approx$ choroid $\approx$ vitreous humor (Chien et al., 1990; Urtti et al., 1990). Aqueous humor flow, blood flow in the iris and ciliary body and the lens barrier prevent effective drug distribution to the posterior segment (Maurice and Mishima, 1984). Typically, drug concentrations in the vitreous are 10 and 100 times less than in the aqueous humor and cornea, respectively, but the concentrations are detectable with sensitive analytical methods (Urtti et al., 1990). It is unlikely that improvements in drug corneal permeation would lead to any significant improvements in retinal drug delivery.

The non-corneal route of drug absorption through the conjunctiva and sclera was demonstrated in the studies in which the corneal and conjunctival drug absorption processes were isolated from each other with a cylinder around the cornea thereby allowing drug instillation only on the corneal or conjunctival surface (Ahmed and Patton, 1987, 1985; Chien et al., 1990; Doane et al., 1978). Drug exposure on only the cornea lead to the typical drug distribution pattern that is seen without the cylinder, lipophilic small molecules (brimonidine, timolol) being delivered transcorneally to the aqueous humor, whereas the conjunctival exposure results in low aqueous humor drug levels, but improved delivery to the posterior segment, and this was seen also in the case of bigger molecules like inulin (Ahmed and Patton, 1985; Chien et al., 1990). The routes of ofloxacin absorption were also explored in a recent study in which hydrogel lenses (corneal and cornea-conjunctival lenses) and rings that are in contact with the conjunctiva were used (Shikamura et al., 2016). All hydrogels showed improved ofloxacin absorption as compared to the eye drops, likely due to the longer contact with the ocular surface. The hydrogel rings resulted in about 10 and 40 times higher ofloxacin levels in the retina-choroid than the corneal hydrogel lens and eye drops, respectively, and to much higher levels in the conjunctiva and sclera. Shikamura et al. (2016) also showed gradually declining levels in the ocular segments from the anterior to the posterior part of the eye, the anterior retina had about 10 times higher levels than the posterior retina. Poly(-hydroxyethyl methacrylate) hydrogel ring released about 1 mg of ofloxacin in 9 h and resulted in the posterior retina concentrations of 0.1 μg/ml (about 10^{-7} M) during the drug release period, but this approach would require daily administration of new hydrogel rings. Note that the dosing rate here is 10–100 times higher than the initial maximal release rate in the sub-conjunctival simulations (Fig. 18). For example, release of 1 mg of the drug during 1–4 months should result the concentrations of about 10^{-10} - 10^{-9} M in the retina, limiting this approach to the retinal delivery for highly potent compounds.

Based on the tissue distributions it is likely that the permeation routes for non-corneal absorption are as shown in Fig. 20. The non-corneal route through the conjunctiva, sclera and choroid might be a useful strategy for the delivery of drugs from the ocular surface to the retina. A major advantage of this approach is that it is non-invasive and allows self-administration of the drugs.

In order to reach higher drug levels in the retina, long acting topical drug delivery systems should be able to localize on the conjunctival surface, incorporate high drug dose, and maintain high dosing rate over prolonged times. With eye drops, bioavailability is lower than with the drug delivery systems, but on the other hand, eye drops can be instilled frequently to maintain high dosing rate. Patient compliance is an important issue in topical self-administered medications. For example, compliance is only 56% in chronic treatment of glaucoma with eye drops (Reardon et al., 2011).

In clinical practice eye drops are not used for drug delivery to the posterior eye segment, because they are not effective treatment. Nevertheless, drug delivery from eye drops to the vitreous and/or retina has been shown in numerous studies (Acheampong, 2002; Hu and Koevary, 2016; Inoue et al., 2004; Kiuchi et al., 2008; Koevary et al., 2002; Takahashi et al., 2003). Many studies have been done in small animals (mice, rats) and these results are probably not translatable to humans. In mice and rats, the barriers are thinner, distances are smaller and drug distribution from blood circulation to the eyes is also more significant than in humans (because the systemic drug clearance and volume are much smaller than in humans). Many studies are based on qualitative methods, such as imaging or histology (Kiuchi et al., 2008; Takahashi et al., 2003). In those cases, it is difficult to assess the quantitative significance of the results. However, also many rabbit, monkey and human studies claim successful drug transfer to the retina and/or choroid from eye drops (Acheampong, 2002; Chastain et al., 2016; Genead and Fishman, 2010; Hughes et al., 2005; Kent et al., 2001; Tajika et al., 2011; Takahashi et al., 2003). We shall discuss these

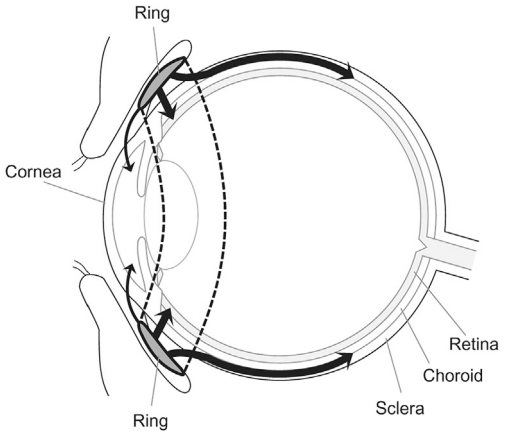

Fig. 20. Potential routes of drug penetration from conjunctival surface to the inner eye tissues are shown. Drug transfer through conjunctiva and sclera leads to different tissue distribution than typical transcorneal absorption from the eye drops (from Shikamura et al. (2016) with permission from Taylor & Francis Group).

studies in more detail.

Clear non-corneal local distribution to the posterior segment was shown for topical brimonidine. About 20 times higher vitreal brimonidine concentrations were seen in the treated cynomolgus monkey eyes as compared to the untreated contralateral eye (Acheampong, 2002). In this case, the pattern of drug concentrations in the ocular tissues resembles the distribution after pure conjunctival exposure (i.e. drug concentrations 10–60 times higher in the anterior sclera than in the aqueous humor) supporting the drug distribution routes shown in Fig. 20. In fact, brimonidine concentration in the vitreous of humans after 1–2 weeks of multiple eye drop dosing was clearly higher (185 nM) than the EC_{50} for α_2-receptors (2 nM) (Kent et al., 2001). It is noteworthy that brimonidine binds strongly to the pigmented tissues around the vitreous. Peak levels and AUC values of ^{14}C-brimonidine borne radioactivity in the pigmented iris, ciliary body and retina/choroid were 400–9000 and 1400–11,000 times higher than in the vitreous, respectively (Acheampong, 2002). It is very difficult to avoid any cross-contamination in this kind of studies, especially when the neighbouring tissues have 10^2–10^4 times higher drug levels than the vitreous. Therefore, it is difficult to judge whether the radioactivities in the vitreous represent free brimonidine concentrations in the retina. The rationale of this study was to provide neuroprotective effects in the retina with topical brimonidine. Neuroprotective efficacy of topical brimonidine was shown in rodent models (Kim et al., 2015), but yet the clinical development of brimonidine is based on the intravitreal implant technology (Holz et al., 2014; Querques et al., 2015).

Even though the efficacy of eye drops in the clinical treatment of retinal conditions is considered to be inadequate, there are reports showing pharmacological effects of eye drops in retinal patients. Patients with either retinitis pigmentosa or Usher syndrome received treatment of cystoid macular oedema with topical dorzolamide eye drops (Fishman and Apushkin, 2007; Genead and Fishman, 2010; Grover et al., 2006). Optical coherence tomography showed a decrease in the central foveal zone thickness in most cases and visual acuity improved in almost one-third of the patients. On the other hand, topical treatment of cystoid macular oedema (after cataract surgery) with non-steroidal anti-inflammatory eye drops (e.g. phenoprofen, ketorolac, indomethacin) was shown to have insufficient efficacy in a compiled analysis of the clinical studies (Sivaprasad et al., 2005). Interestingly, Bayer was developing a topically applied small molecule drug (regorafenib) to treat neovascular age-related macular degeneration. This drug had 200 and 7 times higher drug concentrations in the posterior eye segment than in plasma in rats and monkeys, respectively (Joussen et al., 2016). However, this drug failed due to inadequate efficacy in clinical phase 2b studies.

8.2. Strategies for posterior segment drug delivery

Fig. 20 illustrates the likely route for posterior segment drug distribution after topical administration. The relevant physical barriers are the conjunctiva, sclera and RPE, and the flow barriers include blood and lymphatic flows in the conjunctiva and choroid. Five main factors are affecting the potential success of topical drug delivery to the posterior segment: 1) retention time on the ocular surface; 2) permeability and transport in the barrier membranes (conjunctiva, sclera, RPE); 3) role of the flow factors (drug loss or distribution to the tissues); 4) preferential homing of drug to the retina (e.g. melanin binding); 5) potency of the drug and target (e.g. neural retina, RPE or choroid); 6) drug dose and dosing rate on the ocular surface.

Rapid elimination of eye drops from the ocular surface limits drug absorption, but the bioavailability can be increased with prolonged drug retention on the ocular surface (Maurice and Mishima, 1984). However, the maximal attainable bioavailability is limited to about 10% by the conjunctival systemic drug absorption and tear turnover processes that cannot be stopped (Kyyrönen and Urtti, 1990; Urtti et al., 1990). Retention time on the ocular surface can be increased with various technologies that have been reviewed previously (Cholkar et al., 2013; Kim et al., 2014). The effect of prolonged conjunctival retention on the posterior segment drug delivery was demonstrated recently (Shikamura et al., 2016). In the case of ofloxacin, drug concentrations in the posterior segment were increased 40 fold with the hydrogel ring as compared to the eye drops. The level of improvement depends on the drug, but the retention factor is always important for the improvement of posterior segment drug delivery.

Drugs must be able to permeate in the barrier membranes in order to reach the retina. Two barriers are lipoidal epithelia with tight junctions (conjunctival epithelium and RPE), whereas the sclera is a porous membrane with a mesh size that allows permeation of macromolecules (Prausnitz and Noonan, 1998). Lipophilicity has an impact on drug permeability in the conjunctiva (Ahmed and Patton, 1987) and the RPE (Pitkänen et al., 2005). The extravascular choroid and Bruch's membrane are much more leaky than the RPE and conjunctiva; therefore, they are not considered to be permeation rate limiting barriers (Miller and Edelman, 1990; Pitkänen et al., 2005). Permeability of the conjunctiva, sclera and RPE are compared in Table 3. It is obvious that the sclera is the most permeable membrane, particular in the case of hydrophilic and large compounds. Therefore, permeation enhancement strategies should rather focus on the rate limiting barriers, i.e. conjunctiva and RPE. It is easier to modify the conjunctival transport than the RPE, because the conjunctival epithelium is on the ocular surface and the manipulations can be controlled more accurately. Targeting the drug transporters is one potential approach, but the knowledge of transporters in the conjunctiva and RPE is too limited for this strategy (Mannermaa et al., 2006).

Table 3
Permeability coefficients of drugs in the conjunctiva, RPE and sclera. Typical values for small molecules (lipophilic, hydrophilic) and macromolecules are shown.

Membrane	Permeability of small lipophilic drugs ($\times 10^{-6}$ cm/s)	Permeability of small hydrophilic drugs ($\times 10^{-6}$ cm/s)	Permeability of macromolecule ($\times 10^{-6}$ cm/s)	Data sources
Conjunctiva	2.4–9.8 (tizanidine, dexamethasone, betaxolol, indomethacin, propranolol, fluconazole. fluorometholone)	0.6–1.2 (acetazolamide, nadolol, cephalexin ampicillin, atenolol)	0.01–0.08 (myoglobin, lysozyme, α-lactalbumin	Unpublished data; *ex vivo* porcine tissue in diffusion chambers
Sclera	6.5–71 (timolol, ethoxolamide, hydrocortisone)	6.6–44 (benxolamide, penicillin G, 5-fluorouracil, sucrose)	1.9–4.3 (FITC dextrans 40 and 70 kDa)	Prausnitz and Noonan (1998), *ex vivo* sclera
Retinal pigment epithelium	8.4–16.7 (timolol, betaxolol)	1.0–5.6 (carboxy fluorescein, atenolol, pindolol, nadolol)	0.03–0.05 (FITC dextrans 40 and 80 kDa)	Pitkänen et al. (2005) (*ex vivo* bovine RPE)

On the other hand, drug delivery across the conjunctiva might be improved with nanoparticles that are internalized and transcytosed. Davis et al. (2014) used a topical liposomal drug carrier with anionic phospholipid binding protein annexin A5 to deliver bevacizumab to the rabbit vitreous and retina. These liposomes were able to undergo transcytosis process in the corneal epithelium, and they possibly transcytose in the conjunctiva. Bevacizumab from eye drop solutions had negligible permeation to the rabbit retina and vitreous, but after the liposomal eye drops, a bevacizumab concentration of 18 ng/ml was reached in the retina. This is higher than the anti-VEGF EC_{50} of bevacizumab *in vitro,* but less than the required concentration of bevacizumab *in vivo* (Hutton-Smith et al., 2016). Nevertheless, the study of Davis et al. (2014) shows a rational strategy to overcome the ocular epithelial barriers for posterior segment drug delivery.

Blood flow and lymphatic flow are effective in the conjunctiva and choroid (Robinson et al., 2006; Schroedl et al., 2014). It has been demonstrated that inulin (MW about 5000 Da) permeated at higher amounts to the posterior eye segment than small lipophilic timolol (Ahmed and Patton, 1987, 1985). This result was explained by the slower removal of inulin to the blood flow in the conjunctiva. Rabbit experiments have also shown that small lipophilic prednisolone is cleared from the sub-conjunctival space 64 times more rapidly than Gd-albumin, and most of the sub-conjunctival drug is cleared to the systemic circulation (Kim et al., 2008; Lee and Robinson, 2004; Ranta et al., 2010). Thus, it might be possible to minimize drug loss to the blood circulation using vasoconstrictors, such as phenylephrine. This approach has been used in the context of timolol administration. Even though phenylephrine coadministration reduced the peak concentrations of timolol in plasma by 80% (Kyyrönen and Urtti, 1990) ocular timolol concentrations were not affected, possibly because timolol is primarily absorbing to the eye via the cornea (Ahmed and Patton, 1985). Effects of blood flow may be complex because blood is flowing in many directions. Some surprising results may be due to unexpected blood flow effects. For example, small (70 nm) transferrin targeted liposomes (HSPC/cholesterol/DSPE-PEG-Transferrin/ATTO-DOPE; molar ratios of 2: 1: 0.02: 0.005) were found in the RPE already 5 min after the topical instillation (Lajunen et al., 2014). Normal permeation across the barriers cannot take place so fast. Therefore, some blood flow factor might explain these findings.

Some drugs may also have preferential targeting to the retina or choroid. The most common mechanism is melanin binding in pigmented animals, which leads to increased concentrations in these tissues (Acheampong, 2002; Salminen and Urtti, 1984). Melanin binding may lead to 1–2 orders magnitude increases in the drug concentrations (e.g. pigmented retina and choroid compared to the non-pigmented vitreous). This does not necessarily translate to the increased drug effects, because most of the drug in the pigmented cells is bound to melanin and not free for receptor binding (Rimpelä et al., 2016). Melanin binding will be discussed in more detail later in this review (section 9.2.).

Drug potency and dose are the final strategic points. It is evident that the retinal bioavailability is low after topical administration ($\ll$ 0.1%), but the concentrations that are needed for pharmacological activity are compound dependent. Topical administration may be suitable only for highly potent compounds that are active at low concentrations, preferably in the nanomolar or picomolar range.

Topical drug administration to treat retinal diseases is a major challenge and no solid success has been shown, even though many encouraging results have been published. The route of drug absorption and distribution to the retina is complex and includes many barriers. A combination of beneficial features in the delivery system design may lead to improvements that enable topical non-invasive drug delivery to the back of the eye. Successful delivery system should retain on the ocular surface and release drug at adequate rate.

9. Retinal pharmacokinetics and drug delivery at cellular level

9.1. Challenge of intracellular targets in the retina

Retinal diseases are a large group of different disorders that are affecting different cell types, such as the RPE (dry age-related macular degeneration, proliferative vitreoretinopathy), photoreceptors (rare inherited retinal degenerations), ganglion cells (glaucoma), and endothelial cells (neovascular disorders). New potential cellular and extracellular drug targets and compounds with new mechanisms of action are being developed (Zhang et al., 2012). The emerging compounds are small molecular compounds, proteins, and RNA- and DNA-based therapeutics. The diseases, targets and new compound classes have been presented in more detail elsewhere in the literature. It is also worth noting that the current anti-VEGF therapies have also been put under scrutiny as it is becoming increasingly evident that some VEGF isoforms possess antiangiogenic and neuroprotective properties, thus rendering their inhibition undesirable and emphasizing a need for more selective blocking of pro-angiogenic VEGF isoforms (Amadio et al., 2016).

Drug delivery challenges include prolongation of drug action, drug targeting to the retina and the issues of administration routes, as discussed earlier. However, there are also cellular level factors that are important. The retinal cells are protected by the plasma membrane and they contain complex systems for intracellular organelles. These membranes form cellular level barriers that limit the delivery of drugs to the intracellular targets, especially in the case of hydrophilic drugs and biologicals. The intracellular targets include, for example, intracellular protein aggregation cascades in geographic atrophy, inflammasomes, and genetic defects of the photoreceptors (Arango-Gonzalez et al., 2014; Hanus et al., 2013; Kauppinen et al., 2016). Some of the emerging therapeutic strategies impose major challenges to the cellular drug delivery: CRISPR/Cas9 gene editing approach is a potentially attractive system for the treatment of genetic retinal degenerations (Nash et al., 2015), but the delivery of this system (including both RNA and protein) is difficult. Likewise, siRNA, miRNA and mRNA are not effectively delivered to their target sites in the cytosol and nucleus without carrier systems (Xue et al., 2015). Gene therapy relies on carrier systems that are mostly based on modified viruses, such as AAV-2 (Schön et al., 2015). Also, many proteins have intracellular sites of action, but limited intracellular permeation (e.g. HSP-70, transcription factors) (Subrizi et al., 2015).

Properties of different retinal cell types from a drug targeting point of view have not been investigated systemically. Therefore, this review presents general principles of intracellular and non-viral drug and gene delivery. These principles are applicable with specific modifications to the retinal cells. Intracellular targeted drug delivery requires that the carrier systems reach the surface of the target cells, but several barriers limit their access to the target cells (e.g. the inner limiting membrane, outer limiting membrane, RPE) (section 3.3). In general, drug carrier systems rely on endocytosis or phagocytosis processes for cellular uptake (Friend et al., 1996; Wrobel and Collins, 1995) (Fig. 21). Thus, cellular uptake depends on the inherent activity of the endocytic machinery of the cells. Macrophages, Müller cells and RPE cells are phagocytic and able to ingest even micron sized particles (Tuovinen et al., 2004), but the internalization to the photoreceptors and many other cells is much more difficult (Reinisalo et al., 2003). Even if the nanoparticles can diffuse and reach the cell surface, the cellular uptake may be at least

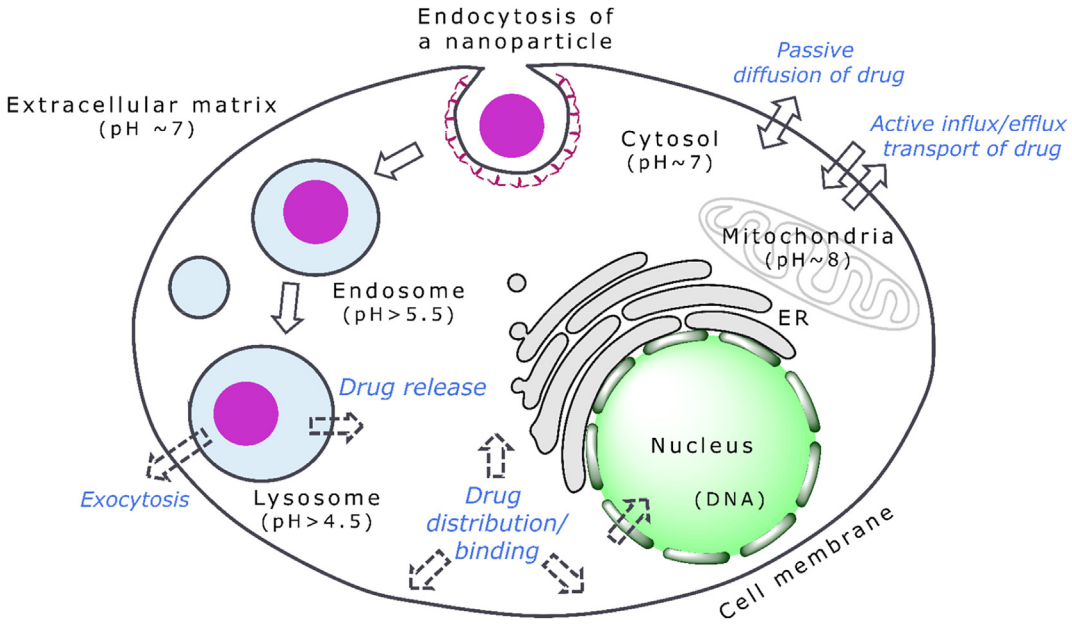

Fig. 21. Illustration of the intracellular routes of nanoparticle delivery, adapted from Soininen (2016).

partly blocked if extracellular proteins and glycosaminoglycans (e.g. from the vitreous) have bound to the nanoparticle surface (Ruponen et al., 1999; Xu and Szoka, 1996). These mechanisms can be effectively studied with cells in culture.

After internalization of the nanoparticles there are still many intracellular hurdles before the impermeable drug can be delivered to the cytosol or nucleus (Fig. 21). A detailed discussion of endocytic pathways is beyond the scope of this review. Certain pathways and cell types may be targeted with ligands that recognize receptors (Conner and Schmid, 2003). Such ligands can be linked to the surface of the nanoparticles or to the conjugates. Generally, endocytic and phagocytic routes are trafficking the cargo to the lysosomes (Gruenberg and van der Goot, 2006) (Fig. 21). Sometimes lysosomes can be relevant target organelles (e.g. lysosomal storage diseases, dry age related macular degeneration), but lysosomal delivery of sensitive drug cargoes should be avoided. For example, RNA, DNA and many proteins are degraded and inactivated due to the enzymatic activity in the lysosomes (Fonseca et al., 2009). There are several technologies that have been used to facilitate drug release from the endosomes to the cytosol to avoid lysosomal localization: 1) pH sensitive materials that will fuse to the endosomal wall (Chu et al., 1990). These systems rely on the acidification of the endosomes during their maturation (pH decrease in about 30 min from 7.4 to 5.0–5.5); 2) Endosomolytic peptides (Fattal et al., 1994; Wagner et al., 1992); 3) Light triggered release from gold nanoparticle containing liposomes (Lajunen et al., 2015); 4) Osmotic effects due to the proton sponge effect (Boussif et al., 1995). Another challenge is the release of the drug from the carrier system, because only the free drug is able to exert the pharmacological actions. The release can take place using pH sensitive structures (e.g. pH sensitive liposomes), enzymatic or hydrolytic mechanisms, external signal based induction (e.g. light activation, magnetic field) or electrostatic exchange of the carrier with endogenous compounds (e.g. oligonucleotide release from the cationic liposomes based on the fusion to the endosomal wall) (Jääskeläinen et al., 1994; Karimi et al., 2016; Zelphati and Szoka, 1996). In the case of nuclear targets, the drug must be able to get across the nuclear envelope (Fig. 21). The nuclear membrane has pores that allow diffusion of molecules that are smaller than 100 kDa; therefore, oligonucleotides can cross this barrier, but plasmid DNA does not (Dowty et al., 1995; Ludtke et al., 1999; Wang and Brattain, 2007). Larger molecules can enter the nucleus if the cells are dividing (Brunner et al., 2000; Männistö et al., 2007), but this is rarely the case in retinal disease.

There are a few retinal examples of intracellular targeted drug delivery. For example, when peptide for ocular delivery (POD), a peptide capable of delivering e.g. siRNA and DNA to murine retinal and ocular tissues *in vivo* (Johnson et al., 2008), was fused together with green fluorescent protein (GFP), this endogenously expressed POD-GFP fusion protein was also observed to localize in the nucleus in human embryonic retinoblast cells *in vitro* (Johnson et al., 2010). Additionally, another study demonstrated how both nucleolin binding peptide-conjugated DNA and GFP were uptaken and guided into the nucleus of retinal and corneal cells *in vivo* (Binder et al., 2011), further attesting the functionality of certain cell penetrating peptides also as nuclear localization signals.

Overall, the cellular level barriers for biologicals are formidable, and currently there are no clinically used biologicals in ophthalmology that have intracellular sites of action. The eye is an attractive target organ, because local drug administration can be used to avoid many complex issues in the systemic circulation.

9.2. Pigment binding

9.2.1. Melanin and melanosomes

Many drugs bind to melanin and this may modify ocular drug distribution significantly (Potts, 1964). Melanin binding can increase total drug concentrations in the pigmented tissues and it can prolong the duration of drug action (Salazar et al. (1976); Salazar and Patil (1976); Salminen and Urtti (1984); Urtti et al. (1984)). Several ocular tissues contain melanin, including the retinal pigment epithelium and choroid.

Melanins are a diverse group of polymers. The most common forms of melanin in the human body are eumelanin and pheomelanin (D'Ischia et al., 2015). In melanin biosynthesis, melanogenesis, L-dihydroxyphenylalanine (L-DOPA) and other intermediates of melanin such as L-dopaquinone, L-cysteinyldopa, 5,6-dihydroxyindole (DHI) and 5,6-dihydroxyindole-2-carboxylic acid

(DHICA) are synthesized from tyrosine by tyrosinase enzyme (Simon et al., 2008). These intermediates polymerize to black or brownish eumelanin and yellow/reddish pheomelanin. The majority of melanin in the RPE is eumelanin whereas melanin in choroidal melanocytes consists of a mixture of eumelanin and pheomelanin (Hu et al., 2008; Wakamatsu et al., 2008).

Melanin is synthesized and packed within melanosomes, cell organelles displaying similarities with lysosomes (Fig. 22) (Raposo and Marks, 2007; Wasmeier et al., 2008). The melanosomes have four developmental stages from depigmented to mature stage IV melanosomes. Synthesized melanin is deposited onto melanosomal PMEL17 protein fibrils that form the protein component in natural melanin. Melanogenesis takes place at neutral melanosomal pH that is optimal for tyrosinase activity. Tyrosinase enzyme displays low or no activity at luminal pH below pH 5. The melanosomal pH in adult RPE cells is unknown, but due to halted melanin synthesis one can assume that the luminal pH is acidic. In contrast to choroidal melanocytes with continuous melanin synthesis through the lifespan, in the RPE, the bulk of melanin/melanosomes is synthesized during fetal development. In the RPE, melanin is stored in melanosomes until senescence, with no turnover (Boulton, 2014; Lopes et al., 2007). Melanosomes protect the retina against solar radiation (Sanyal and Zeilmaker, 1988; Sarna et al., 2003) and maintain the cellular homeostasis of metal ions and oxidative stress (Hong and Simon, 2007; Hu et al., 2008). Peripheral regions of the RPE have the highest melanin concentrations and the macular region has the lowest (Schmidt and Peisch, 1986). Levels of RPE melanin decrease during age-related macular degeneration (Sarna et al., 2003; Thompson et al., 2007). Aging decreases the melanin levels in the RPE, but increases the concentration in the choroid (Boulton and Dayhaw-Barker, 2001; Schmidt and Peisch, 1986; Wakamatsu et al., 2008).

9.2.2. *Binding of drugs to melanin*

Melanin binding of drugs has been observed already decades ago, but the binding still remains poorly known (Leblanc et al., 1998; Potts, 1964). Melanin is a negatively charged polymer with carboxylic groups (Ito, 1986) and melanin granules are about one micron sized particles (Pitkänen et al., 2007). The substances that bind to melanin are a heterogeneous group of drugs (e.g. antibiotics, beta blockers, antipsychotics, antimalarial drugs), dyes, herbicides, alkaloids and metals (Dayhaw-Barker, 2002; Hollo et al., 2006; Larsson, 1993; Leblanc et al., 1998). Both eumelanin and pheomelanin are capable of binding drugs (Mårs and Larsson, 1999). Leblanc et al. (1998) conclude in their review that lipophilic and basic (positive LogP, pKa over 7) bind preferably to melanin. However, the structural features that drive melanin binding of drugs have not been explored systematically.

The mechanisms of drug binding to melanin are not well known, but it is believed that ionic interactions, van der Waals forces, hydrophobic interactions, and charge-transfer interactions may be involved in binding (Larsson, 1993). Many investigators have used one- and two-site Langmuir binding models to describe the binding equilibria of drugs with melanin. Recently, a more realistic Sips binding model was used to take into account the nature of drug binding with melanin, i.e. charged surface without specific binding pockets and drug molecules moving around on the surface (Manzanares et al., 2016). Melanin binding of drugs has typically low affinity (millimolar or micromolar) and high capacity (large quantity of drug can bind to melanin) (Manzanares et al., 2016). In addition to the affinity, also the rate constants for association and dissociation of the drugs are important in defining the effects of binding on pharmacokinetics in the eye.

The effect of melanin binding on drug distribution in the back of the eye has been shown in *in vivo* (Robbie et al., 2013; Salminen and Urtti, 1984; Tanaka et al., 2004) as well as in *in vitro* studies (Pitkänen et al., 2007; Rimpelä et al., 2016). Melanin binding of drugs leads to significantly elevated drug concentrations (differences of 1–3 orders magnitude) in the pigmented tissues compared to the non-pigmented tissues or the tissues of albino animal. In some cases, the retention (chloroquine, ^{14}C-pazopanib, ^{14}C-GW771806, brimonidine) (Acheampong, 2002; Larsson and Tjälve, 1979; Robbie et al., 2013; Tanaka et al., 2004) and duration of drug action (atropine) (Salazar et al., 1976) can change dramatically in pigmented tissues (even to weeks or months). For example, the half-life of brimonidine elimination from pigmented iris of cynomolgus monkeys was 33 days, and the AUC values of brimonidine in iris, ciliary body and retina/choroid were 11,103, 1396 and 1561 times higher than in the vitreous humor after multiple topical drug dosing (Acheampong, 2002).

Cellular melanin binding of the drugs takes place in the melanosomes and there is a complex interplay of drug permeation across the cell membrane. Melanin binding may decrease the free drug concentration that is available for receptor binding, but on the other hand it can prolong drug retention in the cells and drug responses. In order to better understand these relationships melanin binding of drugs was recently studied using pure melanin, RPE cells and pigmented rats (Rimpelä et al., 2016). Melanin binding was modeled at cellular level for timolol and chloroquine (Rimpelä et al., 2016). We now extended this analysis to *in vivo* level to explore the interplay between plasma membrane permeation and melanin binding parameters in the RPE cells. Experimental melanin binding affinities of timolol and chloroquine were used (Rimpelä et al., 2016), the dissociation rate constant was set to 0.1 h^{-1} and plasma membrane permeability was varied. The simulations reveal interesting relationships (Fig. 23): 1) Melanin binding affects free drug concentrations in the RPE cells; 2) Prolonged maintenance of free drug concentrations in the cells is most pronounced when a

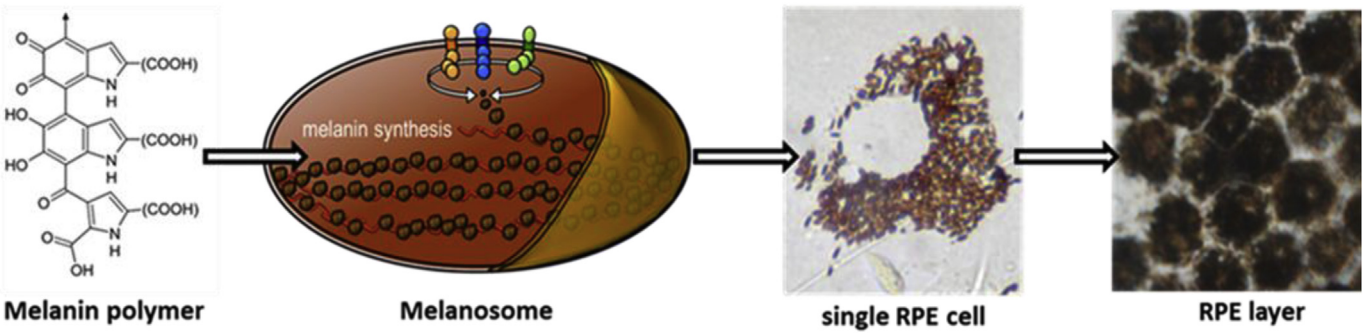

Fig. 22. Organization of melanin in the RPE cells.

low permeability drug binds to melanin, demonstrating that there is an interplay between plasma membrane permeation and melanin binding; 3) The longest retention and extremely slow elimination for chloroquine is seen if membrane permeability is low (10^{-7} cm/s). 4) Only a minor fraction (≪1%) of chloroquine in the RPE cells is in free form. Based on the simulations, the interplay of melanin binding with other transport processes in the cells determines the concentration profile of free drug within the cells. The interplay may explain the high impact of melanin binding on timolol and chloroquine concentrations in the pigmented tissues *in vivo* (Larsson and Tjälve, 1979; Rimpelä et al., 2016; Salminen and Urtti, 1984). It is known that chloroquine is retained in the pigmented ocular tissues for months.

Impact of melanin binding on drug safety is controversial. Melanin binding may protect the tissues from toxic effects (Larsson, 1993). Some melanin binders cause oculotoxicity, for example chloroquine, but others do not, suggesting that melanin binding as such is not causing toxicity (Dayhaw-Barker, 2002; Leblanc et al., 1998). Chronic exposure with toxic compounds that bind to melanin may cause adverse effects (Dayhaw-Barker, 2002; Larsson, 1993).

Overall, melanin binding is a significant factor that should be taken into account in the pharmacokinetics and design of drug delivery strategies. Melanin binding can lead to drug accumulation to the RPE and choroid, and to prolongation of drug effects when the drug is released gradually from the melanin depot (Robbie et al., 2013).

9.3. Transporters

9.3.1. Transporters in the blood-retinal barrier

The transporter proteins facilitate transfer of their substrates across the cell membranes. The transporters can be classified based on their gene family or on their functionality. There are 1555 genes in the human genome that are believed to express membrane transporters (Ye et al., 2014). About 287 transporters in the human genome are related to drug transport (Yan and Sadée, 2000). The largest gene families among these transporters are ABC transporters and SLC solute transporters. Furthermore, the transporters are usually localized to either the apical or basolateral side of epithelia and endothelia, and they transfer their substrates either into the cells (influx transport) or out from the cells (efflux transport). Active transport is a specific process, and therefore, the protein structure and its expression levels affect the rate of molecular transport. Obviously, this may give rise to the differences in the transport among different species, disease states, genetic imprints and ethnic origins. There are useful databases that collect information about the transporters, such as Human Transporter Database (Ye et al., 2014), UCSF-FDA TransPortal (Morrissey et al., 2012) and Transporter Classification Database (TCDB, 2016).

Transporters may have influence on the retinal drug delivery in many ways depending on the route of drug administration. Expression of the transporters in the BRB is the most important factor, because the BRB regulates transfer of small molecules from the eye outwards (intravitreal injection) and inwards into the eye (systemic, topical (trans-scleral route), sub-conjunctival, and suprachoroidal administration). Also, the cells of the BRB (RPE, retinal endothelia) host important drug target sites, for example the RPE cells are key players in the pathogenesis of age-related macular degeneration (Ambati and Fowler, 2012).

The transporter expression in the BRB was reviewed in 2006 (Mannermaa et al., 2006). The conclusion was that there are plenty of ocular drugs that are substrates to the transporters found in humans, but the expression or functionality of those transporters in the BRB was mostly unknown. Thereafter, newer reviews on this specific topic have been published (Hosoya et al., 2011; Jordán and Ruíz-Moreno, 2013). Table 4 shows the key data on the BRB transporters. We have selected to this table those transporters that have significant drug substrates or inhibitors and are known to be expressed at a protein level *in vivo* or in the cultured BRB cells. Note that the expression of some transporters in certain cells is only postulated, without *in vivo* confirmation. Also, it is important to realize that the mRNA and protein level data on expression are not truly quantitative, since no targeted quantitative proteomics have been used. Furthermore, exact localization of the transporters in the BRB is not known. Transporter proteins can be localized either on the blood side or on the retinal side. Expression and localization have a profound impact on the transporter functions. These features are important to study, because many BRB transporters are interacting with important and commonly used drugs (Table 4).

9.3.2. Functionality of transporters

The functionality of the transporters has been investigated in some cell culture studies to prove that the transporters are active. These transporters include MRP1 (Juuti-Uusitalo et al., 2012; Mannermaa et al., 2009; Nevala et al., 2008; Sreekumar et al., 2012), MRP2 (Ryhänen et al., 2008; Vadlapatla et al., 2013), MRP5 (Mannermaa et al., 2009), P-gp (Nevala et al., 2008; Zhang et al., 2012a, 2012b), and BCRP (Vadlapatla et al., 2013). Understanding of the active drug transport in the BRB is still far from complete, but there is evidence for the role of some transporters in drug delivery. For example, ofloxacin efflux in rabbit eyes (Senthilkumari et al., 2009) and the smaller than expected retinal uptake of digoxin and vincristine were explained by P-gp activity (Hosoya et al., 2010). Likewise, higher than expected retinal uptake of L-dopa in rats was explained by the active transport (Hosoya et al., 2010). Furthermore the inner blood-retinal barrier organic anion transporter 3 was shown to transport p-aminohippuric acid, benzylpenicillin, and 6-mercaptopurine from the vitreous/retina to the blood circulation (Hosoya et al., 2009). Intravitreal methotrexate resistance has been explained in one patient case (intraocular lymphoma) to be caused by increased MRP expression (Sen et al., 2008).

Transporters are subject to significant genetic polymorphisms that might cause inter-individual differences in pharmacokinetics and drug responses (Wolking et al., 2015), but this aspect has not been investigated in the context of drug delivery to the posterior eye segment. Likewise, the possible species differences in terms of transporter functions in the BRB are still unclear. Transporter expression should first be reliably quantitated and localized before these aspects can be studied in detail. They can be significant only in those cases (drug − transporter pairs) in which the active transport has a major role in pharmacokinetics, clearly surpassing the role of passive diffusion.

As discussed earlier (section 3) QSPR modeling of drug clearance has been performed from the rabbit vitreous (del Amo et al., 2015). The model was based on data from 40 compounds and it did not show clear outliers when a physico-chemical descriptor equation (including H-bonding and $LogD_{7.4}$) was plotted against the vitreal drug clearance. This indicates that among those 40 compounds, transporter activity did not significantly alter the drug clearance from the vitreous to the blood circulation as good correlation was achieved with purely physico-chemical descriptors, which are important determinants of passive drug diffusion across cellular membranes. The QSPR model for clearance across blood-ocular barriers was used as a component in the pharmacokinetic simulation model for prediction of drug transfer from the blood circulation to the vitreous in rabbits (Vellonen et al., 2016, section 4). Again, good correlation without striking outliers was obtained between the model and real data. However, in this case some over-

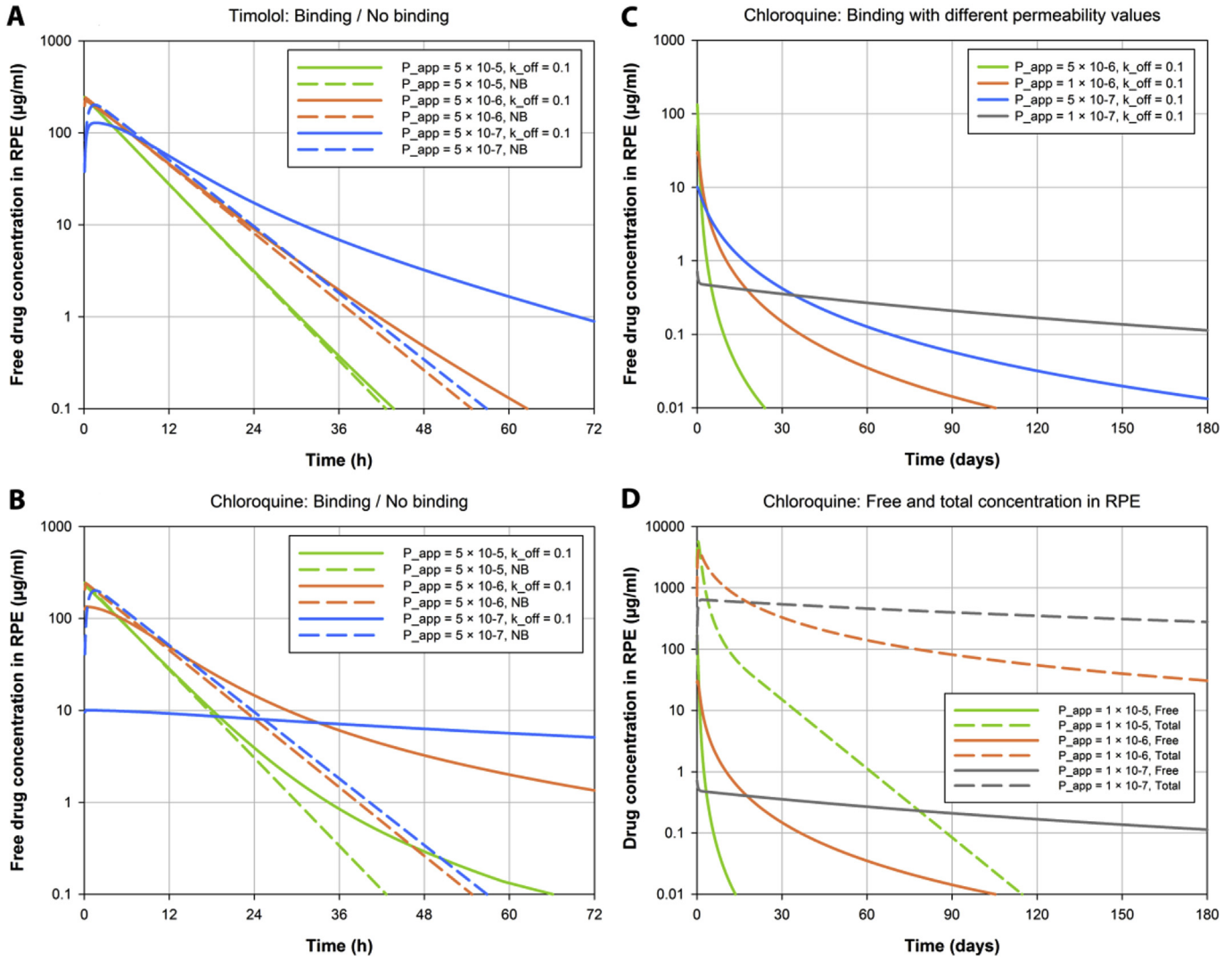

Fig. 23. Simulation of drug concentrations in the RPE cells *in vivo* at different melanin binding conditions (unpublished simulations). Binding affinities of timolol and chloroquine from Rimpelä et al. (2016) were used. The values of melanin binding affinity, rate constants for drug dissociation from melanin (k_{off} = 0.1 h^{-1}) and cell membrane permeability (P_{app} = 10^{-7}–10^{-5} cm/s) were modified in the simulations. A) Free concentration of timolol in the RPE cells at different plasma membrane permeabilities with and without (NB = no binding) melanin. B) Free concentration of chloroquine in the RPE cells at different plasma membrane permeabilities with and without (NB = no binding) melanin. C) Free concentration of chloroquine in the RPE cells. The drug is binding to melanin. Effects of plasma membrane permeability on drug concentration profiles over long time period (6 months) are shown. D) Free and total concentrations of chloroquine in the RPE cells at different plasma membrane permeabilities.

estimations of simulated vitreal drug distribution levels could be explained based on the transporter activity in the BRB (ciprofloxacin, fleroxacin, ofloxacin, mercaptopurine) (Vellonen et al., 2016). It seems that the transporter activity is capable of modulating the drug transport in the BRB, but passive diffusion seems to be the major factor in vitreous to blood clearance. Similarly, passive diffusion seems to be a key player, together with plasma protein binding, as a determinant of drug distribution from the plasma to the vitreous. The BRB data is quite different from the situation in the blood-brain barrier, where simple physico-chemical models do not perform well, and there are significant outliers from the trends, particularly due to the efflux role of P-gp (Dolghih and Jacobson, 2013; Kikuchi et al., 2013).

Another aspect of active transport is its role in the intracellular drug concentrations of the individual cell types in the retina. Expression of influx or efflux transporters on the cell surface may have a big impact on the free drug concentrations in the cells (Chu et al., 2013), possibly also in the context of melanin binding (Fig. 22), even though the transporter activity would not cause pharmacokinetic changes at the level of vitreal drug concentrations. Unfortunately, the transporter expression of different cell types in the retina has not been determined, and therefore, there is no rational basis to design drugs that would be targeted to specific retinal cells via transporter activity.

10. Special issues

10.1. Disease state effects

Diseases may cause pathophysiological alterations in the ocular environment that can lead to changes in pharmacokinetics and drug delivery. This is quite a complicated issue, because the pharmacokinetic outcomes depend on the disease (nature and extent of the changes) and drug properties. For example, it is known that highly permeable lipophilic drugs are relatively insensitive to the changes in the membrane integrity, whereas transport of poorly permeable compounds, such as proteins, may be affected much more.

Table 4
Transporter expression in the blood-retinal barrier. Example substrates and inhibitors are shown in the table. This is not a comprehensive collection, but rather it presents the transporters that have been found in the cells of blood-retinal barrier at protein level.

Transporter	Substrates/inhibitors[a]	Expression in the RPE	Localization in the RPE	Expression in the inner BRB	References
MRP1 (ABCC1)	ofloxacin, erythromycin, clotrimazole, cyclosporine, fluorescein, gluthatione and gluthatione conjugates, verapamil	**mRNA**: ARPE-19, D407, HRPEpiC, bRPE, hESC-RPE, hRetina, hRC, dRetina, mRPE **Protein**: *ARPE-19, D407, HRPEpiC bRPE, hESC-RPE, hRC,* hRetina, hESC-RPE	Apical membrane (hESC-RPE) Basolateral membrane (mRPE)		Chapy et al. (2016); Chen et al. (2013); Dahlin et al. (2013); Haritova et al. (2013); Juuti-Uusitalo et al. (2012); Mannermaa et al. (2009); Nevala et al. (2008); Ryhänen et al. (2008); Sreekumar et al. (2012); Zhang et al. (2008)
MRP2 (ABCC2)	cyclosporine, erythromycin, acyclovir	**mRNA**: ARPE-19, hESC-RPE hRC, D407, hRC **Protein**: *D407, hRC,* hRetina			Chen et al. (2013); Juuti-Uusitalo et al. (2012); Mannermaa et al. (2009); Sreekumar et al. (2012); Vadlapatla et al. (2013); Zhang et al. (2008)
MRP3 (ABCC3)	losartan, diclofenac	**mRNA**: D407, *HRPEpiC,* ARPE-19, hRC, dRetina[b] **Protein**: *hRC*, hRetina		**mRNA**: isolated mouse retinal vascular endothelial cells	Chen et al. (2013); Haritova et al. (2013); Mannermaa et al. (2009); Sreekumar et al. (2012); Tachikawa et al. (2008); Zhang et al. (2008)
MRP4 (ABCC4)	ganciclovir, zidovudine, losartan, diclofenac, p-aminohippuric acid, 6-mercaptopurine, benzylpenicillin	**mRNA**: ARPE-19, hRC, D407, HRPEpiC, hESC-RPE, hRetina, dRetina[b], mRPE **Protein**: *ARPE-19, D407, HRPEpiC, bRPE, hESC-RPE*	Apical membrane (hESC-RPE) Basolateral membrane (mRPE)	**mRNA**: isolated mouse retinal vascular endothelial cells **Protein**: luminal membrane of mouse retinal capillaries	Chapy et al. (2016); Chen et al. (2013); Dahlin et al. (2013); Haritova et al. (2013); Juuti-Uusitalo et al. (2012); Mannermaa et al. (2009); Sreekumar et al. (2012); Tachikawa et al. (2008); Tagami et al. (2009)
MRP5 (ABCC5)	5-fluorouracil, bimatoprost, latanoprost, acyclovir	**mRNA**: ARPE-19, D407, HRPEpiC, bRPE, hESC-RPE, hRetina, hRC **Protein**: *ARPE-19, D407, HRPEpiC, hESC-RPE, hRC,* hRetina, hESC-RPE	Apical membrane (hESC-RPE)		Chen et al. (2013); Dahlin et al. (2013); Juuti-Uusitalo et al. (2012); Mannermaa et al. (2009); Sreekumar et al. (2012)
P-gp (ACB1)	levofloxacin, ofloxacin, erythromycin, miconazole, methylprednisolone, prednisolone, timolol, azelastine, ketotifen, cyclosporine A, acebutolol, verapamil, dexamethasone	**mRNA**: hESC-RPE, hRC, D407, ARPE-19, dRetina **Protein**: *ARPE-19, hRC*, hRetina, *D407*, ARPE-19, hRPE	Both apical and basolateral plasma membrane (hRPE)	**Protein**: luminal membrane of mouse retinal capillaries, luminal membrane of rat retinal capillaries	Chapy et al. (2016); Chen et al. (2013); Dahlin et al. (2013); Hosoya and Tomi (2005); Juuti-Uusitalo et al. (2012); Kennedy and Mangini (2002); Mannermaa et al. (2009); Nevala et al. (2008); Tagami et al. (2009); Vadlapatla et al. (2013); Zhang et al. (2008); Zhang et al. (2012a,b)
BCRP (ABCG2)	ciprofloxacin, norfloxacin, zidovudine, dexamethasone, triamcinolone, cyclosporine, acyclovir, ofloxacin	**mRNA**: D407, ARPE-19, hRetina, hRC, dRetina, mRetina, mRPE **Protein**: *hRC, ARPE-19, D407*, hRetina, ARPE-19, mRPE cell layer	Basolateral membrane (mRPE)	**Protein**: Retinal capillaries in rat and mouse, luminal membrane of mouse retinal capillaries	Asashima et al. (2006); Chapy et al. (2016); Dahlin et al. (2013); Gnana-Prakasam et al. (2011); Haritova et al. (2013); Juuti-Uusitalo et al. (2012); Mannermaa et al. (2009); Nevala et al. (2008); Tagami et al. (2009); Vadlapatla et al. (2013); Zhang et al. (2008)
		Protein: hRPE cell layer, ARPE19		**mRNA**: TR-iBRB cells	

Table 4 (*continued*)

Transporter	Substrates/inhibitors[a]	Expression in the RPE	Localization in the RPE	Expression in the inner BRB	References
MCT1 (SLC16A1)	fluorescein, monocarboxylates, salicylate, valproate, foscarnet, salicylate		Apical membrane (hRPE, ARPE-19, mRPE)		Gnana-Prakasam et al. (2011); Philp et al. (2003)
OCT3 (SLC22A3)	verapamil, brimonidine, atropine, epinephrine, memantine	**mRNA**: hRetina, hRC **Protein**: hRPE cell layer			Dahlin et al. (2013); Zhang et al. (2008)
OATP1B3 (SLCO1B3)	penicillin G, prednisolone phosphate, cyclosporine	**mRNA**: hRetina			Dahlin et al. (2013)
OATP2B1 (SLCO2B1)	unoprostone, cyclosporine	**mRNA**: hChoroid-RPE, hRC **Protein**: hRPE			Kraft et al. (2010); Zhang et al. (2008)

Expression in RPE: *Western blot* or immunochemistry.
Abbreviations: b bovine, c calf, d dog, h human, hf human fetal, m mouse; hESC-RPE human embryonic stem cell derived RPE cells, RC retina-choroid.
[a] From Mannermaa et al. (2006), Dahlin et al. (2013), Zhang et al. (2012a, 2012b), UCSF database (Morrissey et al., 2012).
[b] Found only in 2 dogs out of 6, all different breeds.

Recently, intravitreal clearance for all the drugs with published data in the healthy rabbits and human patients was calculated (del Amo et al., 2015; del Amo and Urtti, 2015). The correlation of clearances between these two groups was excellent (0.91), maximum deviation was only 3-fold, and the mean clearance in humans was 1.4 times higher than in the rabbits (Fig. 24; Human apparent CL_{ivt} = 1.41 × Rabbit CL_{ivt} + 0.04, units are ml/h; $R^2 = 0.82$; note that there was an erroneous equation in the original reference (del Amo and Urtti, 2015)). This difference is explained based on the size difference as the membranes in the human eye have a higher surface area (membrane controlled clearance = permeability x surface area). In these data, the diseases of the patients included choroidal neovascularization, diabetic retinopathy, cytomegalovirus retinitis, and post-operative endophthalmitis with and without core vitrectomy (del Amo and Urtti, 2015). The eight compounds in the data set were relatively hydrophilic as they had been given as intravitreal injections as solutions. Thus, the correlation does not include lipophilic drugs, but on the other hand, the BRB permeability of lipophilic compounds is expected to be less sensitive to the changes in the membrane integrity than the hydrophilic compounds.

We explored the impact of pathological conditions on the pharmacokinetics and compiled the new analysis to this review. We collected the published data where posterior segment pharmacokinetics in animal disease state models and healthy animals has been compared. We determined the essential pharmacokinetic parameters from the published data. The outcome of these analyses is shown in Table 5.

It has been postulated that the vitreal elimination of those compounds that are eliminated via the anterior route (e.g. vancomycin, aminoglycosides, macrolides, rifampicin), and which poorly cross the blood-retinal barrier, should increase in the disease state upon breakdown of the blood-retinal barrier (Coco et al., 1998; Maurice and Mishima, 1984; Radhika et al., 2014). In the case of posteriorly eliminated compounds, drug elimination should be decreased for those drugs that use active transport mechanisms (e.g. penicillin) due to the inactivation of the transporter in the blood-retinal barrier (Maurice and Mishima, 1984). As seen in Table 5 we did not find experimental evidence to support the impact of disease state effects on posterior segment pharmacokinetics.

Breakdown of BRB is considered to be part of clinical diabetic retinopathy. In humans, insulin levels were determined in the post-mortem serum and vitreous (Palmiere et al., 2015). There is a caveolae mediated transport of insulin in the retinal capillaries and, therefore, insulin transport to the eye might involve active transport process in diabetic patients (Klaassen et al., 2013). Based on the data of Klaassen et al. (2013) it is impossible to know if the difference between healthy and diabetic subjects is negligible or substantial. It has been proposed that fluorescein could be used as an early marker for diabetic retinopathy that would report about the leaky BRB, but the results have not been reproducible (Krogsaa et al., 1981; Törnquist et al., 1990). Likewise, fluorometric studies with streptozotocin induced diabetes rats have also given conflicting results on BRB permeability (Klein et al., 1980; Waltman et al., 1978), and no change in the BRB permeability was seen with radioactive tracers after 1–2 weeks of streptozotocin induced diabetes rats (Mäepea et al., 1984).

Overall, there is no strong evidence that would support the notion that diseased BRB would cause major changes in the ocular pharmacokinetics or drug delivery. The data so far suggests that the changes in the pharmacokinetics either do not exist or are only modest. The disease-induced changes shown in Table 5 (less than 1.5-fold) are negligible in relation to the range of clearance values (about 50-fold) that are seen with different molecular structures (Fig. 6A). We have not found quantitative evidence for any major changes that the disease state would cause in the posterior eye segment. Therefore, pharmacokinetic studies in healthy animals should be valid, because the disease effects on pharmacokinetics do not cause major changes in the drug dosing levels.

10.2. Immunological aspects

The eye is considered to be an immunologically privileged organ, but this old paradigm is not quite right, because immunological reactions can be seen in the eye. This is relevant in drug delivery, because human proteins are first tested in laboratory animals where immunological issues may complicate the data interpretation. Also, formulations may cause activation of the immune system.

10.2.1. Protein interactions of biologicals and drug delivery systems

Proteins are the key players in immunology, and knowledge of the ocular proteome is expanding with the Human Eye Proteome Project (open initiative launched in 2012). So far 4842 proteins have been identified from ocular tissues and fluids (Semba et al., 2013). In total, 1317 proteins were found in both the eye and plasma, whereas 3525 were unique to the ocular environment and 611 were only found in plasma. More information can be found in the databases (Peptide Atlas, 2016; The Ocular Tissue Database, 2016). The number of proteins identified in the vitreous humor, retina and choroid are 545, 672 and 897, respectively.

After ocular application, for instance in the vitreous, drugs or formulations may associate with proteins. This is particularly

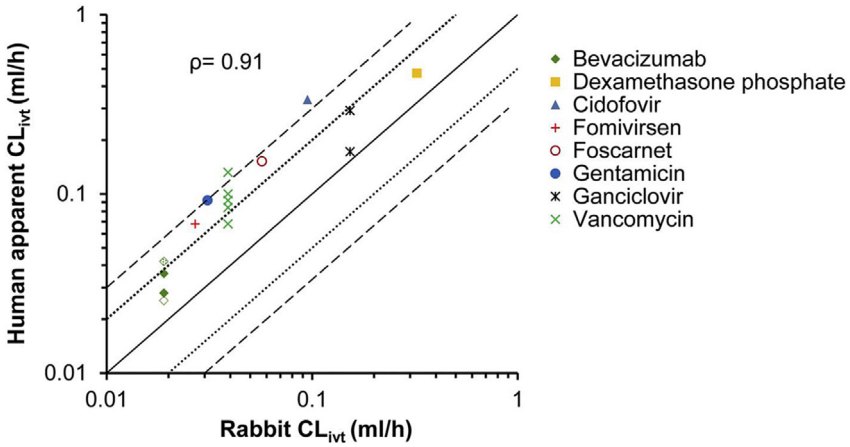

Fig. 24. Intravitreal clearance in the healthy rabbits and human patients. The dotted and dashed lines represent 2 and 3-fold deviation from perfect match (solid line). Human $CL_{ivt,\ apparent} = 1.41 \times$ Rabbit $CL_{ivt} + 0.04$, units are ml/h. For more details of the data, see del Amo and Urtti (2015). Note that in the original article and in later publication of Vellonen et al. (2016) the prediction equation was formulated incorrectly.

relevant in the case of biologicals, viral vectors and nanoparticles. A protein corona may form on the particle surface and this will change and define its biological properties (Docter et al., 2015; Tenzer et al., 2013; Walczyk et al., 2010). This protein corona (or opsonisation) may change the pharmacokinetics, and this is well known in the systemic nanoparticle field (Owens and Peppas, 2006; Vonarbourg et al., 2006). Albumin is one of the major proteins in the vitreous and it is prone to bind to nanoparticles (Docter et al., 2015; Yan et al., 2013). The protein corona can have various effects: 1) A non-specific increase in the particle size can change the distribution and elimination kinetics (Choi et al., 2010); 2) Protein corona, e.g. albumin, may lead to specific cell uptake by macrophages or microglial cells (Ibrahim et al., 2011); 3) Material toxicity may be altered, e.g. masking of positive charges may reduce toxicity (Oh et al., 2010); 4) Protein binding may change the protein conformation and render it immunogenic (Deng et al., 2011; Nel et al., 2009); 5) An active targeting ligand or epitope may be masked, leading to a loss in activity (Lehtinen et al., 2012a; Mirshafiee et al., 2013). It is evident from the systemic drug delivery studies that protein interactions can have profound effects on the behaviour of nanoformulations and biologicals, but how these aspects contribute in the eye is not known.

Most biotechnological products elicit an immune response that leads to formation of neutralizing antibodies in the systemic blood circulation. The neutralizing antibodies interfere at site of action, increase drug clearance, and may lead to adverse effects (Sauerborn et al., 2010). This is also relevant in ocular therapeutics that are administered suprachoroidally, transsclerally or in the subconjunctival space. Although an antibody response does not necessarily affect therapeutic efficacy, immunological assessment of biologicals is required in early development (U.S. Food and Drug Administration, 2013). Impurities, aggregation, modification of proteins by glycosylation or PEGylation, as well as patient and disease-related factors may influence the immunogenicity of protein therapeutics (Sauerborn et al., 2010). Monomeric forms of a proteins are less likely to elicit an immune response than aggregates (Rosenberg, 2006; Sauerborn et al., 2010).

Polyethylene glycol (PEG) that is commonly used to modify therapeutic proteins, drug delivery systems and biomedical devices, reduces the protein adherence and thereby slows down the particle and protein elimination. PEG is not biodegradable and is mostly eliminated via renal filtration. PEG is not completely inert, since it activates the complement system and the production of anti-PEG antibodies (Knop et al., 2010; Schellekens et al., 2013). Interactions of drug delivery devices with the cells and proteins of the immune system may lead to stimulation or suppression of immune function (Elsabahy and Wooley, 2013; Farrera and Fadeel, 2015). In the blood stream, drug delivery systems are taken up in the mononuclear phagocyte system, which is facilitated by opsonisation or plasma proteins adsorption onto their surfaces, resulting in altered biodistribution and accelerated blood clearance (Owens and Peppas, 2006; Vonarbourg et al., 2006). Drug delivery devices are able to activate the complement system but require a co-stimulus to activate immune cells (Farrera and Fadeel, 2015). Immune activation may result in clinical manifestations such as the mild-to-severe pseudoallergic reactions observed with PEGylated liposomal therapeutics (Szebeni, 2005a; Szebeni et al., 2011a). However, safety assessment of drug delivery devices has yet to be standardized and harmonized to the same extent as with protein therapeutics (Nyström and Fadeel, 2012).

10.2.2. Ocular immune defence

Depending on the route of administration, ocular therapeutics may also encounter the immune cells and other components on the ocular surface (conjunctiva, cornea, tear fluid). The cornea, anterior chamber, lens, vitreous cavity and sub-retinal space are immune privileged sites (Bora et al., 1993; Luke et al., 1993). However, a number of immune system effector molecules and cells are present in the inner eye and they can interact with intravitreal therapeutics (Anderson et al., 2010; Rutar et al., 2014). Ocular tissues produce complement system components and rat eyes contain a functional complement system with membrane attack complex (Sohn et al., 2000). This complex could influence also the integrity of liposomes (Sohn et al., 2000). The effect of age-related changes in ocular proteins on the function of the ocular immune system have yet to be established (Perez and Caspi, 2015). Particulate-associated antigens can also bypass the immune privilege and induce a normal immune response in the eye (D'Orazio and Niederkorn, 1998). As a result of immune deviation, the eye is less able to deal with an exaggerated immune response (Forrester et al., 2016). Sterile endophthalmitis that resolves without treatment has been reported with the anti-VEGF therapeutics bevacizumab, ranibizumab, pegaptanib, and aflibercept (Agawa et al., 2014; Agrawal et al., 2013). In most cases, ocular inflammation is transient and considered as an acceptable safety risk in the treatment of posterior eye diseases (Short, 2008). However, animals display significant and

Table 5
Comparison of pharmacokinetics in normal and disease state animal models (unpublished pharmacokinetic parameter analyses). Barza et al., 1982; Barza et al., 1993; Bienert et al., 2012; Ficker et al., 1990; Ozcimen et al., 2015; Coco et al.,1998; Mandell et al., 1993; Meredith, 1993; Park et al., 1999; Shen et al., 2014.

Disease model and species	Drug, administration route, drug properties[1] and primary route of elimination	Pharmacokinetic parameters in healthy and diseased eye	Source
Infection and inflammation: 0.1 ml of 10^9 heat-killed *Staph. epidermis* injected into the vitreous of rabbits	Amikacin intravitreal LogD7.4: -10.59; MW: 585.6; HD: 17 Anterior route	CL_{ivt} (ml/h); $t_{1/2,ivt}$ (h); AUC_{ivt} (h µg/ml) Healthy: 0.039; 29.0; 7,729 Diseased: 0.046; 22.6; 6,518	Mandell et al. (1993)
BRB breakdown: intravitreal injection of 1µg rhVEGF165 in rabbits	Brimonidine intravitreal LogD7.4: 0.73; MW: 292.13; HD: 2 Posterior route	Not possible to curve fit the data. The concentration curves are similar. Time (h); Vitreous conc. (ng/mL) [2] Healthy / Diseased 0.5: 5174.8 / 11266.0 1: 4564.6 / 5579.5 2: 1994.0 / 2979.3 4: 1849.4 / 1038.4 8: 361.9 / 420.7 12: 136.0 / 274.6 24: 100.6 / 108.5	Shen et al. (2014)
Choroidal neovascularization in monkey with lasering	Brimonidine intravitreal Posterior route	CL_{ivt} (ml/h); $t_{1/2,ivt}$ (h); AUC_{ivt} (h.µg/ml) Healthy: 0.161; 17.3; 205.34 Diseased: 0.155; 20.0; 212.27	Shen et al. (2014)
Infection and inflammation: 0.1 ml of 500 cfu/ml *S.aureus* injected into the vitreous of rabbits	Carbenicillin intravitreal LogD7.4: -3.62; MW: 378.4; HD: 3 Posterior route	CL_{ivt} (ml/h); $t_{1/2,ivt}$ (h); AUC_{ivt} (h.µg/ml) Healthy: 0.166; 6.4; 6,030 Diseased: 0.133; 6.5; 7,542	Barza et al. (1982)
Infection and inflammation: 0.1 ml of 10^9 heat-killed *S. epidermis* injected into the vitreous of rabbits	Cefazolin intravitreal LogD7.4: -4.41; MW: 454.51; HD: 2 Posterior route	CL_{ivt} (ml/h); $t_{1/2,ivt}$ (h); AUC_{ivt} (h.µg/ml) Healthy: 0.165; 7.2; 15,182 Diseased: 0.109; 10.4; 22,936	Ficker et al. (1990)
Infection and inflammation: 0.1 ml of 500 cfu/ml *S.aureus* injected into the rabbit vitreous	Intravitreal administration Cefepime: LogD7.4 -2.29; MW 481.57; HD 4 Ceftazidime: -2.95; 547.58; 5 Ceftizoxime: -4.35; 383.4; 4 Ceftriaxone: -5.32; 554.58; 5 Posterior route	No concentrations available. The reported half-life values in the article: $t_{1/2,ivt}$ (h) Healthy / Diseased Cefepime: 14.3 / 15.1 Ceftazidime: 20.0 / 21.5 Ceftizoxime: 5.7 / 9.4 Ceftriaxone: 9.1 / 13.3	Barza et al. (1993)

Infection and inflammation: 0.1 ml of 10^9 heat-killed *S. epidermis* injected into the vitreous of rabbits	Ceftazidime intravitreal Posterior route		Meredih et al. (1993)

	CL_{ivt} (ml/h)	$t_{1/2,ivt}$ (h)	AUC_{ivt} (h.µg/ml)
Healthy	0.077	13.3	29,236
Diseased	0.076	13.3	29,653

Inflammation: 100 ng of lipopolysaccharide from *Escherichia coli* injected into the rabbit vitreous	Daptomycin intravitreal Anterior route		Ozcimen et al. (2015)

$LogD_{7.4}$	MW	HD
-8.81	1620.7	25

	CL_{ivt} (ml/h)	$t_{1/2,ivt}$ (h)	AUC_{ivt} (h.µg/ml)
Healthy	0.041	24.6	4,850
Diseased	0.028	34.8	6,898

Diabetes model: by intravenous injection of alloxan 90 mg/kg in rabbits	Paracetamol intravenous	Drug concentrations in plasma and aqueous humour but not in vitreous. Similar ratio & aqueous humour concentrations values	Bienert et al. (2012)

At 30 min	Plasma conc. (mg/l) [2]	Aqueous humour conc. (mg/l)	Conc. Ratio
Healthy	24.61	5.68	4.3
Diseased	13.13	2.71	4.8

Infection and inflammation: 0.1 ml of 2,000 cfu/ml *S.aureus* injected into the rabbit vitreous	Vancomycin intravitreal Anterior route		Coco (1998)

$LogD_{7.4}$	MW	HD
-4.49	1449.25	21

	CL_{ivt} (ml/h)	$t_{1/2,ivt}$ (h)	AUC_{ivt} (h.µg/ml)
Healthy	0.041	26.9	23,796
Diseased	0.063	14.3	15,387

Infection and inflammation: 2,000 cfu *S.pneumoniae* injected into the rabbit vitreous	Vancomycin intravitreal Anterior route	Not possible to curve fit the data. The concentration curves are similar.	Park et al. (1999)

Time (h)	Vitreous conc. (µg/mL)[2]	
	Healthy	Diseased
24	280.8	197.5
48	204.3	129.7
72	110.4	67.0

1: calculated using ACDlabs® software (version 12, Advanced Chemistry Development, Inc., Toronto, Canada)
2: obtained from the pharmacokinetic graphs using GetData Graph Digitizer® (version 2.24. Digital River, Inc., Cologne, Germany).

unpredictable interspecies differences in their responses to intravitreal therapeutics and are poor predictors of ocular inflammation in humans (Short, 2008). It is likely that this conclusion also applies to drug delivery devices.

In the posterior segment of the eye, microglial cells distributed around blood vessels represent the mononuclear phagocytic system in the retina (Zeng et al., 2008). The macroglial Müller cells of the retina are able to phagocytose foreign material and produce proinflammatory cytokines upon activation (Bringmann et al., 2006). Müller cell gliosis, or the activation of microglial and macroglial cells is central in the retinal response to damage or a pathogen, including extravasation of plasma immune system components (for review see, Bringmann et al. (2006)). The entry of plasma proteins into the eye as a result of inflammation overcomes the immune privilege of the vitreous (Streilein et al., 2002). Exudative diseases may modulate the immune responses towards

intravitreal therapeutics. RPE cells also have a role in immune responses, like phagocytic antigen-presenting cells (Kumar et al., 2004). RPE cells express several Toll-like receptors and co-stimulatory molecules capable of recognizing pathogen-associated molecular motifs leading to inflammasome activation and production of proinflammatory cytokines, demonstrating their role in both innate and adaptive immune responses (Kumar et al., 2004; Percopo et al., 1990). Photoreceptors (Singh and Kumar, 2015), microglia (Kochan et al., 2012) and Müller cells (Kumar and Shamsuddin, 2012) have been shown to express Toll-like receptors with the ability to initiate an innate immune response. Toll like receptor 4 that is present on photoreceptors, RPE, ciliary body, cornea, conjunctiva and choroid recognizes endotoxins that should be avoided in the intraocular pharmaceutical products (Agrawal et al., 2013; Crist et al., 2013; Kumar et al., 2004; Tu et al., 2011; U.S. Food and Drug Administration, 2015). In preclinical studies, endotoxin contamination may alter clearance and biodistribution and lead to inflammation. Toll like receptors also recognize viral DNA and RNA motifs, lipoproteins and heat shock proteins, and could interact with therapeutic proteins, nanoparticles or viral vectors (Micera et al., 2005).

10.2.3. Interactions of drug delivery systems with ocular immune defence

Immune responses to intravitreal biologics (e.g. bevacizumab, aflibercept) have been shown in many studies (Forooghian et al., 2011, 2009; Ho et al., 2013; Rosenfeld et al., 2006), but a lack of antibody formation has also been reported (Gaudreault et al., 2005). The clinical significance of these phenomena is still unclear, but the possible role of antibody formation in the tachyphylaxis to aflibercept and bevacizumab has been proposed (Forooghian et al., 2009; Ho et al., 2013). Although immune responses in the eye are geared towards an anti-inflammatory response and systemic tolerance, the need for repeated administration of intravitreal biologics in chronic therapies may exacerbate this issue. To our best knowledge, studies on the interactions between drug delivery systems and intraocular complement system components have not been reported. Since the ocular environment contains a functional complement system (Sohn et al., 2000), the possibility of complement-mediated immune responses especially in exudative disease states cannot be ruled out. Drug delivery devices have induced clinically significant complement-mediated hypersensitivity reactions in the blood circulation of susceptible individuals (Szebeni et al., 2011b). However, complement-mediated hypersensitivity reactions typically arise at first exposure, but become milder or absent in repeated administration (Szebeni, 2005b).

There are several studies that report interactions or lack of interactions of drug delivery systems with the ocular immune defence. The individual studies demonstrate different aspects of interactions between the immune system and drug delivery systems. Activation increases the phagocytic capacity of microglial cells and macrophage-related cells in general (Hanisch and Kettenmann, 2007). For example, choroidal neovascularization in age-related macular degeneration is associated with the infiltration of blood-derived macrophages to the retina underlying the choroid (Caicedo et al., 2005). Most were found in close proximity to Müller cells of the retina. Resident microglial cell densities were not increased or decreased as a result of infiltration.

Cationic materials, such as chitosan, are often harmful and may cause inflammatory cell infiltrations in the eye after intravitreal and sub-retinal delivery (Prow et al., 2008). In general, positively charged nanoparticles are phagocytosed efficiently into the mononuclear phagocytic system (Xiao et al., 2011). No immune cell infiltration was observed with negatively charged polylactic acid nanoparticles (140 ± 20 nm) in the ciliary body or retina in the first hour, but after 6 and 24 h, some infiltrating cells were found in the vitreous and retina, but signs of inflammation decreased by 48 h (Bourges et al., 2003). Poly-lactic acid particles were present in the RPE cells four months after single intravitreal injection (Bourges et al., 2003). Some of the infiltrating cells were shown to phagocytose the rhodamine-modified nanoparticles (Bourges et al., 2003). On the other hand, negatively charged ganciclovir-loaded bovine serum albumin nanoparticles (size range 257–351 nm) remained in the rat vitreous for two weeks after a single injection, with no inflammatory changes (Merodio et al., 2002).

Barza et al. (1987) used a model of bacterial inflammation to assess the effect of inflammation on the rate of clearance of small and large unilamellar liposomes from the rabbit eye. The authors speculated that the liposomes could be cleared by diffusion through the anterior route, by phagocytic cells (e.g. RPE) or by degradation in the vitreous. The relative contribution of these different routes could not be estimated based on the data. Since only 1–2% of the ^{125}I label was found in the choroid and retina, the contribution of phagocytic cells is likely to be low.

10.3. Non-invasive analytical methods for ocular pharmacokinetics and drug delivery

Ocular pharmacokinetics and drug delivery studies *in vivo* are challenging, because the studies are invasive. It is not possible to withdraw repeated samples from the aqueous humor and vitreous of humans or animals, because the sampling would cause changes in the fluid volumes and other reactions in the eye that might hamper the reliability of the pharmacokinetic results. Furthermore, ocular pharmacokinetics are usually studied in rabbits or monkeys, because the sampling is even more difficult from small animals and pharmacokinetics in the small rodents do not translate well to the human situation. An invasive pharmacokinetic rabbit study involves use of many rabbits. For example, a simple pharmacokinetic comparison of three drugs or formulations requires 36 rabbits (i.e. 3 formulations x 6 time points x 4 eyes/time point).

Non-invasive imaging is an attractive option for pharmacokinetics and drug delivery studies, since it would replace, reduce and refine the animal experiments. Imaging allows observations from the same animal at many time points thereby decreasing the number of animals in the test (in the aforementioned experiment 6 rabbits would be enough). This approach also reduces the data variability that is due to the variation among the animals. The imaging modalities include optical, radiochemical and magnetic resonance methods.

10.3.1. Optical imaging

Optical fluorescence based imaging has been used in ophthalmology since the 1980's. Originally, *in vivo* fluorometers were developed as clinical instruments to determine blood-retinal barriers (in diabetes), early cataract formation, tear flow rates and aqueous turnover (Knudsen, 2002). *In vivo* fluorophotometry has been used to monitor the fluorescence levels mainly in humans and rabbits. The fluorometer is detecting the emission signals after excitation through the transparent ocular tissues (cornea, aqueous humor different depths of visual axis over time).

The drawbacks of *in vivo* fluorophotometry are obvious. Firstly, exact quantitation is very difficult, because the fluorescence signal depends on the geometrical factors, and the properties of the fluorescent probe. Most widely used probes of ocular *in vivo* fluorophotometry (e.g. fluorescein) show fluorescence emission, which is dependent on the environment (e.g. pH), concentration (i.e. non-linear relationship between the signal and fluorophore concentration), and light exposure (i.e. photo-quenching) (Song et al.,

1995). Secondly, only a few drugs have intrinsic fluorescence spectra that would allow their non-invasive fluorometric imaging. In general, fluorometric imaging cannot be used for pharmacokinetic monitoring of small molecular drugs. Thirdly, the stability of the fluorophore in the studied object (e.g. drug or delivery system) is a crucial issue. If the label is detached from the study object, the imaging will thereafter follow only the kinetics of the label. The stability of the label should be checked *in vitro* in relevant media to avoid such artefacts in the imaging study.

Despite its limitations, optical imaging can give useful information about the pharmacokinetics of macromolecules and drug delivery systems in the eye. Recently, intravitreal kinetics of ranibizumab was studied using *in vivo* fluorophotometry (AlexaFluor 488 label) and ELISA (Dickmann et al., 2015). Similar pharmacokinetic parameters were obtained with both approaches. This study demonstrated that it is crucially important to use a minimal number of fluorophores for labelling and select fluorophores that have maximal brightness, photostability and minimal pH sensitivity. Currently, there are various fluorophores (such as Alexa dyes) available that are compatible with the wavelengths of *in vivo* fluorophotometers. They have improved brightness, stability in the presence of light excitation and more robust fluorescence spectra in changing environments (Wysocki and Lavis, 2011). These features provided broader dynamic range of linearity (fluorescence emission vs drug concentration) that enabled intravitreal pharmacokinetic monitoring of ranibizumab over a 20-fold concentration range (Dickmann et al., 2015).

Potential uses of this technique include monitoring the retention of drug delivery systems on the ocular surface or in the vitreous. Also, the effects of drugs and delivery systems on the blood-ocular barrier can be detected by following the entrance of intravenous FITC-dextran to the eye. Several groups have also demonstrated the use of this method to study transscleral drug delivery (Berezovsky et al., 2011; Ghate et al., 2007; Lee et al., 2008). Currently, there are also new *in vivo* fluorometers that are more robust than the classic ocular *in vivo* fluorometer potentially expanding the use of this metholodology.

10.3.2. Radiochemical imaging

Radiochemical imaging is based on the detection of the radioisotopes that are emitting gamma irradiation. The isotopes can be used in single photon emission computed tomography (SPECT) or positron emission tomography (PET). The isotopes in SPECT/CT imaging include technetium (^{99m}Tc), indium (^{111}In) and iodine (^{131}I, ^{123}I), whereas PET isotopes include, e.g. ^{18}F. Radio imaging has a quantitation advantage over optical imaging: the sensitivity is high (about 1 nM), the radioactive signal is insensitive to changes in the environment thereby giving excellent depth and dynamic linear range of the measurements. However, these are expensive techniques, since special labelling techniques and isotopes are needed and the imaging equipment is very expensive. Another challenge is the spatial resolution: typically, the resolution with mouse, rat and rabbit collimators range from 0.5 to 2 mm, respectively. This resolution allows only coarse imaging of the eyes, but not to the levels of individual tissues (e.g. retina). Computed tomography and MRI are used for the anatomical localization of the tissues (spatial resolution MRI: 25–100 μm, CT: 50–200 μm).

The investigator should be aware that the labelling might change the properties of the compound, potentially leading to the alterations in the biodistribution. Labelling is challenging, particularly in the case of small molecules. Pharmacokinetics of proteins, other large molecules and drug delivery systems may not be as sensitive to the labelling changes. Typical labelling strategies include the use of peptide linkers in labelling of proteins (Liu, 2008), encapsulation of hydrophilic or lipophilic compounds to liposomes or nanoparticles (Lehtinen et al., 2012b; Psimadas et al., 2012), radiometal complexation radiotracers with DOTA (Liu, 2008). In the case of ocular studies BRB is an important consideration, because changes in the molecular size and lipophilicity may change the permeability in the BRB and cause changes in the vitreal clearance (Fig. 6). Different labelling techniques have been reviewed in detail in specialized review articles (Hom and Katzenellenbogen, 1997; Liu, 2008).

SPECT/CT has been used to study ocular distribution of intravenously injected radio labelled 3-^{123}I-iodochloroquine in rats (Rimpelä et al., 2016). This study showed that the SPECT/CT is a suitable technique for drug distribution studies, since it allowed non-invasive quantitation of the drug in the eyes over time. Another application of SPECT/CT approach was imaging the vitreal kinetics of HSP-70 protein in *ex vivo* bovine eyes (Subrizi et al., 2015).

Micro-PET has not been used for ocular drug delivery studies.

10.3.3. Magnetic resonance imaging (MRI)

Magnetic resonance imaging has been used to study ocular structures (Fanea and Fagan, 2012; Shih et al., 2011) and ocular drug delivery (Li et al., 2008). This method relies on nuclear magnetic resonance signals emitted by magnetically labelled nuclei (e.g. Gd) (Fanea and Fagan, 2012). A nice feature of MRI is its excellent spatial resolution, but its usefulness is limited in ocular pharmacokinetic studies, because the linear range of quantitation and sensitivity (about 0.1 mM) are quite limited compared to the radioimaging and optical imaging techniques. These are serious shortcomings and currently MRI imaging is not an attractive option for ocular pharmacokinetic studies. However, MRI may be a useful technique to improve the localization in association with SPECT and PET imaging. Also, it is useful in monitoring the fate of the delivery systems in the eye (Li et al., 2008).

10.3.4. Summary

Imaging techniques, especially optical imaging, have been used in ocular pharmacokinetics. At the moment their utility is still limited, but the situation may improve significantly in the future. Imaging methods are continuously developing, optical coherence tomography being a nice example in ophthalmology. It is likely that various imaging methods will be developed, alone and as combinations, towards better quantification, resolution and label free approaches. Such a progress will also facilitate the studies in ocular drug delivery, hopefully allowing non-invasive quantification both in animals and humans.

10.4. Species differences

Ocular research on mechanisms of diseases and pharmacology of drug candidates are usually carried out using *in vitro* methods and mouse models, but ocular drug delivery and pharmacokinetics are studied in larger animals with bigger eyes (e.g. rabbits, monkeys). Obviously, translation tools between animal species and from preclinical models to man are essential in ocular drug development. Currently, there are some tools for translation, but much more progress is still needed. Ocular pharmacokinetic data in rabbits and monkeys exist, but it is sparse in humans, and even less in rodents. Therefore, inter-species translation cannot be done at the current stage. We shall discuss some aspects of the species differences for each route of drug application.

Physiologically based pharmacokinetic models and inter-species scaling is based on anatomical and physiological values. We have collected some key values from rabbit, mouse, cynomolgus monkeys and humans in Table 6.

10.4.1. Topical and sub-conjunctival delivery

After topical drug delivery, the eye drop is subject to the factors that are removing the applied solutions from the ocular surface (Mishima, 1981). In humans, the blinking frequency is much higher than in the rabbits and this leads to faster clearance of applied solutions (Mishima, 1981), but this factor has not been investigated in mice and rats. It is known that the mouse and rat studies are giving over-optimistic results on the posterior segment drug delivery after topical administration (Joussen et al., 2016). This is probably due to the geometric factors, because the distance to the posterior segment tissues is much shorter in mice and rats as compared to rabbits and humans. Also, mouse and rat sclera are much thinner and thus more permeable than the sclera in rabbits and man. The same factors are relevant in the case of sub-conjunctival injections, probably leading to over-optimistic results in retinal drug delivery. Furthermore, drug distribution to the contralateral eye via systemic circulation is more pronounced in the mice, rats and rabbits than in man. One should be particularly cautious when making conclusions based on the rodent studies in terms of posterior segment drug delivery after topical administration.

10.4.2. Intravitreal delivery

The species differences of intravitreal pharmacokinetics have been mostly discussed in the case of rabbits and humans. It is known that there are differences between the human and rabbit eye (Laude et al., 2010; Rowe-Rendleman et al., 2014): 1) Vitreal viscosity in the rabbit eyes may be higher than in elderly human patients; 2) Retinal capillaries are different and sparser in rabbits than in humans; 3) The relative size of the lens is bigger in the rabbit than in the human eye; 4) Overall, the human eyes are bigger than the rabbit eyes. The significance of these differences on the intravitreal drug clearance was analysed after collecting all available literature on drug concentrations in the human patients and rabbits (del Amo and Urtti, 2015). The clearance values were determined and good correlation of the rabbit and human clearance values was obtained (Fig. 24) indicating that the intravitreal drug clearance can be scaled up reliably from rabbit to patients. As discussed earlier, disposition of the delivery systems in the vitreous may differ between man and rabbit (section 3.4), but pharmacokinetic significance of these differences have not been either proven or quantitated in the scientific literature.

Translation of intravitreal pharmacokinetics from rodents (mice, rats) to rabbits or man has not been shown in the literature. Intravitreal injections are given often in mouse and rat studies for pharmacological drug responses, but intravitreal pharmacokinetics in mice and rats has not been investigated and there are no pharmacokinetic data for human translation. We have recently carried out SPECT/CT imaging after intravitreal drug injections to mice. As an example, Fig. 25 illustrates elimination of ^{111}In-pentetreotide (molecular weight of 1394 Da) from the mouse vitreous. The images show that the injected compound is first seen only in the posterior segment, presumably mostly in the vitreous, but the label is later localized in the anterior chamber and during the final time points the compound seems to be primarily localized in the anterior chamber suggesting significant elimination via anterior route. Interestingly, it seems that major part of ^{111}In-pentetreotide was eliminated from the mouse vitreous during 230 min and hardly any tracer is seen in the vitreous at 270 min. These observations can be compared to the intravitreal pharmacokinetics in rabbits and humans.

The intravitreal elimination rate constant and half-life of a compound depend on its clearance (CL) and volume of distribution (V_d): $t_{1/2} = \ln 2\ V_d/CL$ (del Amo et al., 2015). These values in the mouse eye can be compared to the rabbit and human data (Figs. 6A and 24). As we discussed in section 3, the volume of intravitreal drug distribution almost equals the anatomical volume of the vitreous (Fig. 6B). These values are 1.15 ml and 5 μl in the rabbit and mouse, respectively (del Amo et al., 2015; Remtulla and Hallett, 1985). Posterior drug clearance can be roughly related to the surface area of the RPE (assuming similar permeability in two species): the surface area in a rabbit is 520 mm^2 (Reichenbach et al., 1994) and in mouse 16.5 mm^2 (Jeon et al., 1998). Then, the volume/area ratio is related to the vitreal half-life from the elimination via BRB. This calculated half-life for posterior drug elimination is about seven times shorter in the mouse than in the rabbit.

Drug elimination via the anterior route is a complex function that depends on the diffusivity in the vitreous, geometrical factors (distance in the vitreous, open space between the lens and iris, viscosity of the vitreous humor), and aqueous humor outflow. Most of these factors are difficult to estimate, but aqueous humor outflow values are known; rabbit: 0.18 ml/h (Barany and Kinsey, 1949); mouse: 0.0108 ml/h (Aihara et al., 2003). Half-lives ($t_{1/2} = \ln 2\ V_d/CL$) based on the values of outflow clearance and ocular volumes are 0.3 h in mouse and 4.4 h in rabbit (14 times longer in the rabbit). These rough calculations hint that the intravitreal half-life in the mouse is approximately one order of magnitude shorter in mouse than in the rabbit.

The volume of the mouse vitreous is 230 times smaller than in the rabbit eye, but the clearance is about 20–30 times smaller in the mouse, partly cancelling out the volume factor. We cannot obtain exact experimental value for the half-life from Fig. 25, but based on the intensity of SPECT images the half-life is in the range of 1.5–4 h in mouse. Based on the previous rabbit experiments, the

Table 6
Physiological values that are relevant in ocular pharmacokinetics.

	Aqueous humor flow	Vitreous volume	Ciliary body blood flow	Iridial blood flow	RPE surface area	Retinal blood vessels	Choroidal blood flow
Rabbit	0.1950 ml/h (Barany and Kinsey, 1949)	1.15 ml (del Amo et al., 2015)	4.91 ml/h (Nilsson and Alm, 2012)	4.91 ml/h (Nilsson and Alm, 2012)	520 mm^2 (Reichenbach et al., 1991)	**Flow**: 0.66 ml/h (Nilsson and Alm, 2012) **Surface area**: 20–25 mm^2 (Maurice and Street, 1957)	62 ml/h (Nilsson and Alm, 2012)
Monkey (Cynomolgus)	0.0996 ml/h (Rasmussen et al., 2007)	2 ml (Struble et al., 2014)	5.34 ml/h (Alm and Bill, 1973)	5.34 ml/h (Alm and Bill, 1973)	730 mm^2 (Wikler et al., 1990)		
Mice	0.0108 ml/h (Aihara et al., 2003)	5 μl (Remtulla and Hallett, 1985)			16.5 mm^2 (Jeon et al., 1998)		
Human	0.1440 ml/h (Brubaker, 1982)	4 ml (Ruby et al., 2006)			1204 ± 184 mm^2 (Panda-Jonas et al., 1994)	**Flow:** 0.26 ml/h (Feke et al., 1989)	43 ml/h (Sebag et al., 1994)

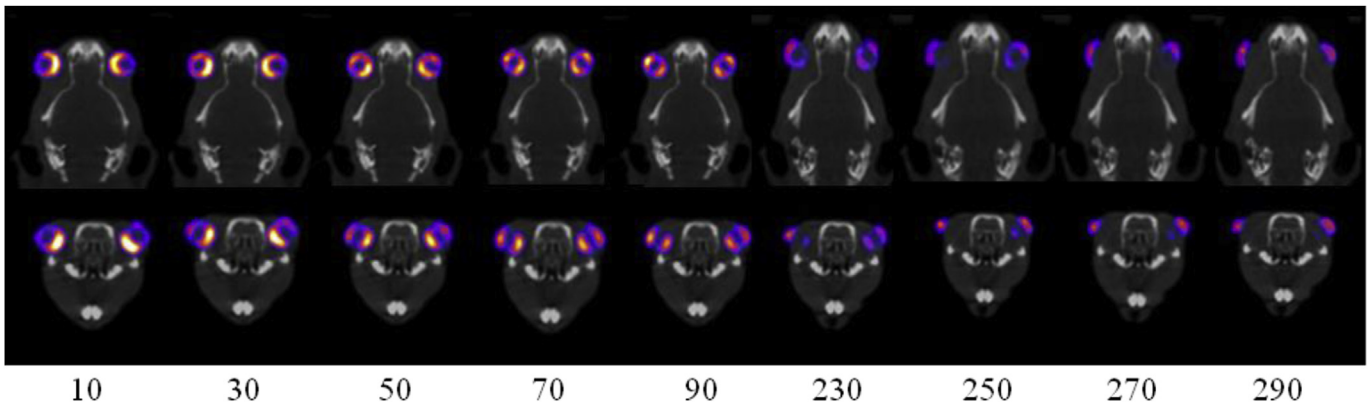

Fig. 25. SPECT/CT imaging of mouse eyes after intravitreal injection of ^{111}In-pentetreotide (unpublished data). The numbers indicate the time after injection (minutes). The anterior eye segment is seen as the lateral part of the images.

intravitreal clearance from the rabbit eye for this peptide (MW = 1394 Da) is expected to be in the range of 0.02–0.04 ml/h (Fig. 6A) meaning half-lives around 20–40 h, values that are one order magnitude higher than in the mouse (Fig. 24). These calculations suggest that following scaling factors (rabbit/mouse) can be used in the interspecies scaling between mouse and rabbit: half-life ≈10, volume ≈230 and clearance ≈ 20–30. The scaling factors man/rabbit are half-life 1.5–3, volume 2–4 and clearance 1.4 (del Amo and Urtti, 2015). Drug exposure after intravitreal injection is best described with AUC values that are dependent on the clearance. Therefore, intravitreal doses in the rabbit should be about 20–30 times larger than in the mouse. In man, the doses should be about 1.4 times higher than in the rabbit.

10.4.3. Systemic delivery

There are only limited experimental data to support rabbit-to-man translation for ocular distribution of systemic drugs, but the good correlation of intravitreal clearance between rabbit and man (Fig. 24) suggests that the modeling approach of Vellonen et al. (2016) that was used in rabbits (chapter 4) may be useful for human predictions. No systemic-to-vitreous drug distribution data exists for rats or mice. It is obvious that the systemic contribution to the ocular drug concentrations is higher in small animals due to the smaller systemic volume and clearance. This may be one factor that leads to the over-optimistic results for posterior drug delivery after topical administration (Joussen et al., 2016).

10.4.4. Prospects for inter-species translation

PBPK modeling is a tool that is used for inter-species scaling. The models are based on the physiology, anatomy and compound properties. PBPK modeling can serve as an approach to integrate the information from the scientific community to the models that can be used to predict *in vivo* pharmacokinetics in animals and humans, thereby helping in the design of preclinical and clinical studies. With increasing data, the models will be more and more reliable in the future, finally enabling inter-species scaling.

11. Future perspectives

Intravitreal delivery is currently the method of choice for retinal drug delivery. New delivery systems are needed to prolong the injection intervals in the new retinal drug treatments, but the development of intravitreal drug delivery systems is difficult particularly due to the tolerability issues. More basic research is needed to improve understanding of the injected material behaviour in the vitreal cavity, including the immunological aspects, biodegradation, release control and toxicity. Obviously the delivery systems must fulfil also the important technological requirements (e.g. sterility, lack of endotoxins, reproducible manufacturing and clinical performance).

Systematic understanding of ocular pharmacokinetics and model building helps to integrate the pharmacological drug properties, delivery system related factors, anatomy and physiology and inter-species scaling in the same package. Integration of pharmacodynamics is an important future challenge, because some drugs may have prolonged response after biochemical switch is turned on, while other drugs require continuous presence of drug molecules. The drug features should be taken into account in the delivery system design. Applicability of different routes of ocular drug delivery depend on the drug properties, for example the drug potency. It is important to integrate drug information in the design of the delivery system, dosing rate and route of drug administration.

Basic research is needed in the field of intracellularly acting biologicals, since they must be delivered within certain cell types in the retina. Unfortunately, knowledge about drug targeting to the key cell types in the retina and choroid is still sparse. This field may benefit from the advances in the fields of cellular and retinal imaging and nanomedicine. These advances are important for the development of treatments to the unmet needs in retinal ophthalmology.

Acknowledgements

This study was supported from the following granting agencies: Academy of Finland (grants: 268868, 263615, 283721, 263573, 272597), European Union FP7 (ALEXANDER, PANOPTES), the Finnish Funding Agency for Technology and Innovation (637/31/2015 TEKES), Sigrid Jusélius Foundation (64578), and University of Eastern Finland (Graduate School Funds for Laura Pelkonen and Emma Heikkinen).

Appendix A. Supplementary data

Supplementary data related to this article can be found at http://dx.doi.org/10.1016/j.preteyeres.2016.12.001.

References

Abarca, E.M., Salmon, J.H., Gilger, B.C., 2013. Effect of choroidal perfusion on ocular tissue distribution after intravitreal or suprachoroidal injection in an arterially perfused ex vivo pig eye model. J. Ocul. Pharmacol. Ther. 29, 715–722.
Acheampong, A.A., 2002. Distribution of brimonidine into anterior and posterior tissues of monkey, rabbit, and rat eyes. Drug Metab. Dispos. 30, 421–429.

Agawa, T., Usui, Y., Wakabayashi, Y., Okunuki, Y., Juan, M., Umazume, K., Kezuka, T., Takeuchi, M., Yamauchi, Y., Goto, H., 2014. Profile of intraocular immune mediators in patients with age-related macular degeneration and the effect of intravitreal bevacizumab injection. Retina 34, 1811–1818.

Agrawal, S., Joshi, M., Christoforidis, J.B., 2013. Vitreous inflammation associated with intravitreal anti-VEGF pharmacotherapy. Mediat. Inflamm. article ID 943409, 2013, 6 pages.

Ahmed, I., Patton, T.F., 1987. Disposition of timolol and inulin in the rabbit eye following corneal versus non-corneal absorption. Int. J. Pharm. 38, 9–21.

Ahmed, I., Patton, T.F., 1985. Importance of the noncorneal absorption route in topical ophthalmic drug delivery. Investig. Ophthalmol. Vis. Sci. 26, 584–587.

Aihara, M., Lindsey, J.D., Weinreb, R.N., 2003. Aqueous humor dynamics in mice. Investig. Ophthalmol. Vis. Sci. 44, 5168–5173.

Algvere, P., Bill, A., 1979. Drainage of microspheres and RBCs from the vitreous of aphakic and phakic eyes. Arch. Ophthalmol. 97, 1333–1336.

Alm, A., Bill, A., 1973. Ocular and optic nerve blood flow at normal and increased intraocular pressures in monkeys (Macaca irus): a study with radioactively labelled microspheres including flow determinations in brain and some other tissues. Exp. Eye Res. 15, 15–29.

Amadio, M., Govoni, S., Pascale, A., 2016. Targeting VEGF in eye neovascularization: what's new?: A comprehensive review on current therapies and oligonucleotide-based interventions under development. Pharmacol. Res. 103, 253–269.

Ambati, J., Canakis, C.S., Miller, J.W., Gragoudas, E.S., Edwards, A., Weissgold, D.J., Kim, I., Delori, F.C., Adamis, A.P., 2000. Diffusion of high molecular weight compounds through sclera. Investig. Ophthalmol. Vis. Sci. 41, 1181–1185.

Ambati, J., Fowler, B.J., 2012. Mechanisms of age-related macular degeneration. Neuron 75, 26–39.

Amrite, A.C., Edelhauser, H.F., Kompella, U.B., 2008. Modeling of corneal and retinal pharmacokinetics after periocular drug administration. Investig. Ophthalmol. Vis. Sci. 49, 320–332.

Anderson, D.H., Radeke, M.J., Gallo, N.B., Chapin, E.A., Johnson, P.T., Curletti, C.R., Hancox, L.S., Hu, J., Ebright, J.N., Malek, G., Hauser, M.A., Bowes Rickman, C., Bok, D., Hageman, G.S., Johnson, L.V., 2010. The pivotal role of the complement system in aging and age-related macular degeneration: Hypothesis re-visited. Prog. Retin. Eye Res. 29, 95–112.

Andrés-Guerrero, V., Zong, M., Ramsay, E., Rojas, B., Sarkhel, S., Gallego, B., De Hoz, R., Ramírez, A.I., Salazar, J.J., Triviño, A., Ramírez, J.M., Del Amo, E.M., Cameron, N., De-Las-Heras, B., Urtti, A., Mihov, G., Dias, A., Herrero-Vanrell, R., 2015. Novel biodegradable polyesteramide microspheres for controlled drug delivery in ophthalmology. J. Control. Release 211, 105–117.

Angi, M., Kalirai, H., Coupland, S.E., Damato, B.E., Semeraro, F., Romano, M.R., 2012. Proteomic analyses of the vitreous humour. Mediat. Inflamm. 2012, 1–7.

Araie, M., Maurice, D.M., 1991. The loss of fluorescein, fluorescein glucuronide and fluorescein isothiocyanate dextran from the vitreous by the anterior and retinal pathways. Exp. Eye Res. 52, 27–39. http://dx.doi.org/10.1016/0014-4835(91)90125-X.

Arango-Gonzalez, B., Trifunović, D., Sahaboglu, A., Kranz, K., Michalakis, S., Farinelli, P., Koch, S., Koch, F., Cottet, S., Janssen-Bienhold, U., Dedek, K., Biel, M., Zrenner, E., Euler, T., Ekström, P., Ueffing, M., Paquet-Durand, F., 2014. Identification of a common non-apoptotic cell death mechanism in hereditary retinal degeneration. PLoS One 9, e112142.

Aretz, S., Krohne, T.U., Kammerer, K., Warnken, U., Hotz-Wagenblatt, A., Bergmann, M., Stanzel, B.V., Kempf, T., Holz, F.G., Schnölzer, M., Kopitz, J., 2013. In-depth mass spectrometric mapping of the human vitreous proteome. Proteome Sci. 11, 22.

Asashima, T., Hori, S., Ohtsuki, S., Tachikawa, M., Watanabe, M., Mukai, C., Kitagaki, S., Miyakoshi, N., Terasaki, T., 2006. ATP-binding cassette transporter G2 mediates the efflux of phototoxins on the luminal membrane of retinal capillary endothelial cells. Pharm. Res. 23, 1235–1242.

Ashton, N., Cunha-Vaz, J.G., 1965. Effect of histamine on the permeability of the ocular vessels. Arch. Ophthalmol. 73, 211–223.

Audren, F., Tod, M., Massin, P., Benosman, R., Haouchine, B., Erginay, A., Caulin, C., Gaudric, A., Bergmann, J.-F., 2004. Pharmacokinetic–pharmacodynamic modeling of the effect of triamcinolone acetonide on central macular thickness in patients with diabetic macular edema. Investig. Opthalmology Vis. Sci. 45, 3435–3441.

Awwad, S., Lockwood, A., Brocchini, S., Khaw, P.T., 2015. The PK-Eye: a novel in vitro ocular flow model for use in preclinical drug development. J. Pharm. Sci. 104, 3330–3342.

Bainbridge, J.W.B., Mehat, M.S., Sundaram, V., Robbie, S.J., Barker, S.E., Ripamonti, C., Georgiadis, A., Mowat, F.M., Beattie, S.G., Gardner, P.J., Feathers, K.L., Luong, V.A., Yzer, S., Balaggan, K., Viswanathan, A., de Ravel, T.J.L., Casteels, I., Holder, G.E., Tyler, N., Fitzke, F.W., Weleber, R.G., Nardini, M., Moore, A.T., Thompson, D.A., Petersen-Jones, S.M., Michaelides, M., van den Born, L.I., Stockman, A., Smith, A.J., Rubin, G., Ali, R.R., 2015. Long-term effect of gene therapy on Leber's congenital amaurosis. N. Engl. J. Med. 372, 1887–1897. http://dx.doi.org/10.1056/NEJMoa1414221.

Bakri, S.J., Snyder, M.R., Reid, J.M., Pulido, J.S., Singh, R.J., 2007. Pharmacokinetics of intravitreal bevacizumab (Avastin). Ophthalmology 114, 855–859.

Balazs, E., 1983. Functional anatomy of the Vitreus. In: Duane, T., Jaeger, E. (Eds.), Biomedical Foundations of Ophthalmology, pp. 1–16.

Barany, Y.E., Kinsey, V.E., 1949. The rate of flow of aqueous humor; the rate of disappearance of para-aminohippuric acid, radioactive rayopake, and radioactive diodrast from the aqueous humor of rabbits. Am. J. Ophthalmol. 32 (Pt. 2), 177–188.

Barcia, E., Herrero-Vanrell, R., Díez, A., Alvarez-Santiago, C., López, I., Calonge, M., 2009. Downregulation of endotoxin-induced uveitis by intravitreal injection of polylactic-glycolic acid (PLGA) microspheres loaded with dexamethasone. Exp. Eye Res. 89, 238–245.

Bartlett, J.D., Cullen, A.P., 1989. Clinical administration of ocular drugs. In: Bartlett, J.D., Jaanus, S.D. (Eds.), Clinical Ocular Pharmacology. Butterworth-Heinemann, USA, pp. 29–66.

Barza, M., Kane, A., Baum, J., 1982. The effects of infection and probenecid on the transport of carbenicillin from the rabbit vitreous humor. Investig. Ophthalmol. Vis. Sci. 22, 720–726.

Barza, M., Lynch, E., Baum, J.L., 1993. Pharmacokinetics of newer cephalosporins after subconjunctival and intravitreal injection in rabbits. Arch. Ophthalmol. 111, 121–125.

Barza, M., Stuart, M., Szoka, F., 1987. Effect of size and lipid composition on the pharmacokinetics of intravitreal liposomes. Investig. Ophthalmol. Vis. Sci. 28, 893–900.

Berezovsky, D.E., Patel, S.R., McCarey, B.E., Edelhauser, H.F., 2011. In vivo ocular fluorophotometry: delivery of fluoresceinated dextrans via transscleral diffusion in rabbits. Investig. Ophthalmol. Vis. Sci. 52, 7038–7045.

Berman, E.R., 1991. Biochemistry of the Eye, first. ed. Plenum Press, New York.

Bienert, A., Kamińska, A., Olszewski, J., Gracz, J., Grabowski, T., Wolc, A., Grześkowiak, E., 2012. Pharmacokinetics and ocular disposition of paracetamol and paracetamol glucuronide in rabbits with diabetes mellitus induced by alloxan. Pharmacol. Rep. 64, 421–427.

Bill, A., 1975. Blood circulation and fluid dynamics in the eye. Physiol. Rev. 55, 383–417.

Bill, A., 1968. Capillary permeability to and extravascular dynamics of myoglobin, albumin and gammaglobulin in the uvea. Acta Physiol. Scand. 73, 204–219.

Bill, A., Törnquist, P., Alm, A., 1980. Permeability of the intraocular blood vessels. Trans. Ophthalmol. Soc. U. K. 100, 332–336.

Binder, C., Read, S.P., Cashman, S.M., Kumar-Singh, R., 2011. Nuclear targeted delivery of macromolecules to retina and cornea. J. Gene Med. 13, 158–170.

Bishop, P., 1996. The biochemical structure of mammalian vitreous. Eye 10, 664–670.

Blair, N.P., Rusin, M.M., 1986. Blood-retinal barrier permeability to carboxyfluorescein and fluorescein in monkeys. Graefe's Arch. Clin. Exp. Ophthalmol. 224, 419–422.

Blomquist, P.H., Palmer, B.F., 2011. Ocular complications of systemic medications. Am. J. Med. Sci. 342, 62–69.

Bora, N.S., Gobleman, C.L., Atkinson, J.P., Pepose, X.J.S., Kaplan, H.J., 1993. Differential expression of the complement regulatory proteins in the human eye. Investig. Ophthalmol. Vis. Sci. 34, 3579–3584.

Boruchoff, S.A., Woodin, A.M., 1956. Viscosity and composition of solutions derived from rabbit vitreous humour. Br. J. Ophthalmol. 40, 113–118.

Bos, K.J., Holmes, D.F., Meadows, R.S., Kadler, K.E., McLeod, D., Bishop, P.N., 2001. Collagen fibril organisation in mammalian vitreous by freeze etch/rotary shadowing electron microscopy. Micron 32, 301–306.

Boulton, M., Dayhaw-Barker, P., 2001. The role of the retinal pigment epithelium: topographical variation and ageing changes. Eye (Lond) 15, 384–389.

Boulton, M.E., 2014. Studying melanin and lipofuscin in RPE cell culture models. Exp. Eye Res. 126, 61–67.

Bourges, J.L., Gautier, S.E., Delie, F., Bejjani, R.A., Jeanny, J.C., Gurny, R., BenEzra, D., Behar-Cohen, F.F., 2003. Ocular drug delivery targeting the retina and retinal pigment epithelium using polylactide nanoparticles. Investig. Ophthalmol. Vis. Sci. 44, 3562–3569.

Boussif, O., Lezoualc'h, F., Zanta, M.A., Mergny, M.D., Scherman, D., Demeneix, B., Behr, J.P., 1995. A versatile vector for gene and oligonucleotide transfer into cells in culture and in vivo: polyethylenimine. Proc. Natl. Acad. Sci. U. S. A. 92, 7297–7301.

Bringmann, A., Pannicke, T., Grosche, J., Francke, M., Wiedemann, P., Skatchkov, S.N., Osborne, N.N., Reichenbach, A., 2006. Müller cells in the healthy and diseased retina. Prog. Retin. Eye Res. 25, 397–424.

Brubaker, R.F., 1982. The flow of aqueous humor in the human eye. Trans. Am. Ophthalmol. Soc. 80, 391–474.

Brunner, S., Sauer, T., Carotta, S., Cotten, M., Saltik, M., Wagner, E., 2000. Cell cycle dependence of gene transfer by lipoplex, polyplex and recombinant adenovirus. Gene Ther. 7, 401–407.

Buitrago, E., Winter, U., Williams, G., Asprea, M., Chantada, G., Schaiquevich, P., 2016. Pharmacokinetics of melphalan after intravitreal injection in a rabbit model. J. Ocul. Pharmacol. Ther. 32, 230–235.

Bunt-Milam, A.H., Saari, J.C., Klock, I.B., Garwin, G.G., 1985. Zonulae adherentes pore size in the external limiting membrane of the rabbit retina. Investig. Ophthalmol. Vis. Sci. 26, 1377–1380.

Butler, J.M., Unger, W.G., Grierson, I., 1988. Recent experimental studies on the blood-aqueous barrier: the anatomical basis of the response to injury. Eye (Lond) 2 (Suppl. l), S213–S220.

Caicedo, A., Espinosa-Heidmann, D.G., Piña, Y., Hernandez, E.P., Cousins, S.W., 2005. Blood-derived macrophages infiltrate the retina and activate Muller glial cells under experimental choroidal neovascularization. Exp. Eye Res. 81, 38–47.

Campochiaro, P.A., 2015. Molecular pathogenesis of retinal and choroidal vascular diseases. Prog. Retin. Eye Res. 49, 67–81. http://dx.doi.org/10.1016/j.preteyeres.2015.06.002.

Chapy, H., Saubaméa, B., Tournier, N., Bourasset, F., Behar-Cohen, F., Declèves, X., Scherrmann, J.-M., Cisternino, S., 2016. Blood-brain and retinal barriers show

dissimilar ABC transporter impacts and concealed effect of P-glycoprotein on a novel verapamil influx carrier. Br. J. Pharmacol. 173, 497–510.
Chastain, J.E., Sanders, M.E., Curtis, M.A., Chemuturi, N.V., Gadd, M.E., Kapin, M.A., Markwardt, K.L., Dahlin, D.C., 2016. Distribution of topical ocular nepafenac and its active metabolite amfenac to the posterior segment of the eye. Exp. Eye Res. 145, 58–67.
Chen, C.-H., Chen, S.C., 1981. Studies on soluble proteins of vitreous in experimental animals. Exp. Eye Res. 32, 381–388.
Chen, M., Li, X., Liu, J., Han, Y., Cheng, L., 2015. Safety and pharmacodynamics of suprachoroidal injection of triamcinolone acetonide as a controlled ocular drug release model. J. Control. Release 203, 109–117.
Chen, P., Chen, H., Zang, X., Chen, M., Jiang, H., Han, S., Wu, X., 2013. Expression of efflux transporters in human ocular tissues. Drug Metab. Dispos. 41, 1934–1948.
Chiang, B., Kim, Y.C., Edelhauser, H.F., Prausnitz, M.R., 2016. Circumferential flow of particles in the suprachoroidal space is impeded by the posterior ciliary arteries. Exp. Eye Res. 145, 424–431.
Chien, D.-S., Homsy, J.J., Gluchowskil, C., Tang-liu, D.D., 1990. Corneal and conjunctival/scleral penetration of p-aminoclonidine, AGN 190342, and clonidine in rabbit eyes. Curr. Eye Res. 9, 1051–1059.
Choi, H.S., Ashitate, Y., Lee, J.H., Kim, S.H., Matsui, A., Insin, N., Bawendi, M.G., Semmler-Behnke, M., Frangioni, J.V., Tsuda, A., 2010. Rapid translocation of nanoparticles from the lung airspaces to the body. Nat. Biotechnol. 28, 1300–1303.
Cholkar, K., Patel, S.P., Vadlapudi, A.D., Mitra, A.K., 2013. Novel strategies for anterior segment ocular drug delivery. J. Ocul. Pharmacol. Ther. 29, 106–123.
Chu, C.J., Dijkstra, J., Lai, M.Z., Hong, K., Szoka, F.C., 1990. Efficiency of cytoplasmic delivery by pH-sensitive liposomes to cells in culture. Pharm. Res. 7, 824–834.
Chu, X., Korzekwa, K., Elsby, R., Fenner, K., Galetin, A., Lai, Y., Matsson, P., Moss, A., Nagar, S., Rosania, G.R., Bai, J.P.F., Polli, J.W., Sugiyama, Y., Brouwer, K.L.R., International Transporter Consortium, 2013. Intracellular drug concentrations and transporters: measurement, modeling, and implications for the liver. Clin. Pharmacol. Ther. 94, 126–141.
Coco, R.M., López, M.I., Pastor, J.C., Nozal, M.J., 1998. Pharmacokinetics of intravitreal vancomycin in normal and infected rabbit eyes. J. Ocul. Pharmacol. Ther. 14, 555–563.
Cohen, S.Y., Mimoun, G., Oubraham, H., Zourdani, A., Malbrel, C., Queré, S., Schneider, V., LUMIERE Study Group, 2013. Changes in visual acuity in patients with wet age-related macular degeneration treated with intravitreal ranibizumab in daily clinical practice: the LUMIERE study. Retina 33, 474–481.
Cole, D.F., 1974. The site of breakdown of the blood-aqueous barrier under the influence of vaso-dilator drugs. Exp. Eye Res. 19, 591–607.
Conner, S.D., Schmid, S.L., 2003. Regulated portals of entry into the cell. Nature 422, 37–44.
Crist, R.M., Grossman, J.H., Patri, A.K., Stern, S.T., Dobrovolskaia, M. a, Adiseshaiah, P.P., Clogston, J.D., McNeil, S.E., 2013. Common pitfalls in nanotechnology: lessons learned from NCI's Nanotechnology Characterization Laboratory. Integr. Biol. (Camb) 5, 66–73.
Cunha-Vaz, J., Maurice, D., 1969. Fluorescein dynamics in the eye. Doc. Ophthalmol. 26, 61–72.
Cunha-Vaz, J., Maurice, D., 1967. The active transport of fluorescein by the retinal vessels and the retina. J. Physiol. 191, 467–486.
D'Ischia, M., Wakamatsu, K., Cicoira, F., Di Mauro, E., Garcia-Borron, J.C., Commo, S., Galvan, I., Ghanem, G., Kenzo, K., Meredith, P., Pezzella, A., Santato, C., Sarna, T., Simon, J.D., Zecca, L., Zucca, F.A., Napolitano, A., Ito, S., 2015. Melanins and melanogenesis: from pigment cells to human health and technological applications. Pigment. Cell Melanoma Res. 28, 520–544.
D'Orazio, T.J., Niederkorn, J.Y., 1998. The nature of antigen in the eye has a profound effect on the cytokine milieu and resultant immune response. Eur. J. Immunol. 28, 1544–1553.
Dahlin, A., Geier, E., Stocker, S.L., Cropp, C.D., Grigorenko, E., Bloomer, M., Siegenthaler, J., Xu, L., Basile, A.S., Tang-Liu, D.D.S., Giacomini, K.M., 2013. Gene expression profiling of transporters in the solute carrier and ATP-binding cassette superfamilies in human eye substructures. Mol. Pharm. 10, 650–663.
Dalkara, D., Kolstad, K.D., Caporale, N., Visel, M., Klimczak, R.R., Schaffer, D.V., Flannery, J.G., 2009. Inner limiting membrane barriers to AAV-mediated retinal transduction from the vitreous. Mol. Ther. 17, 2096–2102.
Davis, B.M., Normando, E.M., Guo, L., Turner, L.A., Nizari, S., O'Shea, P., Moss, S.E., Somavarapu, S., Cordeiro, M.F., 2014. Topical delivery of Avastin to the posterior segment of the eye in vivo using annexin A5-associated liposomes. Small 10, 1575–1584.
Dayhaw-Barker, P., 2002. Retinal pigment epithelium melanin and ocular toxicity. Int. J. Toxicol. 21, 451–454.
de Almeida, F.P.P., Saliba, J.B., Ribeiro, J.A.S., Siqueira, R.C., Fialho, S.L., Silva-Cunha, A., Jorge, R., Messias, A., 2015. In vivo release and retinal toxicity of cyclosporine-loaded intravitreal device. Doc. Ophthalmol. 131, 207–214.
De Kozak, Y., Andrieux, K., Villarroya, H., Klein, C., Thillaye-Goldenberg, B., Naud, M.-C., Garcia, E., Couvreur, P., 2004. Intraocular injection of tamoxifen-loaded nanoparticles: a new treatment of experimental autoimmune uveoretinitis. Eur. J. Immunol. 34, 3702–3712.
Deissler, H.L., Lang, G.K., Lang, G.E., 2016. Internalization of bevacizumab by retinal endothelial cells and its intracellular fate: evidence for an involvement of the neonatal Fc receptor. Exp. Eye Res. 143, 49–59.
del Amo, E.M., 2015. Ocular and Systemic Pharmacokinetic Models for Drug Discovery and Development. University of Helsinki. https://helda.helsinki.fi/handle/10138/156330.
del Amo, E.M., Urtti, A., 2015. Rabbit as an animal model for intravitreal pharmacokinetics: clinical predictability and quality of the published data. Exp. Eye Res. 137, 111–124.
del Amo, E.M., Urtti, A., 2008. Current and future ophthalmic drug delivery systems. A shift to the posterior segment. Drug Discov. Today 13, 135–143.
Del Amo, E.M., Vellonen, K.S., Kidron, H., Urtti, A., 2015. Intravitreal clearance and volume of distribution of compounds in rabbits: in silico prediction and pharmacokinetic simulations for drug development. Eur. J. Pharm. Biopharm. 95, 215–226.
Deng, Z.J., Liang, M., Monteiro, M., Toth, I., Minchin, R.F., 2011. Nanoparticle-induced unfolding of fibrinogen promotes Mac-1 receptor activation and inflammation. Nat. Nanotechnol. 6, 39–44.
Dias, C.S., Anand, B.S., Mitra, A.K., 2002. Effect of mono- and di-acylation on the ocular disposition of ganciclovir: physicochemical properties, ocular bioreversion, and antiviral activity of short chain ester prodrugs. J. Pharm. Sci. 91, 660–668.
Dias, C.S., Mitra, A.K., 2000. Vitreal elimination kinetics of large molecular weight FITC-labeled dextrans in albino rabbits using a novel microsampling technique. J. Pharm. Sci. 89, 572–578.
Dickmann, L.J., Yip, V., Li, C., Abundes, J., Maia, M., Young, C., Stainton, S., Hass, P.E., Joseph, S.B., Prabhu, S., Andrew Boswell, C., 2015. Evaluation of fluorophotometry to assess the vitreal pharmacokinetics of protein therapeutics. Investig. Ophthalmol. Vis. Sci. 56, 6991–6999.
Dithmer, M., Hattermann, K., Pomarius, P., Aboul Naga, S.H., Meyer, T., Mentlein, R., Roider, J., Klettner, A., 2016. The role of Fc-receptors in the uptake and transport of therapeutic antibodies in the retinal pigment epithelium. Exp. Eye Res. 145, 187–205.
Dixon, J. a, Oliver, S.C.N., Olson, J.L., Mandava, N., 2009. VEGF Trap-Eye for the treatment of neovascular age-related macular degeneration. Expert Opin. Investig. Drugs 18, 1573–1580.
Doane, M.G., Jensen, A.D., Dohlman, C.H., 1978. Penetration routes of topically applied eye medications. Am. J. Ophthalmol. 85, 383–386.
Docter, D., Westmeier, D., Markiewicz, M., Stolte, S., Knauer, S.K., Stauber, R.H., 2015. The nanoparticle biomolecule corona: lessons learned - challenge accepted? Chem. Soc. Rev. 44, 6094–6121.
Dolghih, E., Jacobson, M.P., 2013. Predicting efflux ratios and blood-brain barrier penetration from chemical structure: Combining passive permeability with active efflux by P-glycoprotein. ACS Chem. Neurosci. 4, 361–367.
Doonan, F., Groeger, G., Cotter, T.G., 2012. Preventing retinal apoptosis — is there a common therapeutic theme? Exp. Cell Res. 318, 1278–1284. http://dx.doi.org/10.1016/j.yexcr.2012.02.003.
Dowty, M.E., Williams, P., Zhang, G., Hagstrom, J.E., Wolff, J.A., 1995. Plasmid DNA entry into postmitotic nuclei of primary rat myotubes. Proc. Natl. Acad. Sci. U. S. A. 92, 4572–4576.
Duvvuri, S., Majumdar, S., Mitra, A.K., 2004. Role of metabolism in ocular drug delivery. Curr. Drug Metab. 5, 507–515.
Einmahl, S., Behar-Cohen, F., Tabatabay, C., Savoldelli, M., D'Hermies, F., Chauvaud, D., Heller, J., Gurny, R., 2000. A viscous bioerodible poly(ortho ester) as a new biomaterial for intraocular application. J. Biomed. Mater. Res. 50, 566–573.
Einmahl, S., Ponsart, S., Bejjani, R.A., D'Hermies, F., Savoldelli, M., Heller, J., Tabatabay, C., Gurny, R., Behar-Cohen, F., 2003. Ocular biocompatibility of a poly(ortho ester) characterized by autocatalyzed degradation. J. Biomed. Mater. Res. A 67, 44–53.
Einmahl, S., Savoldelli, M., D'Hermies, F., Tabatabay, C., Gurny, R., Behar-Cohen, F., 2002. Evaluation of a novel biomaterial in the suprachoroidal space of the rabbit eye. Investig. Ophthalmol. Vis. Sci. 43, 1533–1539.
Elsabahy, M., Wooley, K.L., 2013. Cytokines as biomarkers of nanoparticle immunotoxicity. Chem. Soc. Rev. 42, 5552–5576.
Fanea, L., Fagan, A.J., 2012. Review: magnetic resonance imaging techniques in ophthalmology. Mol. Vis. 18, 2538–2560.
Farrera, C., Fadeel, B., 2015. It takes two to tango: understanding the interactions between engineered nanomaterials and the immune system. Eur. J. Pharm. Biopharm. 95, 3–12.
Fattal, E., Nir, S., Parente, R.A., Szoka, F.C., 1994. Pore-forming peptides induce rapid phospholipid flip-flop in membranes. Biochemistry 33, 6721–6731.
Feke, G.T., Tagawa, H., Deupree, D.M., Goger, D.G., Sebag, J., Weiter, J.J., 1989. Blood flow in the normal human retina. Invest. Ophthalmol. Vis. Sci. 30, 58–65.
Ficker, L., Meredith, T.A., Gardner, S., Wilson, L.A., 1990. Cefazolin levels after intravitreal injection. Effects of inflammation and surgery. Investig. Ophthalmol. Vis. Sci. 31, 502–505.
Fishman, G.A., Apushkin, M.A., 2007. Continued use of dorzolamide for the treatment of cystoid macular oedema in patients with retinitis pigmentosa. Br. J. Ophthalmol. 91, 743–745.
Fonseca, S.B., Pereira, M.P., Kelley, S.O., 2009. Recent advances in the use of cell-penetrating peptides for medical and biological applications. Adv. Drug Deliv. Rev. 61, 953–964.
Forooghian, F., Chew, E.Y., Meyerle, C.B., Cukras, C., Wong, W.T., 2011. Investigation of the role of neutralizing antibodies against bevacizumab as mediators of tachyphylaxis. Acta Ophthalmol. 89, e206–e207.
Forooghian, F., Cukras, C., Meyerle, C.B., Chew, E.Y., Wong, W.T., 2009. Tachyphylaxis after intravitreal bevacizumab for exudative age-related macular degeneration. Retina 29, 723–731.
Forrester, J.V., Dick, A.D., McMenamin, P.G., Roberts, F., Pearlman, E., 2016. The Eye, Basic Sciences in Practice, fourth. ed. Elsevier.

Friend, D.S., Papahadjopoulos, D., Debs, R.J., 1996. Endocytosis and intracellular processing accompanying transfection mediated by cationic liposomes. Biochim. Biophys. Acta 1278, 41–50.
Fujii, S., Setoguchi, C., Kawazu, K., Hosoya, K., 2015. Functional characterization of carrier-mediated transport of pravastatin across the blood-retinal barrier in rats. Drug Metab. Dispos. 43, 1956–1959.
Gadkar, K., Pastuskovas, C.V., Le Couter, J.E., Elliott, J.M., Zhang, J., Lee, C.V., Sanowar, S., Fuh, G., Kim, H.S., Lombana, T.N., Spiess, C., Nakamura, M., Hass, P., Shatz, W., Meng, Y.G., Scheer, J.M., 2015. Design and pharmacokinetic characterization of novel antibody formats for ocular therapeutics. Investig. Ophthalmol. Vis. Sci. 56, 5390–5400.
Gal-Or, O., Dotan, A., Dachbash, M., Tal, K., Nisgav, Y., Weinberger, D., Ehrlich, R., Livnat, T., 2016. Bevacizumab clearance through the iridocorneal angle following intravitreal injection in a rat model. Exp. Eye Res. 145, 412–416. http://dx.doi.org/10.1016/j.exer.2016.02.006.
Gan, L., Wang, J., Zhao, Y., Chen, D., Zhu, C., Liu, J., Gan, Y., 2013. Hyaluronan-modified core–shell liponanoparticles targeting CD44-positive retinal pigment epithelium cells via intravitreal injection. Biomaterials 34, 5978–5987.
Gao, B.B., Chen, X., Timothy, N., Aiello, L.P., Feener, E.P., 2008. Characterization of the vitreous proteome in diabetes without diabetic retinopathy and diabetes with proliferative diabetic retinopathy. J. Proteome Res. 7, 2516–2525.
Gaudreault, J., Fei, D., Rusit, J., Suboc, P., Shiu, V., 2005. Preclinical pharmacokinetics of ranibizumab (rhuFabV2) after a single intravitreal administration. Investig. Ophthalmol. Vis. Sci. 46, 726–733.
Genead, M.A., Fishman, G.A., 2010. Efficacy of sustained topical dorzolamide therapy for cystic macular lesions in patients with retinitis pigmentosa and usher syndrome. Arch. Ophthalmol. 128, 1146–1150.
Ghate, D., Brooks, W., McCarey, B.E., Edelhauser, H.F., 2007. Pharmacokinetics of intraocular drug delivery by periocular injections using ocular fluorophotometry. Investig. Ophthalmol. Vis. Sci. 48, 2230–2237.
Gilger, B.C., Abarca, E.M., Salmon, J.H., Patel, S., 2013. Treatment of acute posterior uveitis in a porcine model by injection of triamcinolone acetonide into the suprachoroidal space using microneedles. Investig. Ophthalmol. Vis. Sci. 54, 2483–2492.
Giordano, G.G., Chevez-Barrios, P., Refojo, M.F., Garcia, C.A., 1995. Biodegradation and tissue reaction to intravitreous biodegradable poly (D, L-lactic-co-glycolic) acid microspheres. Curr. Eye Res. 14, 761–768.
Gisladottir, S., Loftsson, T., Stefansson, E., 2009. Diffusion characteristics of vitreous humour and saline solution follow the Stokes Einstein equation. Graefe's Arch. Clin. Exp. Ophthalmol 247, 1677–1684.
Gnana-Prakasam, J.P., Reddy, S.K., Veeranan-Karmegam, R., Smith, S.B., Martin, P.M., Ganapathy, V., 2011. Polarized distribution of heme transporters in retinal pigment epithelium and their regulation in the iron-overload disease hemochromatosis. Investig. Ophthalmol. Vis. Sci. 52, 9279–9286.
Goldman, D., 2014. Müller glial cell reprogramming and retina regeneration. Nat. Rev. Neurosci. 15, 431–442.
Goyal, K., Koul, V., Singh, Y., Anand, A., 2014. Targeted drug delivery to central nervous system (CNS) for the treatment of neurodegenerative disorders: trends and advances. Cent. Nerv. Syst. Agents Med. Chem. 14, 43–59.
Grassmann, F., Fauser, S., Weber, B.H.F., 2015. The genetics of age-related macular degeneration (AMD) – novel targets for designing treatment options? Eur. J. Pharm. Biopharm. 95, 194–202. http://dx.doi.org/10.1016/j.ejpb.2015.04.039.
Gregoriadis, G., Ryman, B.E., 1972. Lysosomal localization of -fructofuranosidase-containing liposomes injected into rats. Biochem. J. 129, 123–133.
Gross, N., Ranjbar, M., Evers, C., Hua, J., Martin, G., Schulze, B., Michaelis, U., Hansen, L.L., Agostini, H.T., 2013. Choroidal neovascularization reduced by targeted drug delivery with cationic liposome-encapsulated paclitaxel or targeted photodynamic therapy with verteporfin encapsulated in cationic liposomes. Mol. Vis. 19, 54–61.
Grover, S., Apushkin, M.A., Fishman, G.A., 2006. Topical dorzolamide for the treatment of cystoid macular edema in patients with retinitis pigmentosa. Am. J. Ophthalmol. 141, 850–858.
Gruenberg, J., van der Goot, F.G., 2006. Mechanisms of pathogen entry through the endosomal compartments. Nat. Rev. Mol. Cell Biol. 7, 495–504.
Guadagni, V., Novelli, E., Piano, I., Gargini, C., Strettoi, E., 2015. Pharmacological approaches to retinitis pigmentosa: a laboratory perspective. Prog. Retin. Eye Res. 48, 62–81. http://dx.doi.org/10.1016/j.preteyeres.2015.06.005.
Guo, W., Zhu, Y., Yu, P.K., Yu, X., Sun, X., Cringle, S.J., Su, E.-N., Yu, D.-Y., 2012. Quantitative study of the topographic distribution of conjunctival lymphatic vessels in the monkey. Exp. Eye Res. 94, 90–97.
Hämäläinen, K.M., Kananen, K., Auriola, S., Kontturi, K., Urtti, A., 1997. Characterization of paracellular and aqueous penetration routes in cornea, conjunctiva, and sclera. Investig. Ophthalmol. Vis. Sci. 38, 627–634.
Hamdi, Y., Lallemand, F., Benita, S., 2015. Drug-loaded nanocarriers for back-of-the-eye diseases- formulation limitations. J. Drug Deliv. Sci. Technol. 30, 331–341.
Hanisch, U.-K.K., Kettenmann, H., 2007. Microglia: active sensor and versatile effector cells in the normal and pathologic brain. Nat. Neurosci. 10, 1387–1394.
Hanus, J., Zhang, H., Wang, Z., Liu, Q., Zhou, Q., Wang, S., 2013. Induction of necrotic cell death by oxidative stress in retinal pigment epithelial cells. Cell Death Dis. 4, e965.
Haritova, A.M., Krastev, S.Z., Santos, R.R., Schrickx, J.A., Fink-Gremmels, J., 2013. ABC transporters in the eyes of dogs and implications in drug therapy. Curr. Eye Res. 38, 271–277.
Haselton, F.R., Alexander, J.S., Dworska, E., Evans, S.S., Hoffman, L.H., 1996. Modulation of retinal endothelial barrier in a perfused cell-column model of the retinal microvasculature. Investig. Ophthalmol. Vis. Sci. 37, 211–222.
Haselton, F.R., Dworska, E.J., Huffman, L.H., 1998. Glucose-induced increase in paracellular permeability and disruption of beta-receptor signaling in retinal endothelium. Investig. Ophthalmol. Vis. Sci. 39, 1676–1684.
Heegaard, S., 1997. Morphology of the vitreoretinal border region. Acta Ophthalmol. Scand. Suppl. 1–31.
Heegaard, S., Jensen, O.A., Prause, J.U., 1986. Structure and composition of the inner limiting membrane of the retina. SEM on frozen resin-cracked and enzyme-digested retinas of Macaca mulatta. Graefes Arch. Clin. Exp. Ophthalmol. 224, 355–360.
Heiduschka, P., Fietz, H., Hofmeister, S., Schultheiss, S., Mack, A.F., Peters, S., Ziemssen, F., Niggemann, B., Julien, S., Bartz-Schmidt, K.U., Schraermeyer, U., 2007. Penetration of bevacizumab through the retina after intravitreal injection in the monkey. Investig. Ophthalmol. Vis. Sci. 48, 2814–2823.
Herrero-Vanrell, R., Bravo-Osuna, I., Andrés-Guerrero, V., Vicario-de-la-Torre, M., Molina-Martínez, I.T., 2014. The potential of using biodegradable microspheres in retinal diseases and other intraocular pathologies. Prog. Retin. Eye Res. 42, 27–43.
Herrero-Vanrell, R., Refojo, M.F., 2001. Biodegradable microspheres for vitreoretinal drug delivery. Adv. Drug Deliv. Rev. 52, 5–16.
Ho, V.Y., Yeh, S., Olsen, T.W., Bergstrom, C.S., Yan, J., Cribbs, B.E., Hubbard 3rd, G.B., 2013. Short-term outcomes of aflibercept for neovascular age-related macular degeneration in eyes previously treated with other vascular endothelial growth factor inhibitors. Am. J. Ophthalmol. 156, 23–28 e2.
Hollo, G., Whitson, J.T., Faulkner, R., McCue, B., Curtis, M., Wieland, H., Chastain, J., Sanders, M., DeSantis, L., Przydryga, J., Dahlin, D.C., 2006. Concentrations of betaxolol in ocular tissues of patients with glaucoma and normal monkeys after 1 month of topical ocular administration. Investig. Ophthalmol. Vis. Sci. 47, 235–240.
Holmgren, P., Druid, H., Holmgren, A., Ahlner, J., 2004. Stability of drugs in stored postmortem femoral blood and vitreous humor. J. Forensic Sci. 49, 820–825.
Holz, F.G., Strauss, E.C., Schmitz-Valckenberg, S., van Lookeren Campagne, M., 2014. Geographic atrophy: clinical features and potential therapeutic approaches. Ophthalmology 121, 1079–1091.
Holz, F.G., Tadayoni, R., Beatty, S., Berger, A., Cereda, M.G., Cortez, R., Hoyng, C.B., Hykin, P., Staurenghi, G., Heldner, S., Bogumil, T., Heah, T., Sivaprasad, S., 2015. Multi-country real-life experience of anti-vascular endothelial growth factor therapy for wet age-related macular degeneration. Br. J. Ophthalmol. 99, 220–226.
Hom, R.K., Katzenellenbogen, J.A., 1997. Technetium-99m-labeled receptor-specific small-molecule radiopharmaceuticals: recent developments and encouraging results. Nucl. Med. Biol. 24, 485–498.
Hong, L., Simon, J.D., 2007. Current understanding of the binding sites, capacity, affinity, and biological significance of metals in melanin. J. Phys. Chem. B 111, 7938–7947.
Hosoya, K., Makihara, A., Tsujikawa, Y., Yoneyama, D., Mori, S., Terasaki, T., Akanuma, S., Tomi, M., Tachikawa, M., 2009. Roles of inner blood-retinal barrier organic anion transporter 3 in the vitreous/retina-to-blood efflux transport of p-aminohippuric acid, benzylpenicillin, and 6-mercaptopurine. Pharmacology 329, 87–93.
Hosoya, K., Tomi, M., 2005. Advances in the cell biology of transport via the inner blood-retinal barrier: establishment of cell lines and transport functions. Biol. Pharm. Bull. 28, 1–8.
Hosoya, K., Tomi, M., Tachikawa, M., 2011. Strategies for therapy of retinal diseases using systemic drug delivery: relevance of transporters at the blood–retinal barrier. Expert Opin. Drug Deliv. 8, 1571–1587.
Hosoya, K.I., Yamamoto, A., Akanuma, S.I., Tachikawa, M., 2010. Lipophilicity and transporter influence on blood-retinal barrier permeability: a comparison with blood-brain barrier permeability. Pharm. Res. 27, 2715–2724.
Hu, D.-N., Simon, J.D., Sarna, T., 2008. Role of ocular melanin in ophthalmic physiology and pathology. Photochem. Photobiol. 84, 639–644.
Hu, S., Koevary, S., 2016. Efficacy of antibody delivery to the retina and optic nerve by topical administration. J. Ocul. Pharmacol. Ther. 32, 203–210.
Huang, H.-S., Schoenwald, R.D., 1983. Corneal penetration behavior of β-blocking agents I: physicochemical factors. J. Pharm. Sci. 72, 1266–1272.
Hughes, P.M., Olejnik, O., Chang-Lin, J.-E., Wilson, C.G., 2005. Topical and systemic drug delivery to the posterior segments. Adv. Drug Deliv. Rev. 57, 2010–2032.
Hutton-Smith, L.A., Gaffney, E.A., Byrne, H.M., Maini, P.K., Schwab, D., Mazer, N.A., 2016 Sep 6. A mechanistic model of the intravitreal pharmacokinetics of large molecules and the pharmacodynamic suppression of ocular Vascular Endothelial Growth Factor levels by ranibizumab in patients with neovascular age-related macular degeneration. Mol. Pharm. 13 (9), 2941–2950. http://dx.doi.org/10.1021/acs.molpharmaceut.5b00849.
Huttunen, K.M., Rautio, J., 2011. Prodrugs - an efficient way to breach delivery and targeting barriers. Curr. Top. Med. Chem. 11, 2265–2287.
Ibrahim, A.S., El-Remessy, A.B., Matragoon, S., Zhang, W., Patel, Y., Khan, S., Al-Gayyar, M.M., El-Shishtawy, M.M., Liou, G.I., 2011. Retinal microglial activation and inflammation induced by amadori-glycated albumin in a rat model of diabetes. Diabetes 60, 1122–1133.
Illum, L., Davis, S.S., 1984. The organ uptake of intravenously administered colloidal particles can be altered using a non-ionic surfactant (Poloxamer 338). FEBS Lett. 167, 79–82.
Imai, H., Misra, G.P., Wu, L., Janagam, D.R., Gardner, T.W., Lowe, T.L., 2015. Subconjunctivally implanted hydrogels for sustained insulin release to reduce retinal cell apoptosis in diabetic rats. Investig. Opthalmology Vis. Sci. 56,

7839–7846.
Inoue, J., Oka, M., Aoyama, Y., Kobayashi, S., Ueno, S., Hada, N., Takeda, T., Takehana, M., 2004. Effects of dorzolamide Hydrochloride on ocular tissues. J. Ocul. Pharmacol. Ther. 20, 1–13.
Inoue, K., 2014. Managing adverse effects of glaucoma medications. Clin. Ophthalmol. 8, 903–913.
Ito, S., 1986. Reexamination of the structure of eumelanin. Biochim. Biophys. Acta - Gen. Subj. 883, 155–161.
Jääskeläinen, I., Mönkkönen, J., Urtti, A., 1994. Oligonucleotide-cationic liposome interactions. A physicochemical study. Biochim. Biophys. Acta - Biomembr. 1195, 115–123.
Jackson, T.L., Antcliff, R.J., Hillenkamp, J., Marshall, J., 2003. Human retinal molecular weight exclusion limit and estimate of species variation. Investig. Ophthalmol. Vis. Sci. 44, 2141–2146.
Jansen, J., Koopmans, S.A., Los, L.I., van der Worp, R.J., Podt, J.G., Hooymans, J.M.M., Feijen, J., Grijpma, D.W., 2011. Intraocular degradation behavior of crosslinked and linear poly(trimethylene carbonate) and poly(d,l-lactic acid). Biomaterials 32, 4994–5002.
Järvinen, K., Järvinen, T., Urtti, A., 1995. Ocular absorption following topical delivery. Adv. Drug Deliv. Rev. 16, 3–19.
Jeon, C.J., Strettoi, E., Masland, R.H., 1998. The major cell populations of the mouse retina. J. Neurosci. 18, 8936–8946.
Johnson, F., Maurice, D., 1984. A Simple Method of Measuring Aqueous Humor Flow with Intravitreal Fluoresceinated Dextrans, vol. 39, pp. 791–805. http://dx.doi.org/10.1016/0014-4835(84)90078-2.
Johnson, L.N., Cashman, S.M., Kumar-Singh, R., 2008. Cell-penetrating peptide for enhanced delivery of nucleic acids and drugs to ocular tissues including retina and cornea. Mol. Ther. 16, 107–114.
Johnson, L.N., Cashman, S.M., Read, S.P., Kumar-Singh, R., 2010. Cell penetrating peptide POD mediates delivery of recombinant proteins to retina, cornea and skin. Vis. Res. 50, 686–697.
Jordán, J., Ruíz-Moreno, J.M., 2013. Advances in the understanding of retinal drug disposition and the role of blood-ocular barrier transporters. Expert Opin. Drug Metab. Toxicol. 5255, 1–12.
Joussen, A., Wolf, S., Kaiser, P., Boyer, D., Schmelter, T., Sandbrink, R., Zeitz, O., Boettger, M., Stemper, B., 2016. A Combined Phase 2a/b Study of the Efficacy, Safety, and Tolerability of Repeated Topical Doses of Regorafenib Eye Drops in Treatment-naïve Patients with Neovascular Age-related Macular Degeneration (NAMD). ARVO Conference, Presentation, p. 4720.
Julien, S., Biesemeier, A., Taubitz, T., Schraermeyer, U., 2014. Different effects of intravitreally injected ranibizumab and aflibercept on retinal and choroidal tissues of monkey eyes. Br. J. Ophthalmol. 98, 813–825. http://dx.doi.org/10.1136/bjophthalmol-2013-304019.
Juuti-Uusitalo, K., Vaajasaari, H., Ryhanen, T., Narkilahti, S., Suuronen, R., Mannermaa, E., Kaarniranta, K., Skottman, H., 2012. Efflux protein expression in human stem cell-derived retinal pigment epithelial cells. PLoS One 7, e30089.
Kamei, M., Misono, K., Lewis, H., 1999. A study of the ability of tissue plasminogen activator to diffuse into the subretinal space after intravitreal injection in rabbits. Am. J. Ophthalmol. 128, 739–746.
Kamizuru, H., Kimura, H., Yasukawa, T., Tabata, Y., Honda, Y., Ogura, Y., 2001. Monoclonal antibody-mediated drug targeting to choroidal neovascularization in the rat. Investig. Ophthalmol. Vis. Sci. 42, 2664–2672.
Karimi, M., Ghasemi, A., Sahandi Zangabad, P., Rahighi, R., Moosavi Basri, S.M., Mirshekari, H., Amiri, M., Shafaei Pishabad, Z., Aslani, A., Bozorgomid, M., Ghosh, D., Beyzavi, A., Vaseghi, A., Aref, A.R., Haghani, L., Bahrami, S., Hamblin, M.R., 2016. Smart micro/nanoparticles in stimulus-responsive drug/gene delivery systems. Chem. Soc. Rev. 45, 1457–1501.
Kauppinen, A., Paterno, J.J., Blasiak, J., Salminen, A., Kaarniranta, K., 2016. Inflammation and its role in age-related macular degeneration. Cell. Mol. Life Sci. 73, 1765–1786.
Kennedy, B.G., Mangini, N.J., 2002. P-glycoprotein expression in human retinal pigment epithelium. Mol. Vis. 8, 422–430.
Kent, A.R., Nussdorf, J.D., David, R., Tyson, F., Small, D., Fellows, D., 2001. Vitreous concentration of topically applied brimonidine tartrate 0.2%. Ophthalmology 108, 784–787.
Khoobehi, B., Peyman, G.A., Mcturnan, W.G., Niesman, M.R., Magin, R.L., 1988. Externally triggered release of dye and drugs from liposomes into the eye: an in vitro and in vivo study. Ophthalmology 95, 950–955.
Kidron, H., del Amo, E.M., Vellonen, K.-S., Urtti, A., 2012. Prediction of the vitreal half-life of small molecular drug-like compounds. Pharm. Res. 29, 3302–3311.
Kidron, H., Vellonen, K.S., del Amo, E.M., Tissari, A., Urtti, A., 2010. Prediction of the corneal permeability of drug-like compounds. Pharm. Res. 27, 1398–1407.
Kikuchi, R., De Morais, S.M., Kalvass, J.C., 2013. In vitro P-glycoprotein efflux ratio can predict the in vivo brain penetration regardless of biopharmaceutics drug disposition classification system class. Drug Metab. Dispos. 41, 2012–2017.
Kim, H., Robinson, M.R., Lizak, M.J., Tansey, G., Lutz, R.J., Yuan, P., Wang, N.S., Csaky, K.G., 2004. Controlled drug release from an ocular implant: an evaluation using dynamic three-dimensional magnetic resonance imaging. Investig. Ophthalmol. Vis. Sci. 45, 2722–2731.
Kim, H., Robinson, S.B., Csaky, K.G., 2009a. FcRn receptor-mediated pharmacokinetics of therapeutic IgG in the eye. Mol. Vis. 15, 2803–2812.
Kim, H., Robinson, S.B., Csaky, K.G., 2009b. Investigating the movement of intravitreal human serum albumin nanoparticles in the vitreous and retina. Pharm. Res. 26, 329–337.
Kim, J.H., Kim, J.H., Kim, K.-W., Kim, M.H., Yu, Y.S., 2009. Intravenously administered gold nanoparticles pass through the blood-retinal barrier depending on the particle size, and induce no retinal toxicity. Nanotechnology 20, 505101.
Kim, K.E., Jang, I., Moon, H., Kim, Y.J., Jeoung, J.W., Park, K.H., Kim, H., 2015. Neuroprotective effects of human serum albumin nanoparticles loaded with brimonidine on retinal ganglion cells in optic nerve crush model. Investig. Opthalmology Vis. Sci. 56, 5641–5649.
Kim, S.H., Csaky, K.G., Wang, N.S., Lutz, R.J., 2008. Drug elimination kinetics following subconjunctival injection using dynamic contrast-enhanced magnetic resonance imaging. Pharm. Res. 25, 512–520.
Kim, T., Kim, S.J., Kim, K., Kang, U.-B., Lee, C., Park, K.S., Yu, H.G., Kim, Y., 2007. Profiling of vitreous proteomes from proliferative diabetic retinopathy and nondiabetic patients. Proteomics 7, 4203–4215.
Kim, Y.C., Chiang, B., Wu, X., Prausnitz, M.R., 2014. Ocular delivery of macromolecules. J. Control. Release 190, 172–181.
Kimura, M., Araie, M., Koyano, S., 1996. Movement of carboxyfluorescein across retinal pigment epithelium-choroid. Exp. Eye Res. 63, 51–56.
Kiuchi, K., Matsuoka, M., Wu, J.C., Lima e Silva, R., Kengatharan, M., Verghese, M., Ueno, S., Yokoi, K., Khu, N.H., Cooke, J.P., Campochiaro, P.A., 2008. Mecamylamine suppresses basal and nicotine-stimulated choroidal neovascularization. Investig. Ophthalmol. Vis. Sci. 49, 1705–1711.
Klaassen, I., Van Noorden, C.J.F., Schlingemann, R.O., 2013. Molecular basis of the inner blood-retinal barrier and its breakdown in diabetic macular edema and other pathological conditions. Prog. Retin. Eye Res. 34, 19–48.
Klein, R., Wallow, I.I., Ernest, J.T., 1980. Fluorophotometry. III. Streptozocin-treated rats and rats with pancreatectomy. Arch. Ophthalmol. 98, 2235–2237.
Knop, K., Hoogenboom, R., Fischer, D., Schubert, U.S., 2010. Poly(ethylene glycol) in drug delivery: pros and cons as well as potential alternatives. Angew. Chem. - Int. Ed. 49, 6288–6308.
Knudsen, L.L., 2002. Ocular fluorophotometry in human subjects and in swine - with particular reference to long-term pharmacokinetics. Acta Ophthalmol. Scand. 80, 6–24.
Kochan, T., Singla, A., Tosi, J., Kumar, A., 2012. Toll-like receptor 2 ligand pretreatment attenuates retinal microglial inflammatory response but enhances phagocytic activity toward Staphylococcus aureus. Infect. Immun. 80, 2076–2088.
Koevary, S.B., Nussey, J., Lake, S., 2002. Accumulation of topically applied porcine insulin in the retina and optic nerve in normal and diabetic rats. Investig. Ophthalmol. Vis. Sci. 43, 797–804.
Kohn, J., Abramson, S., Langer, R., 2004. Bioresorbable and bioerodible materials. In: Ratner, B., Hoffman, A., Schoen, F., Lemons, J. (Eds.), An Introduction to Materials in Medicine. Academic Press, Cambridge, pp. 115–127. Biomaterials Science.
Kompella, U.B., Bandi, N., Ayalasomayajula, S.P., 2003. Subconjunctival nano- and microparticles sustain retinal delivery of budesonide, a corticosteroid capable of inhibiting VEGF expression. Investig. Opthalmology Vis. Sci. 44, 1192–1201.
Koo, H., Moon, H., Han, H., Na, J.H., Huh, M.S., Park, J.H., Woo, S.J., Park, K.H., Chan Kwon, I., Kim, K., Kim, H., 2012. The movement of self-assembled amphiphilic polymeric nanoparticles in the vitreous and retina after intravitreal injection. Biomaterials 33, 3485–3493.
Koyama, R., Nakanishi, T., Ikeda, T., Shimizu, A., 2003. Catalogue of soluble proteins in human vitreous humor by one-dimensional sodium dodecyl sulfate–polyacrylamide gel electrophoresis and electrospray ionization mass spectrometry including seven angiogenesis-regulating factors. J. Chromatogr. B 792, 5–21.
Kraft, M.E., Glaeser, H., Mandery, K., König, J., Auge, D., Fromm, M.F., Schlötzer-Schrehardt, U., Welge-Lüssen, U., Kruse, F.E., Zolk, O., 2010. The prostaglandin transporter OATP2A1 is expressed in human ocular tissues and transports the antiglaucoma prostanoid latanoprost. Investig. Ophthalmol. Vis. Sci. 51, 2504–2511.
Krogsaa, B., Lund-Andersen, H., Mehlsen, J., Sestoft, L., Larsen, J., 1981. The blood-retinal barrier permeability in diabetic patients. Acta Ophthalmol. 59, 689–694.
Krohne, T.U., Eter, N., Holz, F.G., Meyer, C.H., 2008. Intraocular pharmacokinetics of bevacizumab after a single intravitreal injection in humans. Am. J. Ophthalmol. 146, 508–512.
Krohne, T.U., Liu, Z., Holz, F.G., Meyer, C.H., 2012. Intraocular pharmacokinetics of ranibizumab following a single intravitreal injection in humans. Am. J. Ophthalmol. 154, 682–686. http://dx.doi.org/10.1016/j.ajo.2012.03.047.
Kubo, Y., Shimizu, Y., Kusagawa, Y., Akanuma, S.-I., Hosoya, K.-I., 2013. Propranolol transport across the inner blood-retinal barrier: potential involvement of a novel organic cation transporter. J. Pharm. Sci. 102, 3332–3342.
Kumar, A., Shamsuddin, N., 2012. Retinal Muller glia initiate innate response to infectious stimuli via toll-like receptor signaling. PLoS One 7, e29830.
Kumar, M.V., Nagineni, C.N., Chin, M.S., Hooks, J.J., Detrick, B., 2004. Innate immunity in the retina: toll-like receptor (TLR) signaling in human retinal pigment epithelial cells. J. Neuroimmunol. 153, 7–15.
Kuo, T.T., Aveson, V.G., 2011. Neonatal Fc receptor and IgG-based therapeutics. MAbs 3, 422–430.
Kyyrönen, K., Urtti, A., 1990. Improved ocular: systemic absorption ratio of timolol by viscous vehicle and phenylephrine. Investig. Ophthalmol. Vis. Sci. 31, 1827–1833.
Lai, T.Y.Y., Wong, R.L.M., Chan, W.-M., 2015. Long-term outcome of half-dose verteporfin photodynamic therapy for the treatment of central serous chorioretinopathy (An American Ophthalmological Society thesis). Trans. Am. Ophthalmol. Soc. 113, T81–T827.
Laicine, E.M., Haddad, A., 1994. Transferrin, one of the major vitreous proteins, is produced within the eye. Exp. Eye Res. 59, 441–445.

Lajunen, T., Hisazumi, K., Kanazawa, T., Okada, H., Seta, Y., Yliperttula, M., Urtti, A., Takashima, Y., 2014. Topical drug delivery to retinal pigment epithelium with microfluidizer produced small liposomes. Eur. J. Pharm. Sci. 62, 23–32.
Lajunen, T., Kontturi, L.-S., Viitala, L., Manna, M., Cramariuc, O., Róg, T., Bunker, A., Laaksonen, T., Viitala, T., Murtomäki, L., Urtti, A., 2016a. Indocyanine green-loaded liposomes for light-triggered drug release. Mol. Pharm. 13, 2095–2107.
Lajunen, T., Nurmi, R., Kontturi, L.-S., Viitala, L., Yliperttula, M., Murtomäki, L., Urtti, A., 2016b. Light activated liposomes: functionality and prospects in ocular drug delivery. J. Control. Release 244, 157–166.
Lajunen, T., Viitala, L., Kontturi, L.-S., Laaksonen, T., Liang, H., Vuorimaa-Laukkanen, E., Viitala, T., Le Guevel, X., Yliperttula, M., Murtomäki, L., Urtti, A., 2015. Light induced cytosolic drug delivery from liposomes with gold nanoparticles. J. Control. Release 203, 85–98.
Larsson, B., Tjälve, H., 1979. Studies on the mechanism of drug-binding to melanin. Biochem. Pharmacol. 28, 1181–1187.
Larsson, B.S., 1993. Interaction between chemicals and melanin. Pigment. Cell Res. 6, 127–133.
Laude, A., Tan, L.E., Wilson, C.G., Lascaratos, G., Elashry, M., Aslam, T., Patton, N., Dhillon, B., 2010. Intravitreal therapy for neovascular age-related macular degeneration and inter-individual variations in vitreous pharmacokinetics. Prog. Retin. Eye Res. 29, 466–475.
Le, K.N., Gibiansky, L., Van Lookeren Campagne, M., Good, J., Davancaze, T., Loyet, K.M., Morimoto, A., Strauss, E.C., Jin, J.Y., 2015. Population pharmacokinetics and pharmacodynamics of lampalizumab administered intravitreally to patients with geographic atrophy. CPT Pharmacometrics Syst. Pharmacol. 4, 595–604.
Le Goff, M.M., Bishop, P.N., 2008. Adult vitreous structure and postnatal changes. Eye (Lond) 22, 1214–1222.
Leblanc, B., Jezequel, S., Davies, T., Hanton, G., Taradach, C., 1998. Binding of drugs to eye melanin is not predictive of ocular toxicity. Regul. Toxicol. Pharmacol. 28, 124–132.
Lee, D.A., Fefeu, S., Edo-Ukeh, A.A., Orengo, C.A., Slingsby, C., 2004. A semi-automated database of protein families in the eye. Nucleic Acids Res. 32, D148–D152. EyeSite.
Lee, S.J., Kim, E.S., Geroski, D.H., McCarey, B.E., Edelhauser, H.F., 2008. Pharmacokinetics of intraocular drug delivery of Oregon green 488-labeled triamcinolone by subtenon injection using ocular fluorophotometry in rabbit eyes. Investig. Ophthalmol. Vis. Sci. 49, 4506–4514.
Lee, T.W.-Y., Robinson, J.R., 2004. Drug delivery to the posterior segment of the eye II: development and validation of a simple pharmacokinetic model for subconjunctival injection. J. Ocul. Pharmacol. Ther. 20, 43–53.
Lehtinen, J., Magarkar, A., Stepniewski, M., Hakola, S., Bergman, M., Róg, T., Yliperttula, M., Urtti, A., Bunker, A., 2012a. Analysis of cause of failure of new targeting peptide in PEGylated liposome: molecular modeling as rational design tool for nanomedicine. Eur. J. Pharm. Sci. 46, 121–130.
Lehtinen, J., Raki, M., Bergström, K.A., Uutela, P., Lehtinen, K., Hiltunen, A., Pikkarainen, J., Liang, H., Pitkänen, S., Määttä, A.-M., Ketola, R.A., Yliperttula, M., Wirth, T., Urtti, A., 2012b. Pre-targeting and direct immunotargeting of liposomal drug carriers to ovarian carcinoma. PLoS One 7, e41410.
Li, J., Lan, B., Li, X., Sun, S., Lu, P., Cheng, L., 2016. Effect of intraocular pressure (IOP) and choroidal circulation on controlled episcleral drug delivery to retina/vitreous. J. Control. Release 243, 78–85. http://dx.doi.org/10.1016/j.jconrel.2016.10.001.
Li, S.K., Liddell, M.R., Wen, H., 2011. Effective electrophoretic mobilities and charges of anti-VEGF proteins determined by capillary zone electrophoresis. J. Pharm. Biomed. Anal. 55, 603–607.
Li, S.K., Lizak, M.J., Jeong, E.-K., 2008. MRI in ocular drug delivery. NMR Biomed. 21, 941–956.
Linnankoski, J., Mäkelä, J., Palmgren, J., Mauriala, T., Vedin, C., Ungell, A., Lazorova, L., Artursson, P., Urtti, A., Yliperttula, M., 2010. Paracellular porosity and pore size of the human intestinal epithelium in tissue and cell culture models. J. Pharm. Sci. 99, 2166–2175.
Liu, K.R., Peyman, G.A., She, S.C., Niesman, M.R., Khoobehi, B., 1989. Reduced toxicity of intravitreally injected liposome-encapsulated cytarabine. Ophthalmic Surg. 20, 358–361.
Liu, S., 2008. Bifunctional coupling agents for radiolabeling of biomolecules and target-specific delivery of metallic radionuclides. Adv. Drug Deliv. Rev. 60, 1347–1370.
Lopes, V.S., Wasmeier, C., Seabra, M.C., Futter, C.E., 2007. Melanosome maturation defect in Rab38-deficient retinal pigment epithelium results in instability of immature melanosomes during transient melanogenesis. Mol. Biol. Cell 18, 3914–3927.
Los, L.I., 2008. The rabbit as an animal model for post-natal vitreous matrix differentiation and degeneration. Eye 22, 1223–1232. http://dx.doi.org/10.1038/eye.2008.39.
Loukovaara, S., Nurkkala, H.L., Tamene, F., Gucciardo, E., Liu, X., Repo, P., Lehti, K., Varjosalo, M., 2015. Quantitative proteomics analysis of vitreous humor from diabetic retinopathy patients. J. Proteome Res. 14, 5131–5143.
Ludtke, J.J., Zhang, G., Sebestyén, M.G., Wolff, J.A., 1999. A nuclear localization signal can enhance both the nuclear transport and expression of 1 kb DNA. J. Cell Sci. 112, 2033–2041.
Luke, Q.J., Jorquera, M., Streilein, J.W., 1993. Subretinal space and vitreous cavity as immunologically privileged sites for retinal allografts. Investig. Ophthalmol. Vis. Sci. 34, 3347–3354.
Maeda, H., 2001. The enhanced permeability and retention (EPR) effect in tumor vasculature: the key role of tumor-selective macromolecular drug targeting. Adv. Enzyme Regul. 41, 189–207.
Mäepea, O., Karlsson, C., Alm, A., 1984. Blood-ocular and blood-brain barrier function in streptozocin-induced diabetes in rats. Arch. Ophthalmol. 102, 1366–1369.
Maguire, A.M., Simonelli, F., Pierce, E.A., Pugh, E.N., Mingozzi, F., Bennicelli, J., Banfi, S., Marshall, K.A., Testa, F., Surace, E.M., Rossi, S., Lyubarsky, A., Arruda, V.R., Konkle, B., Stone, E., Sun, J., Jacobs, J., Dell'Osso, L., Hertle, R., Ma, J., Redmond, T.M., Zhu, X., Hauck, B., Zelenaia, O., Shindler, K.S., Maguire, M.G., Wright, J.F., Volpe, N.J., McDonnell, J.W., Auricchio, A., High, K.A., Bennett, J., 2008. Safety and efficacy of gene transfer for Leber's congenital amaurosis. N. Engl. J. Med. 358, 2240–2248. http://dx.doi.org/10.1056/NEJMoa0802315.
Majumdar, S., Kansara, V., Mitra, A.K., 2006. Vitreal pharmacokinetics of dipeptide monoester prodrugs of ganciclovir. J. Ocul. Pharmacol. Ther. 22, 231–241.
Mandell, B.A., Meredith, T.A., Aguilar, E., El-Massry, A., Sawant, A., Gardner, S., 1993. Effects of inflammation and surgery on amikacin levels in the vitreous cavity. Am. J. Ophthalmol. 115, 770–774.
Mannermaa, E., Reinisalo, M., Ranta, V.-P., Vellonen, K.-S., Kokki, H., Saarikko, A., Kaarniranta, K., Urtti, A., 2010. Filter-cultured ARPE-19 cells as outer blood–retinal barrier model. Eur. J. Pharm. Sci. 40, 289–296.
Mannermaa, E., Vellonen, K.-S., Ryhänen, T., Kokkonen, K., Ranta, V.-P., Kaarniranta, K., Urtti, A., 2009. Efflux protein expression in human retinal pigment epithelium cell lines. Pharm. Res. 26, 1785–1791.
Mannermaa, E., Vellonen, K.-S., Urtti, A., 2006. Drug transport in corneal epithelium and blood-retina barrier: emerging role of transporters in ocular pharmacokinetics. Adv. Drug Deliv. Rev. 58, 1136–1163.
Manning, M.C., Chou, D.K., Murphy, B.M., Payne, R.W., Katayama, D.S., 2010. Stability of protein pharmaceuticals: an update. Pharm. Res. 27, 544–575.
Männistö, M., Reinisalo, M., Ruponen, M., Honkakoski, P., Tammi, M., Urtti, A., 2007. Polyplex-mediated gene transfer and cell cycle: effect of carrier on cellular uptake and intracellular kinetics, and significance of glycosaminoglycans. J. Gene Med. 9, 479–487.
Manzanares, J.A., Rimpelä, A.-K., Urtti, A., 2016. Interpretation of ocular melanin drug binding assays. Alternatives to the model of multiple classes of independent sites. Mol. Pharm. 13, 1251–1257.
Marmor, M.F., Negi, A., Maurice, D.M., 1985. Kinetics of macromolecules injected into the subretinal space. Exp. Eye Res. 40, 687–696.
Mårs, U., Larsson, B.S., 1999. Pheomelanin as a binding site for drugs and chemicals. Pigment. Cell Res. 12, 266–274.
Maurice, B.D.M., Street, J., 1957. The exchange of sodium between the vitreous body and the blood and the aqueous humour. J. Physiol. 137, 110–125.
Maurice, D.M., 1976. Injection of drugs into the vitreous body. In: Leopold, I.H. (Ed.), Simposium on Ocular Therapy, Volume Nine. Wiley, pp. 59–72.
Maurice, D.M., 1959. Protein dynamics in the eye studied with labelled proteins. Am. J. Ophthalmol. 47, 361–368.
Maurice, D.M., Mishima, S., 1984. Ocular pharmacology. In: Sears, M. (Ed.), Handbook of Experimental Pharmacology. Springer-Verlag, Berlin-Heidelberg, pp. 16–119.
Meredith, T.A., 1993. Antimicrobial pharmacokinetics in endophthalmitis treatment: studies of ceftazidime. Trans. Am. Ophthalmol. Soc. 91, 653–699.
Merodio, M., Irache, J.M., Valamanesh, F., Mirshahi, M., 2002. Ocular disposition and tolerance of ganciclovir-loaded albumin nanoparticles after intravitreal injection in rats. Biomaterials 23, 1587–1594.
Meyer, C.H., Krohne, T.U., Holz, F.G., 2011. Intraocular pharmacokinetics after a single intravitreal injection of 1.5 mg versus 3.0 mg of bevacizumab in humans. Retina 31, 1877–1884.
Micera, A., Stampachiacchiere, B., Aronni, S., dos Santos, M.S., Lambiase, A., 2005. Toll-like receptors and the eye. Curr. Opin. Allergy Clin. Immunol. 5, 451–458.
Miguel, A., Henriques, F., Azevedo, L.F., Pereira, A.C., 2014. Ophthalmic adverse drug reactions to systemic drugs: a systematic review. Pharmacoepidemiol. Drug Saf. 23, 221–233.
Miller, S.S., Edelman, J.L., 1990. Active ion transport pathways in the bovine retinal pigment epithelium. J. Physiol. 424, 283–300.
Mirshafiee, V., Mahmoudi, M., Lou, K., Cheng, J., Kraft, M.L., 2013. Protein corona significantly reduces active targeting yield. Chem. Commun. (Camb) 49, 2557–2559.
Mishima, S., 1981. Clinical pharmacokinetics of the eye. Proctor lecture. Invest. Ophthalmol. Vis. Sci. 21, 504–541.
Misra, G.P., Singh, R.S.J., Aleman, T.S., Jacobson, S.G., Gardner, T.W., Lowe, T.L., 2009. Subconjunctivally implantable hydrogels with degradable and thermoresponsive properties for sustained release of insulin to the retina. Biomaterials 30, 6541–6547.
Missel, P.J., 2012. Simulating intravitreal injections in anatomically accurate models for rabbit, monkey, and human eyes. Pharm. Res. 29, 3251–3272.
Missel, P.J., Horner, M., Muralikrishnan, R., 2010. Simulating dissolution of intravitreal triamcinolone acetonide suspensions in an anatomically accurate rabbit eye model. Pharm. Res. 27, 1530–1546. http://dx.doi.org/10.1007/s11095-010-0163-1.
Morales-Canton, V., Fromow-Guerra, J., Longoria, S.S., Vera, R.R., Widmann, M., Patel, S., Yerxa, B., 2013. Suprachoroidal microinjection of bevacizumab is well tolerated in human patients. Investig. Ophthalmol. Vis. Sci. 54, 3299 (ARVO Abstract).
Moritera, T., Ogura, Y., Honda, Y., Wada, R., Hyon, S.H., Ikada, Y., 1991. Microspheres of biodegradable polymers as a drug-delivery system in the vitreous. Investig. Ophthalmol. Vis. Sci. 32, 1785–1790.

Morrissey, K.M., Wen, C.C., Johns, S.J., Zhang, L., Huang, S.-M., Giacomini, K.M., 2012. The UCSF-FDA TransPortal: a public drug transporter database. Clin. Pharmacol. Ther. 92, 545–546.
Munger, R.J., Sallee, V.L., Stern, M.E., 1989. 2–ophthalmic surgery on laboratory animals. In: Research Surgery and Care of the Research Animal, pp. 35–74. http://dx.doi.org/10.1016/B978-0-12-278009-7.50006-6.
Murthy, K.R., Goel, R., Subbannayya, Y., Jacob, H.K., Murthy, P.R., Manda, S., Patil, A.H., Sharma, R., Sahasrabuddhe, N.A., Parashar, A., Nair, B.G., Krishna, V., Prasad, T., Gowda, H., Pandey, A., 2014. Proteomic analysis of human vitreous humor. Clin. Proteomics 11, 29.
Muthuchamy, M., Zawieja, D., 2008. Molecular regulation of lymphatic contractility. Ann. N. Y. Acad. Sci. 1131, 89–99.
Nakanishi, T., Koyama, R., Ikeda, T., Shimizu, A., 2002. Catalogue of soluble proteins in the human vitreous humor: comparison between diabetic retinopathy and macular hole. J. Chromatogr. B 776, 89–100.
Nash, B.M., Wright, D.C., Grigg, J.R., Bennetts, B., Jamieson, R.V., 2015. Retinal dystrophies, genomic applications in diagnosis and prospects for therapy. Transl. Pediatr. 4, 139–163.
Nel, A.E., Mädler, L., Velegol, D., Xia, T., Hoek, E.M.V., Somasundaran, P., Klaessig, F., Castranova, V., Thompson, M., 2009. Understanding biophysicochemical interactions at the nano-bio interface. Nat. Mater 8, 543–557.
Nevala, H., Ylikomi, T., Tähti, H., 2008. Evaluation of the selected barrier properties of retinal pigment epithelial cell line ARPE-19 for an in-vitro blood-brain barrier model. Hum. Exp. Toxicol. 27, 741–749.
Nguyen, B.Q., Fife, R.S., 1986. Vitreous contains a cartilage-related protein. Exp. Eye Res. 43, 375–382.
Nieto, A., Hou, H., Moon, S.W., Sailor, M.J., Freeman, W.R., Cheng, L., 2015. Surface engineering of porous silicon microparticles for intravitreal sustained delivery of rapamycin. Investig. Ophthalmol. Vis. Sci. 56, 1070–1080.
Nilsson, S.F.E., Alm, A., 2012. Determination of ocular blood flows with the microsphere method. In: Schmetterer, L., Kiel, J. (Eds.), Ocular Blood Flow. Springer-Verlag, Berlin-Heidelberg, pp. 25–47.
Niwa, Y., Kakinoki, M., Sawada, T., Wang, X., Ohji, M., 2015. Ranibizumab and aflibercept: intraocular pharmacokinetics and their effects on aqueous VEGF level in vitrectomized and nonvitrectomized macaque eyes. Investig. Ophthalmol. Vis. Sci. 56, 6501–6505.
Nomoto, H., Shiraga, F., Kuno, N., Kimura, E., Fujii, S., Shinomiya, K., Nugent, A.K., Hirooka, K., Baba, T., 2009. Pharmacokinetics of bevacizumab after topical, subconjunctival, and intravitreal administration in rabbits. Investig. Ophthalmol. Vis. Sci. 50, 4807–4813.
Novack, G.D., Robin, A.L., 2016. Ocular pharmacology. J. Clin. Pharmacol. 56, 517–527.
Nyström, A.M., Fadeel, B., 2012. Safety assessment of nanomaterials: implications for nanomedicine. J. Control. Release 161, 403–408.
Oguro, Y., Tsukahara, Y., Saito, I., Kondo, T., 1985. Estimation of the permeability of the blood-retinal barrier in normal individuals. Investig. Ophthalmol. Vis. Sci. 26, 969–976.
Oh, W.K., Kim, S., Choi, M., Kim, C., Jeong, Y.S., Cho, B.R., Hahn, J.S., Jang, J., 2010. Cellular uptake, cytotoxicity, and innate immune response of silica - titania hollow nanoparticles based on size and surface functionality. ACS Nano 4, 5301–5313.
Olsen, T.W., Aaberg, S.Y., Geroski, D.H., Edelhauser, H.F., 1998. Human sclera: thickness and surface area. Am. J. Ophthalmol. 125, 237–241. http://dx.doi.org/10.1016/S0002-9394(99)80096-8.
Olsen, T.W., Edelhauser, H.F., Lim, J.I., Geroski, D.H., 1995. Human scleral permeability. Effects of age, cryotherapy, transscleral diode laser, and surgical thinning. Investig. Ophthalmol. Vis. Sci. 36, 1893–1903.
Olsen, T.W., Feng, X., Wabner, K., Conston, S.R., Sierra, D.H., Folden, D.V., Smith, M.E., Cameron, J.D., 2006. Cannulation of the suprachoroidal space: a novel drug delivery methodology to the posterior segment. Am. J. Ophthalmol. 142, 777–787.
Olsen, T.W., Feng, X., Wabner, K., Csaky, K., Pambuccian, S., Cameron, J.D., 2011. Pharmacokinetics of pars plana intravitreal injections versus microcannula suprachoroidal injections of bevacizumab in a porcine model. Investig. Opthalmology Vis. Sci. 52, 4749–4756.
Omri, S., Omri, B., Savoldelli, M., Jonet, L., Thillaye-Goldenberg, B., Thuret, G., Gain, P., Jeanny, J.C., Crisanti, P., Behar-Cohen, F., 2010. The outer limiting membrane (OLM) revisited: clinical implications. Clin. Ophthalmol. 4, 183–195.
Ouchi, M., West, K., Crabb, J.W., Kinoshita, S., Kamei, M., 2005. Proteomic analysis of vitreous from diabetic macular edema. Exp. Eye Res. 81, 176–182.
Owens, D.E., Peppas, N., 2006. Opsonization, biodistribution, and pharmacokinetics of polymeric nanoparticles. Int. J. Pharm. 307, 93–102.
Ozcimen, M., Sakarya, Y., Ozcimen, S., Sakarya, R., Goktas, S., Iyisoy, S., Alpfidan, I., Erdogan, E., 2015. Clearance of intravitreal daptomycin in uveitis-induced rabbit model. Curr. Eye Res. 40, 598–603.
Paasonen, L., Laaksonen, T., Johans, C., Yliperttula, M., Kontturi, K., Urtti, A., 2007. Gold nanoparticles enable selective light-induced contents release from liposomes. J. Control. Release 122, 86–93.
Paasonen, L., Sipilä, T., Subrizi, A., Laurinmäki, P., Butcher, S.J., Rappolt, M., Yaghmur, A., Urtti, A., Yliperttula, M., 2010. Gold-embedded photosensitive liposomes for drug delivery: triggering mechanism and intracellular release. J. Control. Release 147, 136–143.
Palmiere, C., Sabatasso, S., Torrent, C., Rey, F., Werner, D., Bardy, D., 2015. Postmortem determination of insulin using chemiluminescence enzyme immunoassay: preliminary results. Drug Test. Anal. 7, 797–803.
Panda-Jonas, S., Jonas, J.B., Jakobczyk, M., Schneider, U., 1994. Retinal photoreceptor count, retinal surface area, and optic disc size in normal human eyes. Ophthalmology 101, 519–523.
Panoilia, E., Schindler, E., Samantas, E., Aravantinos, G., Kalofonos, H.P., Christodoulou, C., Patrinos, G.P., Friberg, L.E., Sivolapenko, G., 2015. A pharmacokinetic binding model for bevacizumab and VEGF165 in colorectal cancer patients. Cancer Chemother. Pharmacol. 75, 791–803.
Park, S.J., Oh, J., Kim, Y.-K., Park, J.H.Y., Park, J.H.Y., Hong, H.K., Park, K.H., Lee, J.-E., Kim, H.M., Chung, J.Y., Woo, S.J., 2015. Intraocular pharmacokinetics of intravitreal vascular endothelial growth factor-Trap in a rabbit model. Eye (Lond) 29, 561–568.
Park, S.S., Vallar, R.V., Hong, C.H., Gunten, S., Ruoff, K., D'Amico, D.J., 1999. Intravitreal dexamethasone effect on intravitreal vancomycin elimination in endophthalmitis. Arch. Ophthalmol. 117, 1058–1062.
Patel, S., Müller, G., Stracke, J.O., Altenburger, U., Mahler, H.C., Jere, D., 2015. Evaluation of protein drug stability with vitreous humor in a novel ex-vivo intraocular model. Eur. J. Pharm. Biopharm. 95, 407–417.
Patel, S.R., Berezovsky, D.E., McCarey, B.E., Zarnitsyn, V., Edelhauser, H.F., Prausnitz, M.R., 2012. Targeted administration into the suprachoroidal space using a microneedle for drug delivery to the posterior segment of the eye. Investig. Ophthalmol. Vis. Sci. 53, 4433–4441.
Patel, S.R., Lin, A.S.P., Edelhauser, H.F., Prausnitz, M.R., 2011. Suprachoroidal drug delivery to the back of the eye using hollow microneedles. Pharm. Res. 28, 166–176.
Peeters, L., Sanders, N.N., Braeckmans, K., Boussery, K., Van de Voorde, J., De Smedt, S.C., Demeester, J., 2005. Vitreous: a barrier to nonviral ocular gene therapy. Investig. Ophthalmol. Vis. Sci. 46, 3553–3561.
Peptide Atlas, 2016. http://www.peptideatlas.org/ [accessed 8.8.16].
Percopo, C., Hooks, J., Shinohara, T., Caspi, R., Detrick, B., 1990. Cytokine-mediated activation of a neuronal retinal resident cell provokes antigen presentation. J. Immunol. 145, 4101–4107.
Perez, V.L., Caspi, R.R., 2015. Immune mechanisms in inflammatory and degenerative eye disease. Trends Immunol. 36, 354–363.
Petternel, V., Krepler, K., Schauersberger, J., Wedrich, A., 2004. Fosfomycin in human vitreous: –In–vitro investigation of the protein binding of fosfomycin in human vitreous –Fosfomycin levels in the vitreous cavity after intravenous administration. Investig. Ophthalmol. Vis. Sci. 45, 4930 (ARVO Abstract).
Philp, N.J., Wang, D., Yoon, H., Hjelmeland, L.M., 2003. Polarized expression of monocarboxylate transporters in human retinal pigment epithelium and ARPE-19 cells. Investig. Ophthalmol. Vis. Sci. 44, 1716–1721.
Pitkänen, L., Pelkonen, J., Ruponen, M., Rönkkö, S., Urtti, A., 2004. Neural retina limits the nonviral gene transfer to retinal pigment epithelium in an in vitro bovine eye model. AAPS J. 6, e25.
Pitkänen, L., Ranta, V.-P., Moilanen, H., Urtti, A., 2007. Binding of betaxolol, metoprolol and oligonucleotides to synthetic and bovine ocular melanin, and prediction of drug binding to melanin in human choroid-retinal pigment epithelium. Pharm. Res. 24, 2063–2070.
Pitkänen, L., Ranta, V.-P.P., Moilanen, H., Urtti, A., 2005. Permeability of retinal pigment epithelium: effects of permeant molecular weight and lipophilicity. Investig. Opthalmology Vis. Sci. 46, 641–646.
Poste, G., Bucana, C., Raz, A., Bucana, C., Bugelski, P., Kirsh, R., Fidler, I.J., 1982. Analysis of the fate of systemically administered liposomes and implications for their use in drug delivery. Cancer Res. 42, 1412–1422.
Potts, A.M., 1974. Proceedings: drug toxicity as related to ocular melanin. Psychopharmacol. Bull. 10, 40–41.
Potts, A.M., 1964. The reaction of uveal pigment in vitro with polycyclic compounds. Invest. Ophthalmol. 3, 405–416.
Powner, M.B., McKenzie, J.A.G., Christianson, G.J., Roopenian, D.C., Fruttiger, M., 2014. Expression of neonatal Fc receptor in the eye. Investig. Ophthalmol. Vis. Sci. 55, 1607–1615.
Prausnitz, M.R., Noonan, J.S., 1998. Permeability of cornea, sclera, and conjunctiva: a literature analysis for drug delivery to the eye. J. Pharm. Sci. 87, 1479–1488.
Prow, T.W., Bhutto, I., Kim, S.Y., Grebe, R., Merges, C., McLeod, D.S., Uno, K., Mennon, M., Rodriguez, L., Leong, K., Lutty, G.A., 2008. Ocular nanoparticle toxicity and transfection of the retina and retinal pigment epithelium. Nanomedicine Nanotechnol. Biol. Med. 4, 340–349.
Psimadas, D., Georgoulias, P., Valotassiou, V., Loudos, G., 2012. Molecular nanomedicine towards cancer: 111In-labeled nanoparticles. J. Pharm. Sci. 101, 2271–2280.
Querques, G., Capuano, V., Frascio, P., Souied, E.H., 2015. What may and may not be feasible to minimize the worsening of geographic atrophy. Expert Rev. Ophthalmol. 10, 211–214.
Radhika, M., Mithal, K., Bawdekar, A., Dave, V., Jindal, A., Relhan, N., Albini, T., Pathengay, A., Flynn, H.W., 2014. Pharmacokinetics of intravitreal antibiotics in endophthalmitis. J. Ophthalmic Inflamm. Infect. 4, 22.
Rai, U.D.J.P., Young, S.A., Thrimawithana, T.R., Abdelkader, H., Alani, A.W.G., Pierscionek, B., Alany, R.G., 2015. The suprachoroidal pathway: a new drug delivery route to the back of the eye. Drug Discov. Today 20, 491–495.
Ramana, K.V., 2011. Aldose reductase: new insights for an old enzyme. Biomol. Concepts 2, 103–114.
Ranta, V.-P., Mannermaa, E., Lummepuro, K., Subrizi, A., Laukkanen, A., Antopolsky, M., Murtomäki, L., Hornof, M., Urtti, A., 2010. Barrier analysis of periocular drug delivery to the posterior segment. J. Control. Release 148, 42–48.
Ranta, V.-P., Urtti, A., 2006. Transscleral drug delivery to the posterior eye:

prospects of pharmacokinetic modeling. Adv. Drug Deliv. Rev. 58, 1164–1181.
Raposo, G., Marks, M.S., 2007. Melanosomes — dark organelles enlighten endosomal membrane transport. Nat. Rev. Mol. Cell Biol. 8, 786–797.
Rasmussen, C.A., Gabelt, B.T., Kaufman, P.L., 2007. Aqueous humor dynamics in monkeys in response to the kappa opioid agonist bremazocine. Trans. Am. Ophthalmol. Soc. 105, 225–238, 9.
Raviola, G., 1977. The structural basis of the blood-ocular barriers. Exp. Eye Res. 25 (Suppl. l), 27–63.
Raviola, G., 1974. Effects of paracentesis on the blood-aqueous barrier: an electron microscope study on Macaca mulatta using horseradish peroxidase as a tracer. Invest. Ophthalmol. 13, 828–858.
Reardon, G., Kotak, S., Schwartz, G.F., 2011. Objective assessment of compliance and persistence among patients treated for glaucoma and ocular hypertension: a systematic review. Patient prefer. Adherence 5, 441–463.
Reichenbach, A., Schnitzer, J., Friedrich, A., Ziegert, W., Brückner, G., Schober, W., 1991. Development of the rabbit retina - I. Size of eye and retina, and postnatal cell proliferation. Anat. Embryol. Berl. 183, 287–297.
Reichenbach, A., Ziegert, M., Schnitzer, J., Pritz-Hohmeier, S., Schaaf, P., Schober, W., Schneider, H., 1994. Development of the rabbit retina. V. The question of “columnar units”. Brain Res. Dev. Brain Res. 79, 72–84.
Reinisalo, M., Urtti, A., Honkakoski, P., 2003. Retina-specific gene expression and improved DNA transfection in WERI-Rb1 retinoblastoma cells. Biochim. Biophys. Acta - Gene Struct. Expr. 1628, 169–176.
Remtulla, S., Hallett, P.E., 1985. A schematic eye for the mouse, and comparisons with the rat. Vis. Res. 25, 21–31.
Rimpelä, A.-K., Schmitt, M., Latonen, S., Hagström, M., Antopolsky, M., Manzanares, J.A., Kidron, H., Urtti, A., 2016. Drug distribution to retinal pigment epithelium: studies on melanin binding, cellular kinetics, and single photon emission computed tomography/computed tomography imaging. Mol. Pharm. 13, 2977–2986.
Robbie, S.J., von Leithner, P.L., Ju, M., Lange, C.A., King, A.G., Adamson, P., Lee, D., Sychterz, C., Coffey, P., Ng, Y.S., Bainbridge, J.W., Shima, D.T., 2013. Assessing a novel depot delivery strategy for noninvasive administration of VEGF/PDGF RTK inhibitors for ocular neovascular disease. Investig. Ophthalmol. Vis. Sci. 54, 1490–1500.
Robinson, M.R., Lee, S.S., Kim, H., Kim, S., Lutz, R.J., Galban, C., Bungay, P.M., Yuan, P., Wang, N.S., Kim, J., Csaky, K.G., 2006. A rabbit model for assessing the ocular barriers to the transscleral delivery of triamcinolone acetonide. Exp. Eye Res. 82, 479–487.
Rosenberg, A.S., 2006. Effects of protein aggregates: an immunologic perspective. AAPS J. 8, E501–E507.
Rosenfeld, P.J., Heier, J.S., Hantsbarger, G., Shams, N., 2006. Tolerability and efficacy of multiple escalating doses of ranibizumab (Lucentis) for neovascular age-related macular degeneration. Ophthalmology 113, 623–632 e1.
Rowe-Rendleman, C.L., Durazo, S.A., Kompella, U.B., Rittenhouse, K.D., Di Polo, A., Weiner, A.L., Grossniklaus, H.E., Naash, M.I., Lewin, A.S., Horsager, A., Edelhauser, H.F., 2014. Drug and gene delivery to the back of the eye: from bench to bedside. Investig. Ophthalmol. Vis. Sci. 55, 2714–2730.
Ruby, A., Williams, G.A., Mark, S., 2006. Vitreous humor. In: Duane's Ophthalmology. Lippincott Williams & Wilkins.
Ruponen, M., Ylä-Herttuala, S., Urtti, A., 1999. Interactions of polymeric and liposomal gene delivery systems with extracellular glycosaminoglycans: physicochemical and transfection studies. Biochim. Biophys. Acta - Biomembr. 1415, 331–341.
Rutar, M., Valter, K., Natoli, R., Provis, J.M., 2014. Synthesis and propagation of complement C3 by microglia/monocytes in the aging retina. PLoS One 9, e93343.
Ryhänen, T., Mannermaa, E., Oksala, N., Viiri, J., Paimela, T., Salminen, A., Atalay, M., Kaarniranta, K., 2008. Radicicol but not geldanamycin evokes oxidative stress response and efflux protein inhibition in ARPE-19 human retinal pigment epithelial cells. Eur. J. Pharmacol. 584, 229–236.
Sabzevari, A., Adibkia, K., Hashemi, H., De Geest, B.G., Mohsenzadeh, N., Atyabi, F., Ghahremani, M.H., Khoshayand, M.R., Dinarvand, R., 2013. Improved anti-inflammatory effects in rabbit eye model using biodegradable poly beta-amino ester nanoparticles of triamcinolone acetonide. Investig. Ophthalmol. Vis. Sci. 54, 5520–5526.
Salazar, M., Patil, P.N., 1976. An explanation for the long duration of mydriatic effect of atropine in eye. Invest. Ophthalmol. 15, 671–673.
Salazar, M., Shimada, K., Patil, P.N., 1976. Iris pigmentation and atropine mydriasis. J. Pharmacol. Exp. Ther. 197, 79–88.
Salehi-Had, H., Roh, M.I., Giani, A., Hisatomi, T., Nakao, S., Kim, I.K., Gragoudas, E.S., Vavvas, D., Guccione, S., Miller, J.W., 2011. Utilizing targeted gene therapy with nanoparticles binding alpha v beta 3 for imaging and treating choroidal neovascularization. PLoS One 6, e18864.
Salminen, L., Urtti, A., 1984. Disposition of ophthalmic timolol in treated and untreated rabbit eyes. A multiple and single dose study. Exp. Eye Res. 38, 203–206.
Sandhu, S.S., Manvikar, S., Steel, D.H.W., 2010. Displacement of submacular hemorrhage associated with age-related macular degeneration using vitrectomy and submacular tPA injection followed by intravitreal ranibizumab. Clin. Ophthalmol. 4, 637–642.
Sanyal, S., Zeilmaker, G.H., 1988. Retinal damage by constant light in chimaeric mice: implications for the protective role of melanin. Exp. Eye Res. 46, 731–743.
Sarna, T., Burke, J.M., Korytowski, W., Rózanowska, M., Skumatz, C.M.B., Zaręba, A., Zaręba, M., 2003. Loss of melanin from human RPE with aging: possible role of melanin photooxidation. Exp. Eye Res. 76, 89–98.
Sassoon, I., Blanc, V., 2013. Antibody-drug conjugate (ADC) clinical pipeline: a review. Methods Mol. Biol. 1045, 1–27.
Sauerborn, M., Brinks, V., Jiskoot, W., Schellekens, H., 2010. Immunological mechanism underlying the immune response to recombinant human protein therapeutics. Trends Pharmacol. Sci. 31, 53–59.
Saunders, D.J., Muether, P.S., Fauser, S., 2015. A model of the ocular pharmacokinetics involved in the therapy of neovascular age-related macular degeneration with ranibizumab. Br. J. Ophthalmol. 99, 1554–1559.
Schauersberger, J., Jager, W., 2002. In-vitro investigation of the protein binding of different antibiotics in the human vitreous. Investig. Ophthalmol. Vis. Sci. 43, 1853, 1853.
Schellekens, H., Hennink, W.E., Brinks, V., 2013. The immunogenicity of polyethylene glycol: facts and fiction. Pharm. Res. 30, 1729–1734.
Schmidt, S.Y., Peisch, R.D., 1986. Melanin concentration in normal human retinal pigment epithelium. Regional variation and age-related reduction. Investig. Ophthalmol. Vis. Sci. 27, 1063–1067.
Schön, C., Biel, M., Michalakis, S., 2015. Retinal gene delivery by adeno-associated virus (AAV) vectors: strategies and applications. Eur. J. Pharm. Biopharm. 95, 343–352.
Schroedl, F., Kaser-Eichberger, A., Schlereth, S.L., Bock, F., Regenfuss, B., Reitsamer, H.A., Lutty, G.A., Maruyama, K., Chen, L., Lütjen-Drecoll, E., Dana, R., Kerjaschki, D., Alitalo, K., De Stefano, M.E., Junghans, B.M., Heindl, L.M., Cursiefen, C., 2014. Consensus statement on the immunohistochemical detection of ocular lymphatic vessels. Investig. Ophthalmol. Vis. Sci. 55, 6440–6442.
Schwartz, K., Budenz, D., 2004. Current management of glaucoma. Curr. Opin. Ophthalmol. 15, 119–126.
Sebag, J., Tang, M., Brown, S., Sadun, A.A., Charles, M.A., 1994. Effects of pentoxifylline on choroidal blood flow in nonproliferative diabetic retinopathy. Angiology 45, 429–433. http://dx.doi.org/10.1177/000331979404500603.
Semba, R.D., Enghild, J.J., Venkatraman, V., Dyrlund, T.F., Van Eyk, J.E., 2013. The human eye proteome Project: perspectives on an emerging proteome. Proteomics 13, 2500–2511.
Sen, H.N., Chan, C.-C., Byrnes, G., Fariss, R.N., Nussenblatt, R.B., Buggage, R.R., 2008. Intravitreal methotrexate resistance in a patient with primary intraocular lymphoma. Ocul. Immunol. Inflamm. 16, 29–33.
Senthilkumari, S., Velpandian, T., Biswas, N.R., Bhatnagar, A., Mittal, G., Ghose, S., 2009. Evidencing the modulation of P-glycoprotein at blood-ocular barriers using gamma scintigraphy. Curr. Eye Res. 34, 73–77.
Shakib, M., Cunha-Vaz, J.G., 1966. Studies on the permeability of the blood-retinal barrier. IV. Junctional complexes of the retinal vessels and their role in the permeability of the blood-retinal barrier. Exp. Eye Res. 5, 229–234.
Shatz, W., Hass, P.E., Mathieu, M., Kim, H.S., Leach, K., Zhou, M., Crawford, Y., Shen, A., Wang, K., Chang, D.P., Maia, M., Crowell, S.R., Dickmann, L., Scheer, J.M., Kelley, R.F., 2016. Contribution of antibody hydrodynamic size to vitreal clearance revealed through rabbit studies using a species-matched fab. Mol. Pharm. 13, 2996–3003. http://dx.doi.org/10.1021/acs.molpharmaceut.6b00345.
Shelke, N.B., Kadam, R., Tyagi, P., Rao, V.R., Kompella, U.B., 2011. Intravitreal poly(l-lactide) microparticles sustain retinal and choroidal delivery of TG-0054, a hydrophilic drug intended for neovascular diseases. Drug Deliv. Transl. Res. 1, 76–90.
Shen, J., Durairaj, C., Lin, T., Liu, Y., Burke, J., 2014. Ocular pharmacokinetics of intravitreally administered brimonidine and dexamethasone in animal models with and without blood-retinal barrier breakdown. Investig. Ophthalmol. Vis. Sci. 55, 1056–1066.
Shih, Y.-Y.I., Guang, L., Garza, B.H.D., La Muir, E.R., Duong, T.Q., 2011. High resolution ΔR2, ΔR2 *, and vessel density MRI of the rat ocular circulation. In: Proceedings of the International Society for Magnetic Resonance in Medicine, p. 368.
Shikamura, Y., Yamazaki, Y., Matsunaga, T., Sato, T., Ohtori, A., Tojo, K., 2016. Hydrogel ring for topical drug delivery to the ocular posterior segment. Curr. Eye Res. 41, 653–661.
Shitama, T., Hayashi, H., Noge, S., Uchio, E., Oshima, K., Haniu, H., Takemori, N., Komori, N., Matsumoto, H., 2008. Proteome profiling of vitreoretinal diseases by cluster analysis. Proteomics - Clin. Appl. 2, 1265–1280.
Short, B.G., 2008. Safety evaluation of ocular drug delivery formulations: techniques and practical considerations. Toxicol. Pathol. 36, 49–62.
Silva-Cunha, A., Fialho, S.L., Naud, M.C., Behar-Cohen, F., 2009. Poly-ε-caprolactone intravitreous devices: an in vivo study. Investig. Ophthalmol. Vis. Sci. 50, 2312–2318.
Simon, J.D., Hong, L., Peles, D.N., 2008. Insights into melanosomes and melanin from some interesting spatial and temporal properties. J. Phys. Chem. B 112, 13201–13217.
Singh, P.K., Kumar, A., 2015. Retinal photoreceptor expresses toll-like receptors (TLRs) and elicits innate responses following TLR ligand and bacterial challenge. PLoS One 10, e0119541.
Singh, S.R., Grossniklaus, H.E., Kang, S.J., Edelhauser, H.F., Ambati, B.K., Kompella, U.B., 2009. Intravenous transferrin, RGD peptide and dual-targeted nanoparticles enhance anti-VEGF intraceptor gene delivery to laser-induced CNV. Gene Ther. 16, 645–659.
Sivaprasad, S., Bunce, C., Wormald, R., 2005. Non-steroidal anti-inflammatory agents for cystoid macular oedema following cataract surgery: a systematic review. Br. J. Ophthalmol. 89, 1420–1422.
Smedowski, A., Pietrucha-Dutczak, M., Kaarniranta, K., Lewin-Kowalik, J., 2014. A rat experimental model of glaucoma incorporating rapid-onset elevation of intraocular pressure. Sci. Rep. 4, 5910.

Smith, R.S., Rudt, L.A., 1975. Ocular vascular and epithelial barriers to microperoxidase. Invest. Ophthalmol. 14, 556–560.
Sohn, J.H., Kaplan, H.J., Suk, H.J., Bora, P.S., Bora, N.S., 2000. Chronic low level complement activation within the eye is controlled by intraocular complement regulatory proteins. Investig. Ophthalmol. Vis. Sci. 41, 3492–3502.
Soininen, S.K., 2016. Cellular, Placental and in Vivo Pharmacokinetics of Liposomal Doxorubicin. University of Eastern Finland.
Soininen, S.K., Vellonen, K.-S., Heikkinen, A.T., Auriola, S., Ranta, V.-P., Urtti, A., Ruponen, M., 2016. Intracellular PK/PD relationships of free and liposomal doxorubicin: quantitative analyses and PK/PD modeling. Mol. Pharm. 13, 1358–1365.
Song, L., Hennink, E.J., Young, I.T., Tanke, H.J., 1995. Photobleaching kinetics of fluorescein in quantitative fluorescence microscopy. Biophys. J. 68, 2588–2600.
Sreekumar, P.G., Spee, C., Ryan, S.J., Cole, S.P.C., Kannan, R., Hinton, D.R., 2012. Mechanism of RPE cell death in α-crystallin deficient mice: a novel and critical role for MRP1-mediated GSH efflux. PLoS One 7, e33420.
Steichen, S.D., Caldorera-Moore, M., Peppas, N.A., 2013. A review of current nanoparticle and targeting moieties for the delivery of cancer therapeutics. Eur. J. Pharm. Sci. 48, 416–427.
Stewart, M.W., 2014. Pharmacokinetics, pharmacodynamics and pre-clinical characteristics of ophthalmic drugs that bind VEGF. Expert Rev. Clin. Pharmacol. 7, 167–180. http://dx.doi.org/10.1586/17512433.2014.884458.
Stewart, M.W., 2012. Aflibercept (VEGF Trap-eye): the newest anti-VEGF drug. Br. J. Ophthalmol. 96, 1157–1158.
Stingl, K., Bartz-Schmidt, K.U., Besch, D., Chee, C.K., Cottriall, C.L., Gekeler, F., Groppe, M., Jackson, T.L., MacLaren, R.E., Koitschev, A., Kusnyerik, A., Neffendorf, J., Nemeth, J., Naeem, M.A.N., Peters, T., Ramsden, J.D., Sachs, H., Simpson, A., Singh, M.S., Wilhelm, B., Wong, D., Zrenner, E., 2015. Subretinal visual implant alpha IMS - clinical trial interim report. Vis. Res. 111, 149–160. http://dx.doi.org/10.1016/j.visres.2015.03.001.
Streilein, J.W., Ohta, K., Mo, J.S., Taylor, A.W., 2002. Ocular immune privilege and the impact of intraocular inflammation. DNA Cell Biol. 21, 453–459.
Struble, C., Howard, S., Relph, J., 2014. Comparison of Ocular Tissue Weights (Volumes) and Tissue Collection Techniques in Commonly Used Preclinical Animal Species Mean Male and Female. EVER Conference 2014.
Subrizi, A., Toropainen, E., Ramsay, E., Airaksinen, A.J., Kaarniranta, K., Urtti, A., 2015. Oxidative stress protection by exogenous delivery of rhHsp70 chaperone to the retinal pigment epithelium (RPE), a possible therapeutic strategy against RPE degeneration. Pharm. Res. 32, 211–221.
Sugano, K., Kansy, M., Artursson, P., Avdeef, A., Bendels, S., Di, L., Ecker, G.F., Faller, B., Fischer, H., Gerebtzoff, G., Lennernaes, H., Senner, F., 2010. Coexistence of passive and carrier-mediated processes in drug transport. Nat. Rev. Drug Discov. 9, 597–614.
Sutinen, R., Paronen, P., Urtti, A., 2000. Water-activated, pH-controlled patch in transdermal administration of timolol: I. Preclinical tests. Eur. J. Pharm. Sci. 11, 19–24.
Szebeni, J., 2005a. Complement activation-related pseudoallergy: a new class of drug-induced acute immune toxicity. Toxicology 216, 106–121.
Szebeni, J., 2005b. Complement activation-related pseudoallergy: a new class of drug-induced acute immune toxicity. Toxicology 216, 106–121. http://dx.doi.org/10.1016/j.tox.2005.07.023.
Szebeni, J., Muggia, F., Gabizon, A., Barenholz, Y., 2011a. Activation of complement by therapeutic liposomes and other lipid excipient-based therapeutic products: prediction and prevention. Adv. Drug Deliv. Rev. 63, 1020–1030.
Szebeni, J., Muggia, F., Gabizon, A., Barenholz, Y., 2011b. Activation of complement by therapeutic liposomes and other lipid excipient-based therapeutic products: prediction and prevention. Adv. Drug Deliv. Rev. 63, 1020–1030. http://dx.doi.org/10.1016/j.addr.2011.06.017.
Tachikawa, M., Takeda, Y., Tomi, M., Hosoya, K., 2010. Involvement of OCTN2 in the transport of acetyl-lcarnitine across the inner blood-retinal barrier. Investig. Ophthalmol. Vis. Sci. 51, 430–436.
Tachikawa, M., Toki, H., Tomi, M., Hosoya, K., 2008. Gene expression profiles of ATP-binding cassette transporter A and C subfamilies in mouse retinal vascular endothelial cells. Microvasc. Res. 75, 68–72.
Tagami, M., Kusuhara, S., Honda, S., Tsukahara, Y., Negi, A., 2009. Expression of ATP-binding cassette transporters at the inner blood–retinal barrier in a neonatal mouse model of oxygen-induced retinopathy. Brain Res. 1283, 186–193.
Tajika, T., Isowaki, A., Sakaki, H., 2011. Ocular distribution of difluprednate ophthalmic emulsion 0.05% in rabbits. J. Ocul. Pharmacol. Ther. 27, 43–49.
Takahashi, K., Saishin, Y., Saishin, Y., Mori, K., Ando, A., Yamamoto, S., Oshima, Y., Nambu, H., Melia, M.B., Bingaman, D.P., Campochiaro, P.A., 2003. Topical nepafenac inhibits ocular neovascularization. Investig. Ophthalmol. Vis. Sci. 44, 409–415.
Tanaka, M., Takashina, H., Tsutsumi, S., 2004. Comparative assessment of ocular tissue distribution of drug-related radioactivity after chronic oral administration of 14C-levofloxacin and 14C-chloroquine in pigmented rats. J. Pharm. Pharmacol. 56, 977–983.
TCDB, 2016. Transporter Classification Database [WWW Document]. http://www.tcdb.org/ (accessed 7.31.16).
Tenzer, S., Docter, D., Kuharev, J., Musyanovych, A., Fetz, V., Hecht, R., Schlenk, F., Fischer, D., Kiouptsi, K., Reinhardt, C., Landfester, K., Schild, H., Maskos, M., Knauer, S.K., Stauber, R.H., 2013. Rapid formation of plasma protein corona critically affects nanoparticle pathophysiology. Nat. Nanotechnol. 8, 772–781.
The Ocular Tissue Database, 2016. https://genome.uiowa.edu/otdb/ [accessed 8.8.16].
Thompson, C.L., Jun, G., Klein, B.E.K., Klein, R., Capriotti, J., Lee, K.E., Iyengar, S.K., 2007. Genetics of pigment changes and geographic atrophy. Investig. Ophthalmol. Vis. Sci. 48, 3005–3013.
Thornit, D.N., Vinten, C.M., Sander, B., Lund-Andersen, H., La Cour, M., 2010. Blood-retinal barrier glycerol permeability in diabetic macular edema and healthy eyes: estimations from macular volume changes after peroral glycerol. Investig. Ophthalmol. Vis. Sci. 51, 2827–2834.
To, M., Goz, A., Camenzind, L., Oertle, P., Candiello, J., Sullivan, M., Henrich, P.B., Loparic, M., Safi, F., Eller, A., Halfter, W., 2013. Diabetes-induced morphological, biomechanical, and compositional changes in ocular basement membranes. Exp. Eye Res. 116, 298–307. http://dx.doi.org/10.1016/j.exer.2013.09.011.
Tojo, K., Nakagawa, K., Morita, Y., Ohtori, A., 1999. A pharmacokinetic model of intravitreal delivery of ganciclovir. Eur. J. Pharm. Biopharm. 47, 99–104.
Tonjum, A.M., Pedersen, O.O., 1977. The permeability of the human ciliary and iridial epithelium to horseradish peroxidase. An in vitro study. Acta Ophthalmol. 55, 781–788.
Törnquist, P., 1979. Capillary permeability in cat choroid, studied with the single injection technique (II). Acta Physiol. Scand. 106, 425–430.
Törnquist, P., Alm, A., Bill, A., 1990. Permeability of ocular vessels and transport across the blood-retinal-barrier. Eye (Lond) 4, 303–309.
Tsuboi, S., Pederson, J.E., 1986. Permeability of the isolated dog retinal pigment epithelium to carboxyfluorescein. Investig. Ophthalmol. Vis. Sci. 27, 1767–1770.
Tu, Z., Portillo, J.A.C., Howell, S., Bu, H., Subauste, C.S., Al-Ubaidi, M.R., Pearlman, E., Lin, F., 2011. Photoreceptor cells constitutively express functional TLR4. J. Neuroimmunol. 230, 183–187.
Tuovinen, L., Ruhanen, E., Kinnarinen, T., Rönkkö, S., Pelkonen, J., Urtti, A., Peltonen, S., Järvinen, K., 2004. Starch acetate microparticles for drug delivery into retinal pigment epithelium—in vitro study. J. Control. Release 98, 407–413.
Turunen, T., 2016. Diffusion of Nanoparticles in the Porcine Vitreous. University of Helsinki. https://helda.helsinki.fi/handle/10138/161072.
U.S. Food and Drug Administration, 2015. Endotoxin Testing Recommendations for Single-use Intraocular Ophthalmic Devices - Guidance for Industry and Food and Drug Administration Staff.
U.S. Food and Drug Administration, 2013. Guidance for industry: immunogenicity assessment for therapeutic protein products. Biotechnol. Law Rep. 172–185.
Ulrich, J.N., Spannagl, M., Kampik, A., Gandorfer, A., 2008. Components of the fibrinolytic system in the vitreous body in patients with vitreoretinal disorders. Clin. Exp. Ophthalmol. 36, 431–436.
Urtti, A., 2006. Challenges and obstacles of ocular pharmacokinetics and drug delivery. Adv. Drug Deliv. Rev. 58, 1131–1135.
Urtti, A., Pipkin, J.D., Rork, G., Sendo, T., Finne, U., Repta, A.J., 1990. Controlled drug delivery devices for experimental ocular studies with timolol 2. Ocular and systemic absorption in rabbits. Int. J. Pharm. 61, 241–249.
Urtti, A., Salminen, L., 1993. Minimizing systemic absorption of topically administered ophthalmic drugs. Surv. Ophthalmol. 37, 435–456.
Urtti, A., Salminen, L., Kujari, H., Jäntti, V., 1984. Effect of ocular pigmentation on pilocarpine pharmacology in the rabbit eye. II. Drug response. Int. J. Pharm. 19, 53–61.
Urtti, A., Salminen, L., Miinalainen, O., 1985. Systemic absorption of ocular pilocarpine is modified by polymer matrices. Int. J. Pharm. 23, 147–161.
Urtti, A., Sendo, T., Pipkin, J.D., Rork, G., Repta, A.J., 1988. Application site dependent ocular absorption of timolol. J. Ocul. Pharmacol. 4, 335–343.
Vadlapatla, R.K., Vadlapudi, A.D., Ponnaluri, V.K.C., Pal, D., Mukherji, M., Mitra, A.K., 2013. Molecular expression and functional activity of efflux and influx transporters in hypoxia induced retinal pigment epithelial cells. Int. J. Pharm. 454, 444–452.
van Bilsen, K., van Hagen, P.M., Bastiaans, J., van Meurs, J.C., Missotten, T., Kuijpers, R.W., Hooijkaas, H., Dingjan, G.M., Baarsma, G.S., Dik, W.A., 2011. The neonatal Fc receptor is expressed by human retinal pigment epithelial cells and is downregulated by tumour necrosis factor-alpha. Br. J. Ophthalmol. 95, 864–868.
van Deemter, M., Kuijer, R., Harm Pas, H., Jacoba van der Worp, R., Hooymans, J.M.M., Los, L.I., 2013. Trypsin-mediated enzymatic degradation of type II collagen in the human vitreous. Mol. Vis. 19, 1591–1599.
Vaughan-Thomas, A., Gilbert, S.J., Duance, V.C., 2000. Elevated levels of proteolytic enzymes in the aging human vitreous. Investig. Ophthalmol. Vis. Sci. 41, 3299–3304.
Vegge, T., 1971. An electron microscopic study of the permeability of iris capillaries to horseradish peroxidase in the vervet monkey (Cercopithecus aethiops) (Vienna, Austria 1948). Z. für Zellforsch. Mikrosk. Anat. 121, 74–81.
Vellonen, K.-S., Soini, E.-M., del Amo, E.M., Urtti, A., 2016. Prediction of ocular drug distribution from systemic blood circulation. Mol. Pharm. 13, 2906–2911. http://dx.doi.org/10.1021/acs.molpharmaceut.5b00729.
Vonarbourg, A., Passirani, C., Saulnier, P., Benoit, J.-P., 2006. Parameters influencing the stealthiness of colloidal drug delivery systems. Biomaterials 27, 4356–4373.
Wagner, E., Plank, C., Zatloukal, K., Cotten, M., Birnstiel, M.L., 1992. Influenza virus hemagglutinin HA-2 N-terminal fusogenic peptides augment gene transfer by transferrin-polylysine-DNA complexes: toward a synthetic virus-like gene-transfer vehicle. Proc. Natl. Acad. Sci. U. S. A. 89, 7934–7938.
Wakamatsu, K., Hu, D.-N.N., McCormick, S.A., Ito, S., 2008. Characterization of melanin in human iridal and choroidal melanocytes from eyes with various colored irides. Pigment. Cell Melanoma Res. 21, 97–105.
Walczyk, D., Bombelli, F.B., Monopoli, M.P., Lynch, I., Dawson, K. a, 2010. What the cell "sees" in bionanoscience. J. Am. Chem. Soc. 132, 5761–5768.
Waltman, S., Krupin, T., Hanish, S., Oestrich, C., Becker, B., 1978. Alteration of the

blood-retinal barrier in experimental diabetes mellitus. Arch. Ophthalmol. 96, 878–879.
Wang, H., Feng, L., Hu, J., Xie, C., Wang, F., 2012. Characterisation of the vitreous proteome in proliferative diabetic retinopathy. Proteome Sci. 10, 15.
Wang, R., Brattain, M.G., 2007. The maximal size of protein to diffuse through the nuclear pore is larger than 60kDa. FEBS Lett. 581, 3164–3170.
Wasmeier, C., Hume, A.N., Bolasco, G., Seabra, M.C., 2008. Melanosomes at a glance. J. Cell Sci. 121, 3995–3999.
Weijtens, O., Feron, E.J., Schoemaker, R.C., Cohen, A.F., Lentjes, E.G., Romijn, F.P., van Meurs, J.C., 1999. High concentration of dexamethasone in aqueous and vitreous after subconjunctival injection. Am. J. Ophthalmol. 128, 192–197.
Weiss, L., 1897. Über das Wachstum des menschlichen Auges und über die Veränderung der Muskelinsertionen am wachsenden Auge. Ref. Beiträge zur Anat. Entwickelungsgeschichte 8, 191–248.
Weleber, R.G., Pennesi, M.E., Wilson, D.J., Kaushal, S., Erker, L.R., Jensen, L., McBride, M.T., Flotte, T.R., Humphries, M., Calcedo, R., Hauswirth, W.W., Chulay, J.D., Stout, J.T., 2016. Results at 2 Years after gene therapy for RPE65-deficient leber congenital amaurosis and severe early-Childhood–onset retinal dystrophy. Ophthalmology 123, 1606–1620. http://dx.doi.org/10.1016/j.ophtha.2016.03.003.
Wikler, K.C., Williams, R.W., Rakic, P., 1990. Photoreceptor mosaic: number and distribution of rods and cones in the rhesus monkey retina. J. Comp. Neurol. 297, 499–508. http://dx.doi.org/10.1002/cne.902970404.
Wolking, S., Schaeffeler, E., Lerche, H., Schwab, M., Nies, A.T., 2015. Impact of genetic polymorphisms of ABCB1 (MDR1, P-Glycoprotein) on drug disposition and potential clinical implications: update of the literature. Clin. Pharmacokinet. 54, 709–735.
Wong, W.L., Su, X., Li, X., Cheung, C.M.G., Klein, R., Cheng, C.-Y., Wong, T.Y., 2014. Global prevalence of age-related macular degeneration and disease burden projection for 2020 and 2040: a systematic review and meta-analysis. Lancet Glob. heal. 2, e106–e116.
Wrobel, I., Collins, D., 1995. Fusion of cationic liposomes with mammalian cells occurs after endocytosis. Biochim. Biophys. Acta - Biomembr. 1235, 296–304.
Wysocki, L.M., Lavis, L.D., 2011. Advances in the chemistry of small molecule fluorescent probes. Curr. Opin. Chem. Biol. 15, 752–759. http://dx.doi.org/10.1016/j.cbpa.2011.10.013.
Xiao, K., Li, Y., Luo, J., Lee, J.S., Xiao, W., Gonik, A.M., Agarwal, R.G., Lam, K.S., 2011. The effect of surface charge on in vivo biodistribution of PEG-oligocholic acid based micellar nanoparticles. Biomaterials 32, 3435–3446.
Xu, Q., Boylan, N.J., Suk, J.S., Wang, Y.-Y., Nance, E.A., Yang, J.-C., McDonnell, P.J., Cone, R.A., Duh, E.J., Hanes, J., 2013. Nanoparticle diffusion in, and microrheology of, the bovine vitreous ex vivo. J. Control. Release 167, 76–84.
Xu, Y., Szoka, F.C., 1996. Mechanism of DNA release from cationic liposome/DNA complexes used in cell transfection. Biochemistry 35, 5616–5623.
Xue, H., Guo, P., Wen, W.-C., Wong, H., 2015. Lipid-based nanocarriers for RNA delivery. Curr. Pharm. Des. 21, 3140–3147.
Yamane, K., 2003. Proteome analysis of human vitreous proteins. Mol. Cell. Proteomics 2, 1177–1187.
Yan, Q., Sadée, W., 2000. Human membrane transporter database: a Web-accessible relational database for drug transport studies and pharmacogenomics. AAPS PharmSci 2, E20.
Yan, Y., Gause, K.T., Kamphuis, M.M.J., Ang, C.S., O'Brien-Simpson, N.M., Lenzo, J.C., Reynolds, E.C., Nice, E.C., Caruso, F., 2013. Differential roles of the protein corona in the cellular uptake of nanoporous polymer particles by monocyte and macrophage cell lines. ACS Nano 7, 10960–10970.
Yang, W., Yuan, Y., Zong, Y., Huang, Z., Mai, S., Li, Y., Qian, X., Liu, Y., Gao, Q., 2014. Preliminary study on retinal vascular and oxygen-related changes after long-term silicone oil and foldable capsular vitreous body tamponade. Sci. Rep. 4, 5272.
Yanoff, M., Duker, J.S., 2014. Ophthalmology, fourth. ed. Saunders, Philadelphia.
Yasin, M.N., Svirskis, D., Seyfoddin, A., Rupenthal, I.D., 2014. Implants for drug delivery to the posterior segment of the eye: a focus on stimuli-responsive and tunable release systems. J. Control. Release 196, 208–221.
Ye, A.Y., Liu, Q.-R., Li, C.-Y., Zhao, M., Qu, H., 2014. Human Transporter Database: comprehensive knowledge and discovery tools in the human transporter genes. PLoS One 9, e88883.
Yu, Q., Kent, C.R., Tytell, M., 2001. Retinal uptake of intravitreally injected Hsc/Hsp70 and its effect on susceptibility to light damage. Mol. Vis. 7, 48–56.
Yücel, Y.H., Johnston, M.G., Ly, T., Patel, M., Drake, B., Gümüş, E., Fraenkl, S.A., Moore, S., Tobbia, D., Armstrong, D., Horvath, E., Gupta, N., 2009. Identification of lymphatics in the ciliary body of the human eye: a novel “uveolymphatic” outflow pathway. Exp. Eye Res. 89, 810–819.
Zehetner, C., Kralinger, M.T., Modi, Y.S., Waltl, I., Ulmer, H., Kirchmair, R., Bechrakis, N.E., Kieselbach, G.F., 2015. Systemic levels of vascular endothelial growth factor before and after intravitreal injection of aflibercept or ranibizumab in patients with age-related macular degeneration: a randomised, prospective trial. Acta Ophthalmol. 93, e154–e159.
Zelphati, O., Szoka, F.C., 1996. Intracellular distribution and mechanism of delivery of oligonucleotides mediated by cationic lipids. Pharm. Res. 13, 1367–1372.
Zeng, H., Green, W.R., Tso, M.O.M., 2008. Microglial activation in human diabetic retinopathy. Arch. Ophthalmol. 126, 227–232.
Zhang, K., Zhang, L., Weinreb, R.N., 2012. Ophthalmic drug discovery: novel targets and mechanisms for retinal diseases and glaucoma. Nat. Rev. Drug Discov. 11, 541–559.
Zhang, T., Xiang, C.D., Gale, D., Carreiro, S., Wu, E.Y., Zhang, E.Y., 2008. Drug transporter and cytochrome P450 mRNA expression in human ocular barriers: implications for ocular drug disposition. Drug Metab. Dispos. 36, 1300–1307.
Zhang, Y., Li, C., Sun, X., Kuang, X., Ruan, X., 2012a. High glucose decreases expression and activity of p-glycoprotein in cultured human retinal pigment epithelium possibly through iNOS induction. PLoS One 7, e31631.
Zhang, Y., Lu, M., Sun, X., Li, C., Kuang, X., Ruan, X., 2012b. Expression and activity of p-glycoprotein elevated by dexamethasone in cultured retinal pigment epithelium involve glucocorticoid receptor and pregnane X receptor. Investig. Ophthalmol. Vis. Sci. 53, 3508–3515.
Zhang, Y., Schlachetzki, F., Li, J.Y., Boado, R.J., Pardridge, W.M., 2003. Organ-specific gene expression in the rhesus monkey eye following intravenous non-viral gene transfer. Mol. Vis. 9, 465–472.
Zhu, C., Zhang, Y., Pardridge, W.M., 2002. Widespread expression of an exogenous gene in the eye after intravenous administration. Investig. Ophthalmol. Vis. Sci. 43, 3075–3080.